Benha University
Benha Faculty of Engineering
Department of Mechanical Engineering

Performance study of proposed Hybrid Desiccant Air-Conditioning and HDH Desalination Systems in Low Humidity Applications

Thesis Submitted in Partial Fulfillment of the Requirements
of the
M.Sc. in Mechanical Engineering

By:

Eng. Mohamed Ashraf Mohamed Mahmoud
B.Sc. in Mechanical Engineering Technology, 2014

Under the Supervision of:

Prof. Dr. Sameh A. Nada
Mechanical Engineering Department
Benha Faculty of Engineering
Benha University

Dr. Refaat M. H. Khater
Lecturer, Mechanical Engineering Department,
Benha Faculty of Engineering,
Benha University

Benha 2019

The undersigned have examined the thesis entitled

Performance study of proposed hybrid desiccant air-conditioning and HDH desalination systems in low humidity applications

Presented by

Eng. Mohamed Ashraf Mohamed Mahmoud

B.Sc. in Mechanical Engineering Technology, 2014

a candidate for the degree of

Master of Science in Engineering in Mechanical Engineering

and hereby certify that it is worthy of acceptance.

Prof. Dr. Adel Hassan Khalil Professor in Mechanical Power Engineering Department, Faculty of Engineering, Cairo University	**(Committee Chairperson)** ______________________
Prof. Dr. Sayed Ahmed Kaseb Professor in Mechanical Power Engineering Department, Faculty of Engineering, Cairo University	**(Committee Member)** ______________________
Prof. Dr. Sameh Abdelwahed Nada Professor in Mechanical Engineering Department, Benha Faculty of Engineering, Benha University	**(Committee Member)** ______________________
Accepted from Mechanical Engineering Department **Assoc. Prof. Ahmed EL-Betar**	**(Department Chariman)** ______________________
Accepted from the Postgraduate Affairs **Prof. Dr. Hesham M. El-Batsh**	**(Vice Dean for Postgraduate Studies)** ______________________
Accepted for the Faculty **Prof. Dr. Aref Mohamed Ahmed Soliman**	**(Dean of the Faculty)** ______________________

Benha Faculty of Engineering – Benha University

ABSTRACT

The air conditioning systems of low humidity applications using desiccant wheel consume a huge amount of energy to maintain the required low temperature and humidity needed by the application. In the mathematical work of the present study, proposed efficient systems that integrate the technologies of desiccant dehumidification, evaporative cooling, and freshwater production with the air conditioning system of low-humidity applications are presented. Thermodynamics analysis of the systems is conducted and the systems of governing equations are analytically solved and analyzed using EES software. Parametric studies are conducted to investigate the effects of the different operating parameters on the performance of the proposed systems. The power savings and the fresh water productions of the different proposed systems are evaluated and compared to select the optimum system configuration.

The results of the analytical study showed that :

- **(i)** The fresh water production rate and the cooling coil capacity of the air conditioning system increase with increasing the fresh air ratio and outdoor humidity and decrease with increasing the ambient air temperature,
- **(ii)** The saving in power consumption due to using energy recovery in system 2 and 3 remarkably noticed with increasing the outdoor air ratio.
- **(iii)** The system with energy recovery located after the desiccant wheel is operating more efficiently and economically compared to the other systems.

An experimental investigation of the Humidification dehumidification (HDH) water desalination system using new air humidification section (honeycomb packed bed) and new dehumidification coils (un-finned and strips wired finned helical coils) at different orientations were conducted. HDH systems of different dehumidifying helical coils (finned and un-finned) were tested at different orientations (vertical and

horizontal) for a wide range of air flow rate, air temperature, air humidity, water flow rate and water temperature.

The results of the experimental study showed that:

(i) The productivity and performance of the proposed HDH system increases with increasing the air flow rate, air humidity, air temperature, water flow rate and water temperature.

(ii) The proposed HDH system with the new humidification and dehumidification sections has better productivity and performance compared to other systems.

(iii) The dehumidifying finned helical coil always has better performance compared to the un-finned coils whatever the coil orientations, air flow rates, and air properties.

(iv) Placing the coil (finned or un-finned coils) at vertical orientation enhances the coil performance and the system productivity.

(v) The finned and un-finned coils at the vertical and horizontal orientations, the system productivity and the coil performance increases with increasing air flow rate, air humidity and air temperature.

(vi) The effect of using strip fins on the coil surface is more dominant in case of horizontal orientation of the coil compared to the vertical orientation. Finally, the results concluded the recommendation of using finned helical coils at the vertical orientation for the optimal performance of the HDH system.

ACKNOWLEDGEMENTS

- I thank the almighty ALLAH for his mercy and grace, which enabled me to complete this work.
- I wish to express my deep gratitude to my supervisors, **Prof. Sameh A. Nada**, and **Dr. Refaat M. H. Khater** for their inspiring guidance, valuable advice, and constant encouragement throughout the progress of this research. Their suggestions, criticism, and patience have been a great asset.
- I would like to appreciate all the staff of Benha Faculty of Engineering who graciously gave me their time and assistance so that i could accomplished the requirements of this degree.
- I thank my parents for their unceasing encouragement and support.
- Last but not least, my sincere gratitude to my family, especially my wife, my son (**Hamza**) and her family for their continuous support and encouragement.
- I am also grateful to all who directly or indirectly have lent helping hand in this research.

Mohamed Ashraf Mohamed

2019

CONTENTS

continued

LIST OF FIGURES

NOMENCLATURES

C_p	Specific heat, kJ/kg. K
E°	Total power consummation, kW
E°_{pump}	Auxiliary power "Ratio of the auxiliary electricity consumed by blowers and pumps used for air and water circulation per unit amount of water production ≈ 0.029 kWh"
h	Specific enthalpy, kJ/kg
h_{fg}	Heat of water evaporation, kJ/kg
h_s	Sensible heat transfer coefficient, kW/ m^2.K
h_t	Total heat transfer coefficient, kW/ m^2.K
m°	Mass flow rate, kg/sec
m°_{w1}	Fresh water production rate across cooling coil in air cooled chiller unit, kg/sec.
m°_{w2}	Fresh water production rate across cooling coil in water cooled unit, kg/sec.
Q°_{cc}	Cooling coil capacity, kW
Q°_{L}	Latent heat transfer, kW
Q°_{R}	Conditioned space load, TR
Q°_{s}	Sensible heat transfer rate, kW
Q°_{t}	Total heat transfer rate, kW
T	Temperature, ˚C
W°_{c}	Compressor power, kW
ω	Specific humidity, kg_v/ kg_a

Abbreviations

A/C	Air Conditioning
Ac	Surface area of helical coil
CC	Cooling Coil
COP	Coefficient of Performance
DCS	Desiccant Cooling System
DW	Desiccant Wheel
DX	Direct Expansion
EES	Engineering Equation Solver
FWST	Feed Water Storage Tank
HC	Humidification Compression
HDH	Humidification- Dehumidification
HR	Heat Recovery
MVC	Mechanical Vapor Compression

PS	Power Saving
RH	Relative Humidity
RR	Reactivation air Ratio "Reactivation air volume divided by process air volume"
RSHF	Room Sensible Heat Factor "Sensible heat load divided by total heat load in room"
TR	Tone of Refrigeration "1TR= 3.51 KW"
TSC	Total Saving in Cost ($/Kwh)

Subscript

0,3	Fresh air inlet to system
1	Process air inlet
1, air	Air inlet to system
2, 2'	Process air outlet (Dry air)
2, air	Air inlet to helical coil
4	Regeneration air inlet (Hot and dry air)
5	Regeneration air outlet (wat air)
6	Air exit from humidifier inlet to the cooling coil
7	Air exit from the cooling coil
c	Compressor
e	Exit
I	Inlet
o	Outlet/ Outdoor
P	Process air
$P_{s2,3}$	Proposed system 2, 3
Reg	Regeneration air
S	Air supply to room
w	Water
w, hum	Water inlet to humidifier

Greek Symbols

α	Inclination angle
ε_{DW1}	Thermal efficiency of Desiccant wheel
ε_{DW2}	Regeneration Efficiency of Desiccant wheel
η_{eff}	Coil effectiveness

Chapter 1: INTRODUCTION

1.1. Problem Definition

The air conditioning systems of low humidity applications such as pharmaceutical factories consume a huge amount of energy in air conditioning and desiccant wheel processes to maintain the required low temperature and humidity needed by the application. At the same time, a huge amount of water vapor is exhausted to the atmosphere with the regenerated hot air of the desiccant wheel. Fig. 1.1 shows the basic air conditioning system with a desiccant wheel to maintain the space at the required temperature and low humidity. The system consists of air-cooled chiller unit to serve the cooling coil with chilled water required to cool the air supplied to the space required to be air-conditioned, desiccant wheel (DW) to keep the low humidity in the server space, and heating coil to produce the hot air required for the regeneration process of the desiccant wheel.

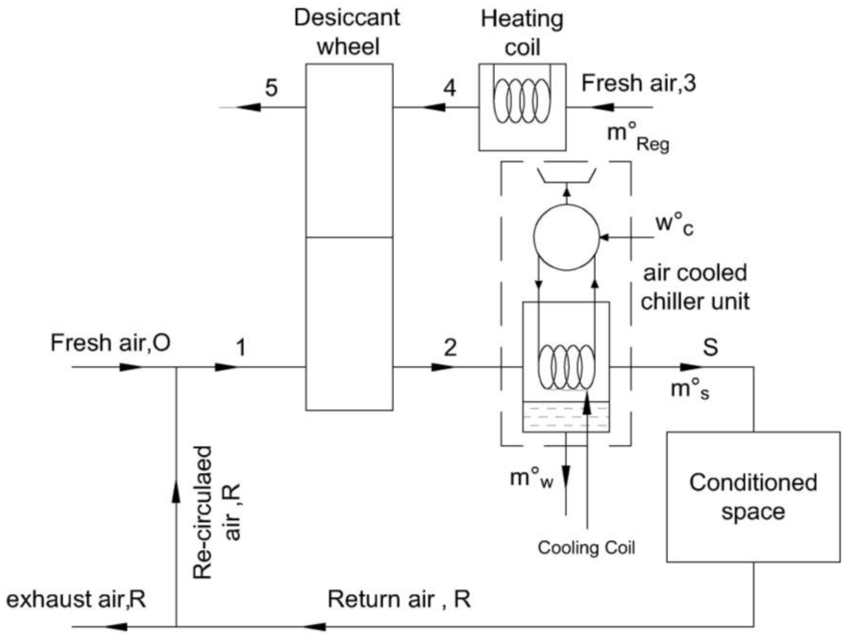

Fig. 1. 1 Basic air conditioning system with desiccant wheel

The system process on the air is described using the psychrometric chart as shown in Fig. 1.2. The outdoor air at state O mixes with the return air at state R to a mixed air at state (1). The outdoor air to the return air ratio and accordingly the location of point 1 on the

Psychrometric chart vary according to the fresh air requirements in the conditioned space. The mixed air is then passed on the desiccant wheel where water vapor is extracted from it leading to the dehumidification and heating of the air to state (2). The air outlet from the desiccant wheel passes through the cooling coil of the air handling unit. Air cooled chiller is used to supply the chilled water required by the cooling coil of the air handling unit to cool and extra dehumidify the air. The air exits the cooling coil at state (S) where it is supplied to the conditioned space to remove its cooling and moisture load and maintain it at the required design conditions. Part of the air returned from the conditioned space is mixed with the outdoor fresh air, and the other part is exhausted to outdoor. To remove the moisture captured in the desiccant rotor, another amount of outdoor air called reactivation air at outdoor ambient condition (O) is heated up in a heating coil before entering the desiccant rotor at state (4). After removing the moisture content from the desiccant wheel section, the humid hot air exit from the desiccant wheel (state 5) is exhausted to the atmosphere.

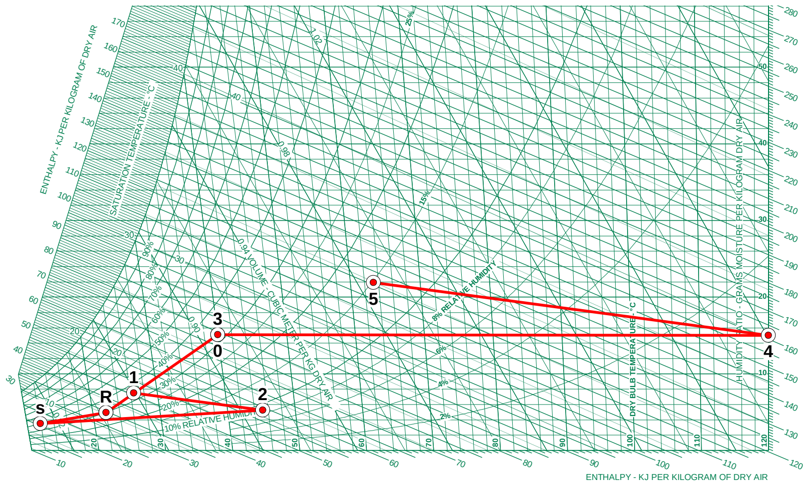

Fig. 1. 2 Psychrometric chart of process air of the AC system with DW

A large part of the energy of the air-conditioning system (AC) of the low humidity applications is required for the removal of moisture. A desiccant wheel (DW) is typically used in this system to remove water (moisture) from processing air before it is mechanically refrigerated. In the desiccant wheel, the process air to be dehumidified passes through the adsorption section of the wheel where the water vapor in the process air is directly removed from the air and holds in the wheel while rotating.

As the desiccant section saturated with water vapor passes through the regeneration sector of the wheel, the water vapor is transferred to a heated regenerative airstream, which is exhausted to outside. The process operates in a steady continuous manner, allowing for highly effective and uninterrupted dehumidification. Fig. 1.3 shows the principle of operation of the desiccant wheel.

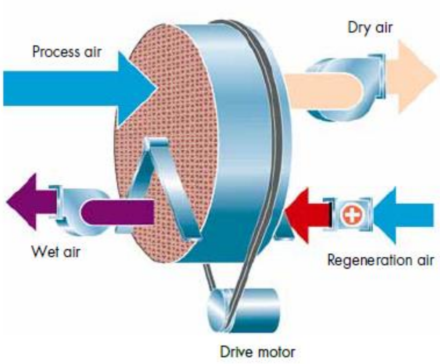

Fig. 1. 3 Principle of desiccant wheel operation

Freshwater production by air humidification dehumidification system is widely used for the sake of fresh water with minimum driving energy. Extra energy in the air and water heating can be used in this system to enhance the performance and productivity of this system. Fig. 1.4 shows a schematic diagram of a water desalination system using air humidification dehumidification system (HDH).

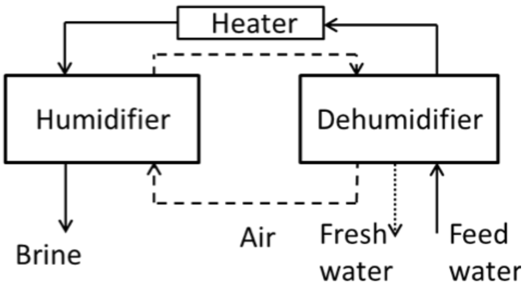

Fig. 1. 4 Schematic diagram of water desalination system using air HDH system.

Combining the purpose and advantages of the above two systems make us thinking of proposing hybrid systems for air conditioning and fresh water production to be used in air conditioning of low humidity applications to remove moisture from the conditioned space and utilizing the high humidity and temperature of the exhaust regenerated air from the desiccant wheel of the air conditioning system in freshwater production. Fig. 1.5 shows the schematic diagram of the hybrid air conditioning and fresh water production system where the hot and humid regeneration air exhausted from the desiccant wheel is utilized as the process air of the humidification-dehumidification system. Doing so, the energy and water used to drive the system to produce fresh water are reduced. Fig. 1.6 shows the air process on the Psychometric chart. The humid hot air exit from the desiccant wheel at state (5) passes through humidifier operated by brackish water to increase the moisture content in reactivation air. The air exits the humidifier at state (6) is dehumidified on the water coil to produce water and the air is then exhausted to the atmosphere at state 7. The water rate given by the water coil is m°_{w2}. The water produced from the water-cooling coil is collected with the water condenses on the cooling coil to produce the total amount of fresh water production. A water chemical treatment unit is used to treat the total condensate water to be fresh water.

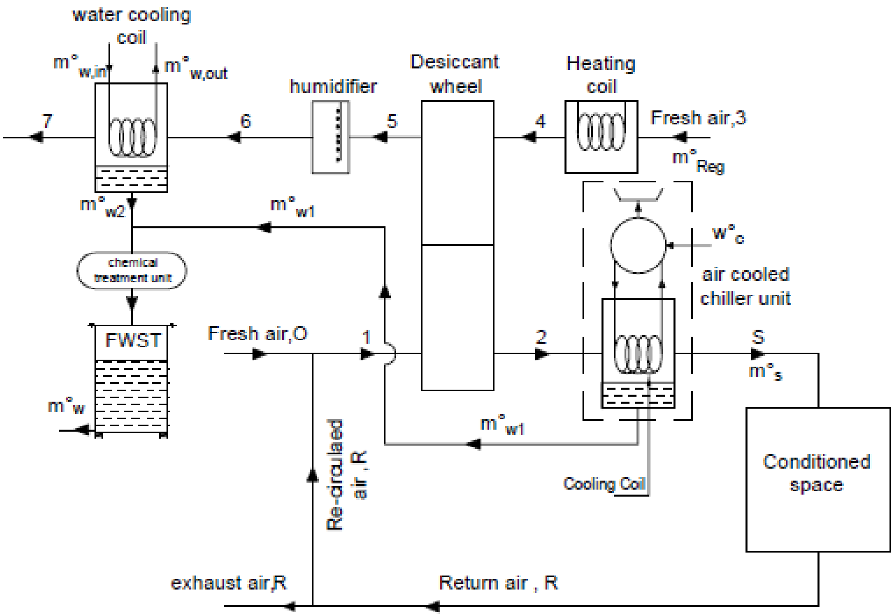

Fig. 1. 5 Schematic diagram of the hybrid AC and HDH water desalination system (system-1)

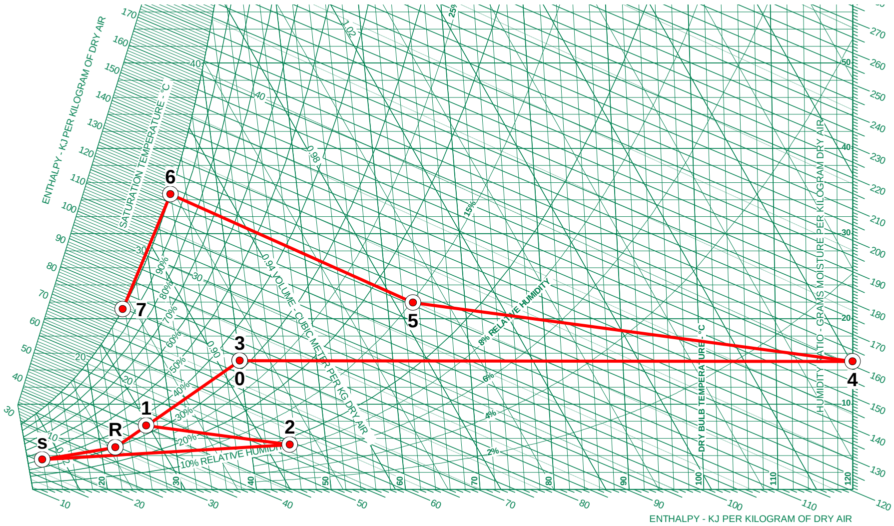

Fig. 1. 6 Psychometric chart of process air of the hybrid AC and HDH water desalination system

1.2. Brief About Previous Work

The desiccant wheel (DW) has been used as an air dehumidifier since the 1930$_s$ for industrial applications such as product dying and corrosion prevention. It has also been used in hospitals, pharmaceutical applications, clean rooms, museums and other areas requiring a low humidity level. Nowadays, to save energy, the desiccant wheel is also used in the air-conditioning system to reduce the latent cooling load. The more moisture is removed from the air, the better the desiccant wheel dehumidifier should perform. To achieve higher moisture reduction, a higher temperature of the heater is required to heat the regeneration air that flows pass the desiccant wheel. After removing the water vapor from the desiccant wheel, the regeneration air is exhausted at very high temperature and humidity. Utilizing this hot and humid regeneration air in fresh water production by air HDH system, the productivity of the system can be increased and the energy used to drive the system can be reduced. Different hybrid systems of air conditioning and fresh water production using HDH system can be proposed for different alternatives of the system components locations. The systems of the minimum power consumption and the maximum freshwater production should be selected. The freshwater productivity of the HDH water desalination system depends on the effectiveness of the system components and the operating conditions. The effectiveness of the dehumidifying coil is the most important parameters that affect the productivity of this system. The effectiveness of the dehumidifying coil depends on the geometric conditions of the coil as well as the orientation of the coil. The operating conditions that affect the system productivity are the air flow rate, air temperature, and air humidity as well as the water flow rate and water temperature.

1.3. Thesis Overview

In the present work, innovated systems that integrate the technologies of desiccant dehumidification, evaporative cooling, traditional chillers system, and HDH water desalination system are proposed for energy saving and fresh water production in the air conditioning of low-humidity applications, as shown in Fig. 1.5. Energy recovery and HDH units are integrated with the convention air Conditioning-Desiccant wheel system of low humidity application for energy saving and freshwater production. Different systems are proposed for different arrangements of the energy recovery unit in the system, as shown in Figs. 1.7, 1.8.

Theoretical analysis and parametric study are conducted to (i) investigate the effects of the operating parameters on the performance of the system, and (ii) compare between the different systems alternatives to select the optimal system that gives maximum fresh water production rate with the minimum driving power. To avoid the high cost of the desiccant wheel system, a prototype experimental set-up was designed and constructed where the desiccant wheel system was replaced by heating and humidification systems as shown in Fig. 1.9. The main objective of the experimental work is (i) study the effects of the different operating parameters on the HDH units for fresh water production, and (ii) study the effect of the dehumidifying coil geometry, the presence of extended surfaces and orientation on the system productivity. The experimental work also aims to test a new helical coil with wired fins for the sake of maximizing the water dehumidification rate. The coil was tested at different orientations and compared with the un-finned coil.

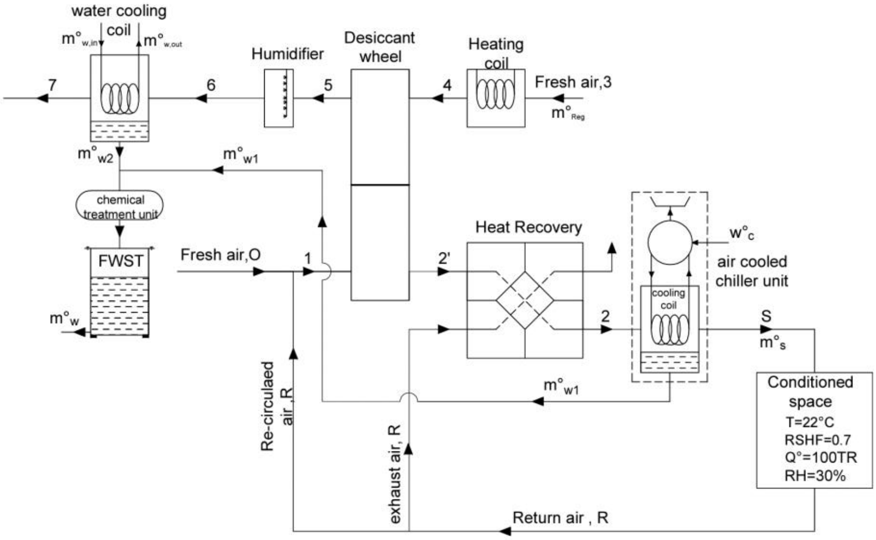

Fig. 1. 7 schematic diagram of the proposed system (system-2)

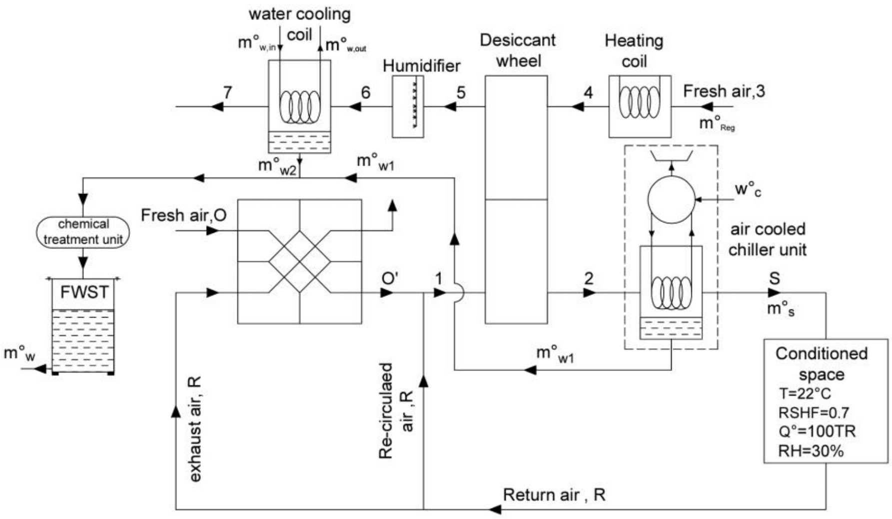

Fig. 1. 8 schematic diagram of the proposed system (system-3)

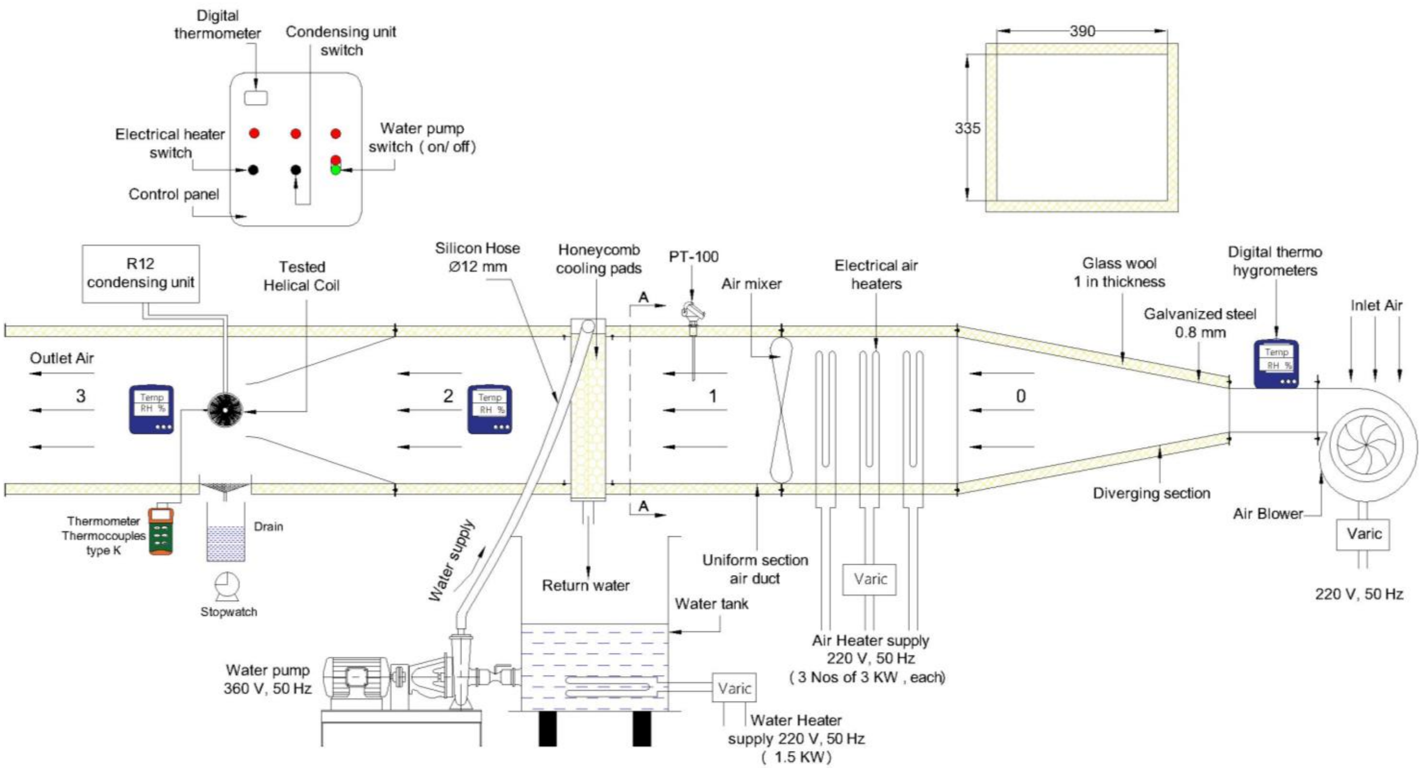

Fig. 1. 9 Experimental setup schematic diagram

1.4. Organization of Thesis

The organization of this thesis is as follows:

Chapter 2 "*Literature Review*": This chapter reviews the previous research papers related to the present study.

Chapter 3 "*Mathematical model of proposed systems*": This chapter Includes proposed efficient systems that integrate the technologies of desiccant dehumidification, evaporative cooling, and freshwater production with the air conditioning system of low-humidity applications.

Chapter 4 *"Experimental Facility and Measuring Instruments"*: This chapter presents the experimental setup to study the performance of the HDH water desalination system at different operating conditions and geometric design parameters of the dehumidifying coil.

Chapter 5 "*Results and Discussions*": This chapter concludes the results of experimental work to investigate and compare the heat transfer characteristics and the air dehumidification/water condensation rates of the finned and the un-finned helical coils at the vertical and horizontal orientations.

Chapter 6 "*Conclusions and Future work*": This chapter concludes the contributions made in this thesis and provides some visions for the future research.

Chapter 2: LITERATURE REVIEW

Different hybrid systems of air conditioning/refrigeration and fresh water production using HDH system have been investigated in the literature by many investigators. The aim of most of these researches was the selection of the system and the operating conditions that give minimum power consumption and maximum freshwater production. The freshwater productivity of the HDH water desalination system depends on the effectiveness of the system components and the operating conditions. The effectiveness of the dehumidifying coil is the most important parameters that affect the productivity of the system. One of the aims of the present study is to propose a dehumidifying coil geometry and orientation that maximize the coil dehumidification capacity. Accordingly, the literature review of the present study was conducted for the following two major areas to support the scope of the present work:

- Hybrid Air Conditioning/refrigeration and HDH Systems.
- Performance of cooling and dehumidifying coils for different geometries and orientations

The concentrated efforts that have been devoted in the literature of these two areas will be reviewed in this chapter.

2.1. Hybrid Air Conditioning/ Refrigeration and HDH Systems

Water desalination can be considered as a solution to fresh water sources depletion but it consumes a considerable amount of energy. Moreover, air conditioning systems consume considerable electrical energy specially in hot and humid areas. Different techniques were proposed to enhance the performance of the water desalination and the air conditioning systems and to reduce the energy consumption. Hybrid air conditioning and HDH fresh water production systems were proposed and discussed by many investigators to enhance the performance and the productivity of the systems and reduce the energy consumption.

Aly NH et al. [1] studied theoretically and experimentally the performance of the mechanical vapor compression (MVC) desalination system. The experimental and theoretical results indicated that the production rate increases by increasing the operating temperature from 70°C to about 98°C, “evaporator designed temperature70°C”. Also, increasing the evaporator temperature has a good effect on the heat transfer coefficient.

Ghalavand Y et al. [2] presented a new humidification-dehumidification process desalination technology named ‘‘Humidification Compression (HC)" which has some advantages (such as high energy performance, high recovery flow rate, energy recovery) in comparison with other similar methods.

Nada SA et al. [3] studied theoretically the performance of integrated A/C and water desalination systems using HDH technique suggested for hot and dry weather areas. Four systems with evaporative cooler and heat recovery units were employed, analyzed and assessed at various operating conditions (fresh air ratio, supply air temperature and outside air wet bulb temperature). The results show that (i) the fresh water production rates of the proposed systems increase with increasing fresh air ratio, supply air temperature and outdoor wet bulb temperature, (ii) powers saving of the proposed systems increase with increasing fresh air ratio and supply air temperature and decreasing of the outdoor air wet bulb temperature.

Later, Nada SA et al. [4] achieved an experimental study to investigate the performance of an integrated HDH water desalination and A/C system using vapor compression refrigeration unit. The performance was studied under different operating parameters (air flow rate, air inlet temperature, specific humidity, and evaporator saturation temperature). The results showed the enhancement of the fresh water production rate, the refrigeration capacity and the compressor work per kilogram of fresh water with increasing air specific humidity and air mass flow rate. The supply air temperature and relative humidity increased remarkably with increasing freshwater rate.

Al-Enezi G et al. [5] measured and analyzed the performance characteristics of the humidification-dehumidification desalination system at low operating temperatures. The highest water production rates were obtained at high hot water temperature, low cooling water temperature, high air flow rate, and low hot water flow rate.

Mohamed and El-Minshawy [6] carried out theoretical work to evaluate the performance of seawater HDH desalination system powered by solar energy. The theoretical simulation model was developed and a comparison study had been presented to show the effect of the different parameters on the system performance and its productivity.

Ghazal et al. [7] carried out an experimental prototype to improve the performance of solar HDH systems. The solar air heater, solar water heater and the evaporator of the traditional HDH systems were replaced with compact system designs.

Nafey et al. [8] presented a numerical investigation of humidification-dehumidification desalination (HDH) process using solar energy. A mathematical model was developed, simulating the HDH system, to study the influence of the different system configurations and operating conditions on the system productivity. The results showed also that the productivity of the unit is strongly influenced by the air flow rate, cooling water flow rate and total solar energy incident through the day. Wind speed and ambient temperature variations show a very small effect on the system productivity. In addition, the obtained results indicate that the solar water collector area strongly affects the system productivity more than the solar air collector area.

Nafey et al. [9] also presented an experimental investigation for desalination system based on humidification– dehumidification desalination (HDH) technique using solar energy at the weather conditions of Suez City, Egypt. Different variables are examined including the feed water flow rate, the air flow rate, the cooling water flow rate in the dehumidifier and the weather conditions. The results showed that the productivity of the system is strongly affected by the saline water temperature at the inlet to the humidifier, dehumidifier cooling water flow rate, air flow rate and solar intensity. The wind speed and ambient temperature variation were found to have a very small effect on the system productivity.

Fouda et al. [10] studied the performance of a proposed innovated solar integrated system for air conditioning (A/C) and humidification-dehumidification (HDH) water desalination in hot and humid regions. The study was conducted under different operating and design conditions. The system performance parameters (fresh water production rate, cooling capacity, electrical power consumption, water recovery and system coefficient of performance) were hourly estimated and daily integrated for different operational and design conditions.

Elattar et al. [11] presented a parametrical and economical study of the performance of integrative A/C and HDH water desalination system assisted by solar energy. The system performance was investigated under steady-state operation utilizing solar thermal storage and auxiliary heating units.

Dayem and Fatouh [12] conducted theoretical and experimental investigations for various HDH solar assisted water desalination systems to present the best efficient system. Three systems were suggested and compared for climatological environments of Cairo (30_N). In the first system, an auxiliary heater was used to switch the temperature of the salt water where it was naturally switched in the second system depending on the weather conditions. The third system was an open system in which the salt water was used as a collector fluid. It was found that the third system is the most efficient one and it has the lowest cost. Moreover, the first one has the greatest distilled water with higher temperatures and flow rates.

Giwa et al. [13] presented a humidification-dehumidification desalination system driven by photovoltaic thermal energy recovery for small-scale sustainable water and power production. The technical analysis of the desalination process was carried out through the modeling of the physical and thermodynamic properties under the environmental conditions of Abu Dhabi, UAE.

Kabeel and El-Said [14] investigated and compared various configurations of hybrid desalination systems based on air HDH–single stage flashing and powered by solar energy.

Yıldırım and Solmus [15] theoretically investigated the performance of HDH water desalination system driven by solar energy for Antalya, Turkey under different design and operational parameters.

Sharshir et al. [16] experimentally investigated the performance of a continuous HDH designation system integrated with evacuated tube solar collector and solar still.

Suyono et al. [17] show the theoretical and experimental analysis of system integrated solar dryer with a desiccant wheel is designed to produce dry air, and then study desiccant wheel performance at low humidity climatic region, where discuss the main factors affected on drying process (temperature, flow rate and humidity of processing air).

Yadav and Bajpai. [18] studied the effect of optimal rotational speed on moisture removed by process area in the desiccant wheel. Also, the effect of air flow rate on the reactivation air and process air has been studied. When process inlet air velocity increases it causes a reduction in process removed moisture. With an increase in reactivation inlet air velocity, there is only a slight increase in process removed moisture.

Dai et al. [19] conducted a comparison study between the cooling vapor compression systems, vapor compression with complementary desiccant and vapor compression evaporative cooler supplemented with desiccant.

Mandegari and Pahlavanzadeh [20] studied the different types of desiccant wheel efficiency. Two kinds of the efficiency of the desiccant wheel dehumidifier were examined, namely thermal and dehumidification efficiency. The study concluded that the efficiency changes due to the change of temperature and humidity of inlet and outlet air streams.

Kamar et al. [21] studied the effect of varying the regeneration air temperature on desiccant wheel performance. Results of the experiments showed that increasing the regeneration air temperature increases the dry bulb temperature of the process outlet air. However, the moisture content of the process outlet air was reduced. The dehumidification efficiency of the desiccant wheel decreased with increasing regeneration air temperature.

Zendehboudi et al. [22] studied the performance evaluation of a system consists of desiccant wheel coupled with AC system for tropical climatic zone of IRAN. The study showed that the amount of energy saving and efficiency increased comparing with those of conventional cooling and dehumidification systems. Results indicated that when the hybrid system was used, the efficiency was increased by 0.76 and energy consumption was reduced by 3.034kW.

Daou et al. [23] investigated the performance of the desiccant systems in different climatic conditions to emphasize the benefits of energy savings. Some commented examples were presented to show how the desiccant cooling can be a perfective supplement to other cooling systems such as traditional vapor compression air conditioning system, the evaporative cooling, and the chilled-ceiling radiant cooling.

Al-Enezi et al. [24] examined and investigated the performance of water desalination system using HDH technique at low operational temperatures. The maximum freshwater rate was observed at elevated hot water and low cooling water temperatures and at high air and low hot water mass flow rates.

Yuan et al. [25] presented an integrative unit for air-conditioning and desalination driven by vapor compression heat pump on basis of direct humidification-dehumidification process. The performance of the system was studied using the mathematical modeling. The flow, heat and mass transfer inside the humidifier was analyzed by Gao et al. [26].

Mehrgoo and Amidpour [27] used the constructed theory for conceptual design of humidification-dehumidification (HDH) desalination unit and showed that the main design features of a direct contact HDH desalination process can be determined based on the method of the constructed design.

2.2 Performance of cooling and dehumidifying coils for different geometries and orientations

In the cooling and dehumidifying coil, condensation of water vapor of the air on the surface of the cooling coil occurs. The characteristics of the heat and mass transfer in the condensation process control the performance of the cooling and dehumidifying coils. The helical coil is an effective device for heat exchange because of its high heat transfer area and heat transfer coefficient in small occupied space. The cooling effect in helical coils tube is high compared to the straight tube due to the tube curvature effect in helical coil. The fluid stream in the outer layer of the helical tube flows faster than the flow of fluid in the inner layer. Helical coils showed the best performance among the other types of the coils due to its compact size and high heat transfer coefficients. The purpose of most of the researches conducted on helical coils was to determine the performance of the helical coils in different application Heat transfer process in helical coil heat exchanger had been extensively studied by man researchers. Most of the researches were devoted to compare the heat transfer characteristics of helical coils and straight tubes heat exchangers. Some of these researches were conducted through analytical/numerical studies and other through experimental studies [28-45].

Prabhanjan et al. [28] studied heat transfer in helically coiled heat exchanger compared to straight tube heat exchanger with similar dimensions. Results showed that, heat transfer coefficient increases in helical coils compared to those of straight tubes.

Coronel and Sandeep [29] tested two helical coils having different curvature ratios versus straight tube heat exchanger at different flow rates to determine and compare heat transfer capability of the different coils with turbulent flow regimes. Results showed that, in helical coil heat exchanger the overall heat transfer coefficient is higher than that of the straight tube heat exchanger and increases with increasing the curvature ratio.

Salimpour [30] carried out experimental work to study heat transfer coefficient of shell and helical coil tube with different coil pitches. Results showed that large coil pitches give higher heat transfer coefficient at constant temperature boundary condition.

Gupta et al. [31] conducted experiments to develop correlations to be used in the design of finned-coil heat exchangers of air conditioning and refrigeration applications. Experiments were conducted in Reynolds number effective range 500-1900. Results showed that the predicted correlations can be utilized in heat exchanger design with reasonable accuracy.

Mohamed et al. [32] conducted experimental study to determine the condensation heat transfer coefficient of the steam flowing into the helical coil. The different operating factors are; diameter of the pipe, diameter of the coil, pitch coil, and coil directions. The results showed that, the heat transfer coefficient increases when the saturation temperature decreases, the diameter of pipe decreases, the e helical-coil diameter decreases, and the coil pitch increases.

Shirgire and Kumar [33] compared between helical coil and straight tube heat exchangers through studying the effect of the heat exchanger geometry on heat transfer and on the heat exchanger effectiveness. The results revealed that the overall heat transfer coefficient increases and the effeteness of the heat exchangers decreases with increasing the flowing fluid velocity.

Jaber et al. [34] used three shells and helically coils heat exchangers of different pitches to conduct experimental work to evaluate and compare the heat transfer coefficients for parallel and counter flow. The results showed that, heat transfer coefficient increases with increasing the pitch of the helical coil.

Gurav [35] conducted comparative study of heat transfer in helical coil and straight tube heat exchangers. From the results, it was reported that increasing the curvature ratio causes the increase of the heat transfer coefficient. The heat transfer coefficient for helical tube-in-tube arrangement was approximately 10 to 20 times of the straight tube's arrangement.

Ankanna and Reddy [36] performed parametric analysis for straight tube and helical coil heat exchangers. Both the tubes were tested for parallel and counter flow configurations. The effects of various parameters on the effectiveness were observed. For helical counter flow arrangement, the overall heat transfer obtained was less than parallel flow arrangement. It was found that the effectiveness of helical coil heat exchanger was always more than that of straight tube and higher values were observed for counter flow configuration.

Naphon [37] conducted experiments on helical coil heat exchanger consisting of a shell and helical coil of 30 turns with and without fins for calculating and comparing heat transfer and coils performances.

N. Ghorbani et al. [38-39] experimentally studied the convection heat transfer in helical coil tube at different diameters, pitches of coil and mass flow rates. The results showed that, when the mass flow rate increases the effectiveness of the heat exchanger decreases.

Bandpy et al. [40] experimentally studied the effect of the coil pitch on heat transfer from the coil to the shell in helical coil-shell heat exchanger. The tests were conducted for laminar as well as turbulent regime at different flow velocities and temperatures. The results showed that with increasing the coil pitch for the same inside tube diameter, the heat transfer coefficient was found to increase.

Nada and Alshaer [41, 42] developed correlations for Nusselt number and pressure drop for double tubes and multi tubes in tube helical coils, respectively. Different numerical investigations were recently conducted for multi tubes in tube helical coil heat exchangers to study the effect of the mass flow rates, number of tubes, heat-flux and temperatures on the flow regime and heat transfer coefficient [43, 44].

Gore et al. [45] experimentally compared the performance of the straight tube and helical coil heat exchangers. The results were compared with the help of verified CFD model to infer that helical coil gives superior heat transfer rates compared with the straight tube coil.

Shriyan [46] conducted a review on heat transfer characteristics of fluids in curved and straight tubes for various parameters and under different experimental conditions. It was reported that, surface geometry modifications like bending of straight tubes into curved coils are effective and efficient method for heat transfer enhancement.

Karmankar, [47] used helical coil tube to promote heat transfer coefficient. It was reported that heat transfer in a coiled tube is higher than that in a straight tube because of the contribution of the secondary vortices formed by the centrifugal force.

Gavade et al. [48] conducted experimental comparative analysis between a helical coil and a straight tube heat exchanger for parallel and counter flow. Based on the results obtained, it was concluded that the helical tube has a larger surface contact area that allows the fluid to contact surface for a longer period and this improves the heat transfer compared to the straight tube.

Sreejith et al. [49] also conducted comparative experimental analysis between helical and straight heat exchanger for parallel flow and counter flow arrangements. It was also reported that the overall heat-transfer coefficient and the heat exchanger effectiveness are relatively high compared to the straight tube heat exchanger.

Khairul et al. [50] conducted thermodynamic analysis of enhanced fluid flow in helical coil heat exchanger using different nanofluids (CuO, Al2O3 and ZnO with water). Results of heat transfer and entropy generation rates were found to depend on nanofluid concentrations and flow rates.

Ehsan et al. [51] experimentally studied the effect of different operating parameters of helical coils such as coil pitch, coil diameter, number of turns, and mass flow rater on Nusselt number. The work was done on seventeen helical coils to study the natural convection heat transfer between the coils and the water tank in which the coils were submerged. Nada et al. [52-53] experimentally investigated the performance of the shell and finned and un-finned helical coils heat exchanger to study shell diameter effect and the existence of external fins on the heat transfer process. Four shells of different diameters were tested in this work for finned and un-finned coils.

Heat and mass transfer characteristics of water vapor condensation on/in helical coils were also extensively studied by many researchers. Most of the researches were devoted to determine the condensation heat transfer coefficient in helical coil at different operating parameter by using analytical or experimental investigation [54-56].

Gupta et al. [54] carried out an experimental study of heat transfer and pressure drop characteristics of R-134a condensing inside a helical coil tube in horizontal position with the counter flow of the water in the shell. The effects of the mass flux, amount of vapor, and the evaporative temperature on Nusselt number and pressure losses were studied.

Ali and Gulhane [55] conducted experiments on condensation heat transfer in a vertical helical coil of 175 mm coil diameter under variable mass flux conditions. The results were used to evaluate coefficient of heat transfer and compare it with the correlations obtained in previous works in the literature.

Yu et al. [56] studied the heat transfer during the condensation of hydrocarbon propane refrigerants in a helical coil. The investigation was carried out at different operating conditions as mass flux and saturated temperature. The effects of flow parameters were analyzed. The result revealed the increase of the heat transfer coefficient with the increase of the mass flow rate and vapour quality. Several researches have been conducted experimental and analytical investigations to explore the effects of the tilt angle and the surface orientation on the heat transfer coefficient by condensation [57-65].

Saffari et al. [57] theoretically and numerically studied stratified condensation heat transfer mechanism in an inclined tube. The heat transfer coefficient for 30° inclination angle was high in comparison with 60° and 90° inclination angles.

Waiker et al. [58] implemented a study to determine the effect of the pipe inclination angle on steam condensation rate in case of steam flow in pipes. The investigation was done analytically and experimentally for vertical and horizontal tubes.

Mozafari et al. [59] investigated the effects of refrigerant mass flux, vapor quality and coil inclination angle of on the condensation and pressure drop processes of R 600a flows in the helical coil oriented at different angles: zero, 30°, 60° and 90°. The study was done at coil diameter, coil pitch, and number of turns of 305 mm, 35 mm, 210 mm and 6, respectively. The results showed that at any inclination angle, when the mass flow rate and vapor quality increase the heat transfer coefficient and pressure drop of condensation process increase.

Ewim et al. [60] experimentally studied condensation of R134a in tube at different parameters such as mass flux, saturation temperature, wall tube temperatures and tube inclination angle to find the effect of these parameters on the condensation heat transfer coefficient.

Abadi et al, [61, 62] presented numerical investigations of the effects of inclination angle on condensation heat transfer coefficients and pressure drops of vapor condensing inside tube. The work was done at different saturation temperatures and different inclination angles in the range -60 to +60°. The results showed that when the saturation temperature increases the pressure drop and heat transfer coefficient decrease.

William et al. [63] presented an experimental study for steam condensation in inclined flatted tubes used in air-cooled condenser. The inclination angle was varying from horizontal 0° to 75°. The overall heat transfer coefficient was found to be increased by increasing the inclination angle of the tube.

Nada and Hussein [64] conducted an experimental work to find a correlation of heat transfer coefficient for steam condensation outside inclined tubes tube in terms of the inclination angle. An experimental and numerical investigation of the effect of the tube curvature on the condensation heat transfer and flow regime for vapor condensing inside horizontal helically coiled tubes was conducted by Naphon and Suwgrai [65]. Three different curvature ratios were tested at constant wall coil temperature. The results were compared between straight tube and helical coil.

The above literature shows that although heat transfer process in helical coil heat exchanger had been extensively studied by many researchers; heat and mass transfer during humidification of moist air on helical coils has not been extensively studies. Moreover, the enhancement of the heat transfer and dehumidification process of moist air on helical coils using extended fins on coil surfaces has not been studied.

2.3. Gap in Literature Review and aim of the present study

It is evident from literature review that there is no comprehensive study for a hybrid air conditioning system using desiccant wheel and HDH water desalination system. Moreover, enhancing the productivity of HDH system using helical dehumidifying coils with ripped fins and the characteristics of water condensation/dehumidification on helical coils during the air dehumidification on the coil was not addressed in the literature. The effects of coil orientations and the existence of fins on the coil outer surface on the water dehumidification rate for different inlet air flow rates, temperatures and humidity are not exist in the literature. The aim of the present work is:

1. Conduct analytical study of proposed efficient hybrid systems that integrate the technologies of desiccant dehumidification, evaporative cooling, and freshwater production with the air conditioning system of low-humidity applications. Thermodynamics analysis of the systems is conducted and the systems of equations are analytically solved and analyzed using EES software. Parametric studies are conducted to investigate the effects of the different operating parameters on the performance of the system. The power savings and the fresh water productions of the different proposed systems are evaluated and compared to select the optimum system configuration.

2. Conduct an experimental investigation of the performance and characteristics of HDH system using honeycomb paced bed for air humidification and helical coils of different surface geometries and orientation for air dehumidification. Heat transfer and vapor condensation/dehumidification characteristics on the helical coils used for fresh air dehumidification in the HDH were investigated in details. A parametric experimental study of the effects of helical coil orientation and the air inlet conditions on the HDH system and the dehumidifying coils performances and water condensation rate was also conducted. The effects of adding rips/wire fins on the external surface of the dehumidifying coil was also investigated by testing two similar coils; one without fins and the second with fins. The study aims to find the geometric, orientation and operating conditions which gives the best performance of the HDH system and dehumidifying helical coils.

Chapter 3: MATHEMATICAL MODEL OF PROPOSED SYSTEMS

3.1. Introduction

The air conditioning systems of low humidity applications consume a huge amount of energy to maintain the required low temperature and humidity needed by the application. A large part of the energy is consumed for the removal of moisture and maintaining the required low humidity and temperature. Desiccant dehumidification is using desiccant wheel is typically used in this system to remove the moisture from the processing air before it is mechanically refrigerated. In the desiccant wheel, the process air to be dehumidified passes through the adsorption section of the wheel where the water vapor in the process air is directly removed from the air and holds in the wheel while rotating. As the desiccant section saturated with water vapor passes through the regeneration sector, the water vapor is transferred to a heated regenerative airstream, which is exhausted to the outside. In the present chapter, proposed efficient systems that integrate the technologies of desiccant dehumidification, evaporative cooling, and freshwater production with the air conditioning system of low-humidity applications are presented. Thermodynamics analysis of the systems is conducted and the systems of equations are analytically solved and analyzed using EES software. Parametric studies are conducted to investigate the effects of the different operating parameters on the performance of the system. The power savings and the fresh water productions of the different proposed systems are evaluated and compared to select the optimum system configuration.

3.2. System Description

Air conditioning, desiccant, and HDH hybrid systems are proposed for low humidity application for energy saving and freshwater production. Three systems are proposed in the present study. The first system (named as system1) is a basic air conditioning system of low-humidity applications that can also be utilized for fresh water production. The other two systems, system 2 and system 3, are a modification of basic system with the integration of heat recovery in the system downstream (system 2) and upstream (system 3) the desiccant wheel. The schematic diagrams of the three systems are shown in Fig. 3.1. For the sake of comparison, the three systems are assumed to serve a space of a 100 TR cooling capacity a room sensible heat factor (RSHF) of 0.7 and are required to be maintained at 22 ˚C temperature and 30% relative humidity. The systems consist of air-cooled chiller unit to serve the cooling coil to cool the air, desiccant wheel to keep the low humidity in the served space, heating coil to produce the hot air required to the regeneration process of the desiccant wheel, and HDH unit consists of humidifier and water-cooling coil for fresh water production from the humid hot air that exit the desiccant wheel. In systems 2 and 3 a heat recover is used for energy recovery by cooling the process air by the cold air exhausted from the air condition space. The thermodynamic processes that occur on the air in the three systems are on the Psychometric chart in Fig. 3.2. Air at ambient condition (O) is mixed with return air (R) to obtain air at state (1). The mixed air is then passed on the desiccant wheel where is heated and dehumidified to obtain air at state (2). The air outlet from desiccant wheel passes through air-cooled chiller unit where it is cooled and water vapor condenses on the cooling coil surface producing fresh water (m°_{w1}) and obtain air at state (S). The air at state (S) which known as air supplied to conditioned space. To remove the moisture captured in the desiccant rotor, the smaller air volume called reactivation air at ambient condition (3) is heated up in a heating coil before entering the rotor (4). The outlet air from the desiccant wheel at state (5) passes through humidifier at constant wet bulb temperature for increasing the moisture content in reactivation air to obtain air at state (6). The air inlet water cooling coil has a high amount of water vapor then this moisture will be condensed on the coil surface producing fresh water (m°_{w2}) and obtain air at state (7). The condensate water from air cooling coil mixing with condensate water from water cooling coil before passes through a chemical water treatment unit where it is treated to be fresh water (m°_{w}). The proposed systems 2 using heat recovery locate after desiccant wheel where process air outlet from desiccant wheel in state (2) inlet to heat recovery for decrease the process air temperature to obtain air at state (2') before the inlet to air cooling coil. The proposed systems 3 by using heat recovery locate before mixing section where inlet ambient air passes into heat recovery to obtain air at state (O') before mixed with return air.

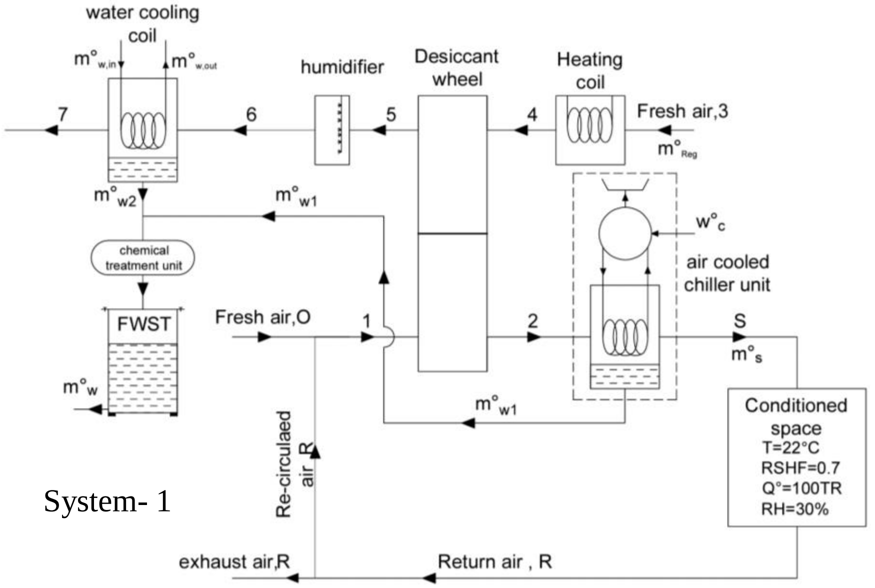

System- 1

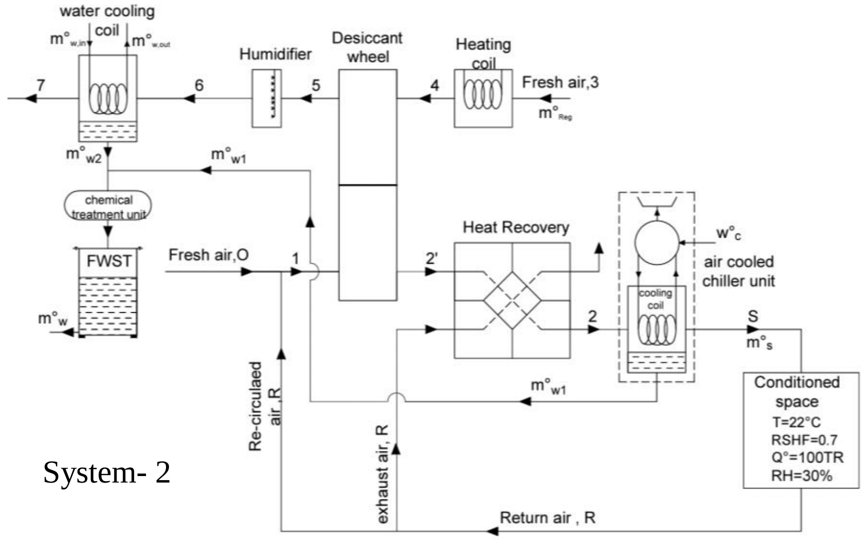

System- 2

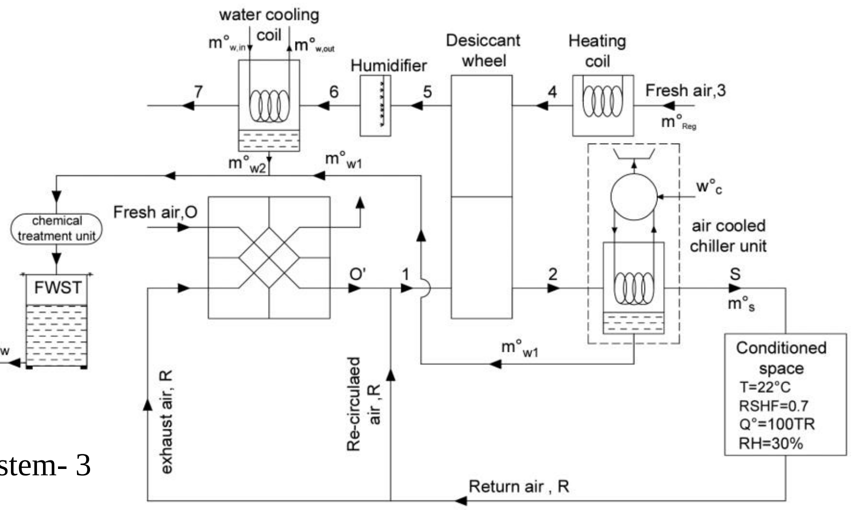

System- 3

Fig. 3. 1 Schematic diagram of the proposed systems

System- 1

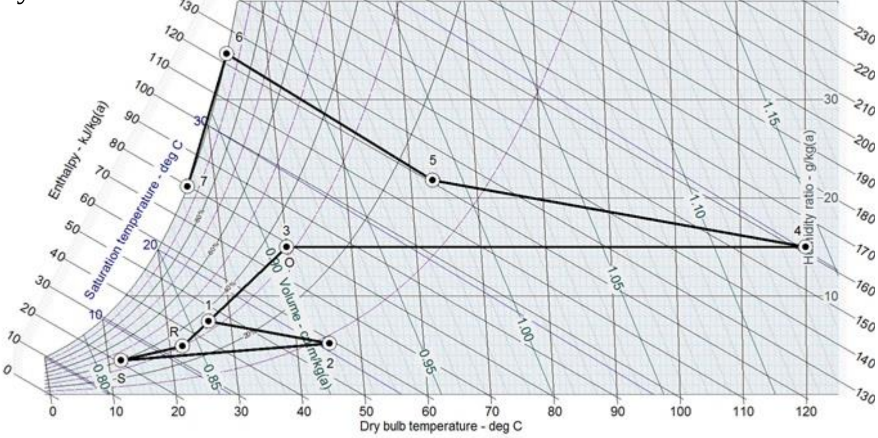

System- 2

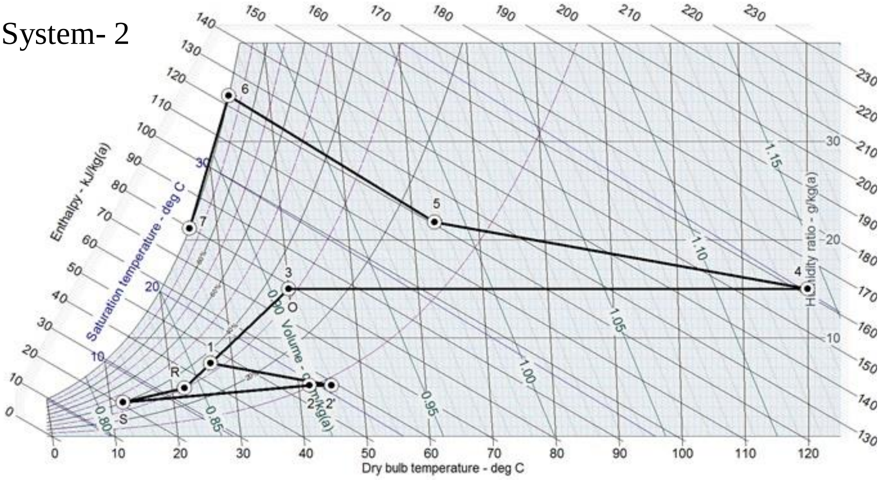

System- 3

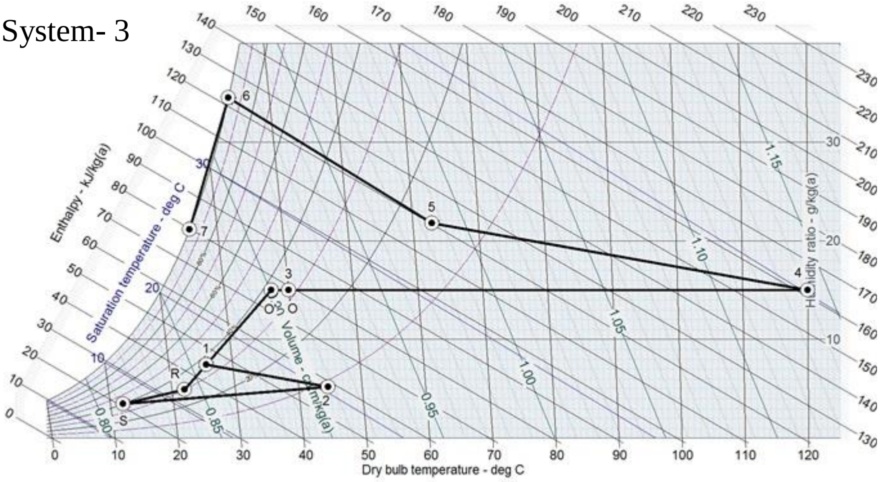

Fig. 3. 2 Psychrometric chart of systems 1, 2 and 3.

3.3. Thermodynamic analysis and mathematical modeling

The governing equations based on energy and mass balance are derived for each of the system components and solved numerically by developing a mathematical model to simulate the systems in equations using EES (Engineering Equation Solver, commercial version 6.883-3D) software see Appendix A for EES formatted equation. The model proposed is based on the following assumptions:

- Thermal/regeneration efficiencies of DW are taken as 20 % [20].
- Heat recovery efficiency is taken 60 % as per typical values of suppliers [66].
- Air and water leakages in the system are neglected.
- Reactivation air ratio is taken 0.33 which depend on the type of DW.
- The air leaves the humidifier at a wet-bulb temperature equal to the leaving water temperature.
- The air humidification in the humidifier occurs until saturation of air
- The dehumidification process in the water coil occurs on the saturation curve.
- Any auxiliary power in the system is negligible as compared to the AC power [67].
- The indoor design conditioned of the production hall is taken to be T_R = 22°C and RH_R = 30% as per the practical pharmaceutical applications.
- The supply cooling air to the production hall is at 12 °C.

- The cooling capacity and the room sensible heat factor (RSHF) are 100 TR and 0.7, respectively.

The amount of water condensate, cooling coil capacity, process and reactivation air flow rates are obtained from the thermodynamic analysis of mixing section, air- and water-cooling coil, conditioned space, and desiccant wheel, as follows:

$$m^{\circ}_{w1} = m^{\circ}_{s} (\omega_2 - \omega_s) \quad (3.1)$$

$$m^{\circ}_{w2} = m^{\circ}_{Reg} (\omega_6 - \omega_7) \quad (3.2)$$

$$m^{\circ}_{w} = m^{\circ}_{w1} + m^{\circ}_{w2} \quad (3.3)$$

$$m^{\circ}_{s} = Q^{\circ}_{R} / (h_R - h_s) \quad (3.4)$$

$$RR = m^{\circ}_{Reg} / m^{\circ}_{s} \quad (3.5)$$

$$Q^{\circ}_{cc} = m^{\circ}_{s} (h_2 - h_s) \quad (3.6)$$

The specific humilities and enthalpies in Eq. (3.1) to Eq. (3.6) are obtained from air properties and desiccant wheel relations as follows:

$$\frac{m^{\circ}_{o}}{m^{\circ}_{s}} = \frac{T_R - T_1}{T_1 - T_o} \quad (3.7)$$

$$\varepsilon_{Dw1} = \frac{T_2 - T_1}{T_4 - T_1} \quad (3.8)$$

$$\varepsilon_{Dw2} = \frac{m^{\circ}_{s}(\omega_1 - \omega_2)h_{fg}}{m^{\circ}_{Reg}(h_4 - h_3)} \quad (3.9)$$

$$\varepsilon_{HR} = \frac{m^{\circ}_{s}(T_{o.HR} - T_{i,HR})}{m^{\circ}_{o}(T_{Room} - T_{i,HR})} \quad (3.10)$$

$$T_5 = T_4 - \left(\frac{T_2 - T_1}{RR}\right) \quad (3.11)$$

$$\omega_5 = \omega_4 + \left(\frac{\omega_1 - \omega_2}{RR}\right) \quad (3.12)$$

The COP of the air conditioning system is calculated from:

$$COP = Q^{\circ}_{cc} / W^{\circ}_{C} \quad (3.13)$$

It is well known that the COP (coefficient of performance) of the air-cooled chillers is a function of the ambient air temperature. The COP correlation in terms of the outdoor temperature was previously expressed by [67]:

$$COP = 11.1 - 0.4T_o + 7.2\times10^{-3}\, T_o^2 - 5.18\times10^{-5}\, T_o^3 \quad (3.14)$$

The total power consumed in the system and the power saving in system 2 and system 3 due to incorporating the energy recovery system can be found from

$$E^{\circ} = W^{\circ}_{C} + E^{\circ}_{pump} \quad (3.15)$$

$$\text{Power saving\%} = \frac{E^{\circ}_{1} - E^{\circ}_{PS\ 2,3}}{E^{\circ}_{1}} 100\% \quad (3.16)$$

The above systems of equations are solved using EES software to find the water production rate, air condition cooling capacity, power consumption and percentage of power and water saving as a function of the operating and ambient conditions. The operating and ambient conditions are assumed to vary in the following given ranges:

- Fresh air ratio $\dot{m}_o / \dot{m}_s$: 0-1
- Ambient air temperature T_o: 30-50 ˚C
- Ambient air specific humidity ω_o: 0.01-0.03 Kg_v / Kg_a.
- Basic Conditions: $\dot{m}_o / \dot{m}_s = 0.25$, $T_o = 40$˚C, $\omega_o = 0.015$ Kg_v / Kg_a, RSHF= 0.7, and $T_s = 12$ ˚C

3.4. Results and Discussions

3.4.1 Effects of outdoor air ratio on the system performances

Fig. 3.3 shows the variation of m°_{w}, E°, Q°_{cc} and percentage of power saving with the outdoor air ratio ($m^{\circ}_{o} / m^{\circ}_{s}$).

Fig. 3.3-a shows that for all the studied systems, the rate of the obtained water from the systems m°_{w} increases with the increase of the outdoor air ratio for the entire ranges of the studied parameters. This may be attributed to the following reasons, **(a)** increasing the fresh air ratio makes state (1) on the Psychometric chart (see Fig. 3.2, system 1) moves along the line O-R to be closer to state O. Accordingly, the humidity of air at the inlet of the cooling coil rises as a result of moving state (2) upwards on the Psychometric chart. This increases the condensation rate on the cooling coil (m°_{w1}) as per Eq. (3.1), and (b) the increase of water vapor removed by the desiccant wheel $(\omega_2 - \omega_s)$ which leads to the increase of the humidity of the reactivation at desiccant wheels exit (state 5) and consequently rising the reactivation air humidity at the water cooling coil inlet (state 6) leading to more vapor condensation and water rate m°_{w2} (see Eq. 3.2).

It can be noted from Fig. 3.3-a that the rate of water obtained for system-1 and system-2 increase with the increase of the outdoor air ratio by the same ratio and this makes the trends of the two lines coincide with each other. However, for system-3, the rate of increase in the water rate is smaller than those of systems-1 and 2, and this is due to the decrease of $(\omega_2 - \omega_s)$ of system (3) as a result of the decrease of (ω_2) due to the free cooling of the outdoor air in the energy recovery.

Fig. 3.3-b shows that the cooling capacity of the air conditioning system $\dot{Q}_{cc}$ increases with increasing the outdoor air ratio for the three systems. The reason of that is the increase of the temperature and humidity of the air (i.e. the increase of the air enthalpy) at cooling coil inlet with the increase of the outdoor air ratio (refer to Eq. (3.6)). Fig. 3.3-b also shows that using the heat recovery in the system reduces the coil cooling capacity where the coil capacity of systems-2 and 3 are lower than that of system-1 at any outdoor air ratio. This is attributed to the free cooling of the fresh air by cooling recovery from the exhaust air. Fig. 3-b also reveals that the cooling capacity of system-2 is lower than that of system-3 for any outdoor air ratio. This proves that locating the heat recovery after the desiccant wheel as in system-2 is more effective than locating it at the entrance of the fresh air intake as in case of system-3.

Fig. 3.3-c shows that the variation of the total electrical power consumption $\dot{E}$ with the fresh air has the same trend of the variation of the cooling coil capacity. This is attributed to the linear relation between the electric power consumption and the cooling coil capacity as given by Eq. (3.13) to Eq. (3.15).

Fig. 3.3-d gives the dependence of the power saving due to using heat recovery in system-2 and system-3 on the fresh air ratio. The Fig.3.3-d shows the increase in the percentage of the power saving with the increase of the outdoor air ratio. The reason for this is the decrease of the hot stream air enthalpy at the inlet to the heat recovery and the increase of the free cooling that can be recovered. Fig. 3.3-d also shows that the power saving of system-2 is always higher than that of system-3 for any outdoor air ratio indicating that locating the heat recovery after the desiccant wheel increases its capacity for the cooling recovery.

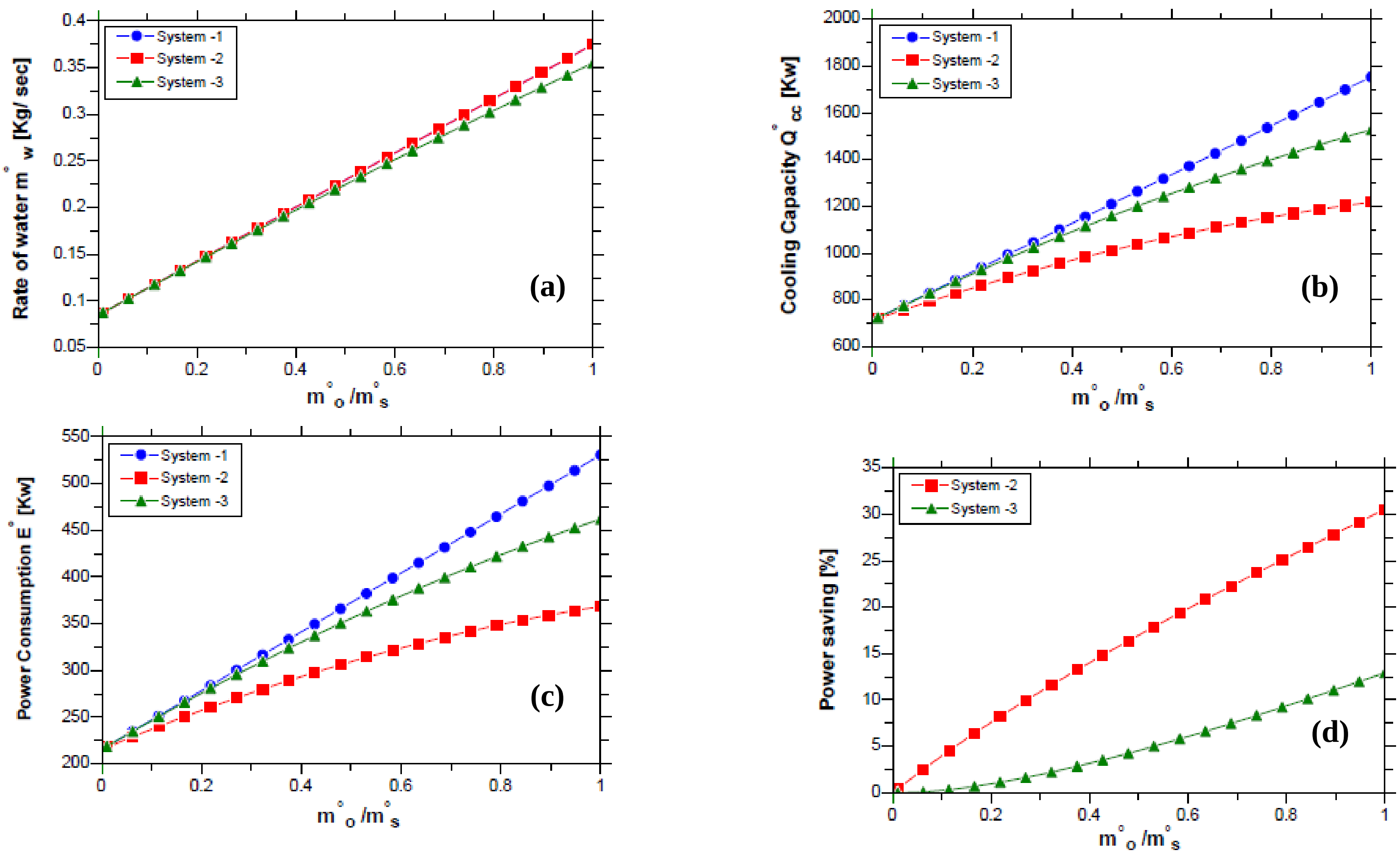

Fig. 3. 3 Effect of outdoor air ratio on (a) m°_{w}, (b) Q°_{cc}, (c) E°, and (d) % power saving.

3.4.2 Effects of ambient temperature on the system performances

Fig. 3.4 gives the variation of m°_w, E°, $Q^\circ cc$ and power saving with the ambient air temperature T_o.

Fig. 3.4-a illustrates the decrease of m°_w with the increase of the ambient air temperature for the three systems. The reason of that is the decrease of the process air humidity at the entrance of the cooling coil (ω_2) and the increase of the wet bulb temperature of the outdoor air with increasing its dry blub temperature leading to the increase of ω_7. Decreasing ω_2 and increasing ω_7 cause the decrease of the water production rates as given by Eq. (3.1) to Eq. (3-3), respectively.

Fig. 3.4-b shows the increase of Q°_{cc} with the increase of T_o which may be attributed to the increase of the enthalpy of the air at the inlet of the cooling coil (h_2) as indicated by the Psychometric charts that are shown in Fig. 3.2. Increasing the cooling coil inlet air enthalpy causes the increase of the cooling coil capacity as per Eq. 3.6. Fig. 3.4-b shows that the coil cooling capacity of system 2 is lower than that of systems 1 and 3 and the that of system 3 is lower than that of system-1.

Fig. 3.4-c shows the variation E° with the ambient air temperature T_o. As shown in the Figure, E° dramatically increases with increasing To. The reason of that is the increase of the cooling coil capacity Q°_{cc}, and the decrease of the COP of the air-cooled chiller with increasing the outdoor air temperature (see Eq. (3.13) to Eq. (3.15)).

Fig. 3.4-d shows the variation of power saving with ambient air temperature. As shown in the Figure, the power saving in system-2 and 3 are approximately constants with T_o. This indicates that the energy consumptions of the three systems increase with the same rates with increasing the outdoor air temperature. This is confirmed by the same slope of the three lines in Fig. 3.4-c. Fig. 3.4-d, confirms that system-2 has higher power saving compared with system-3 for all outdoor air temperature and outdoor air ratio.

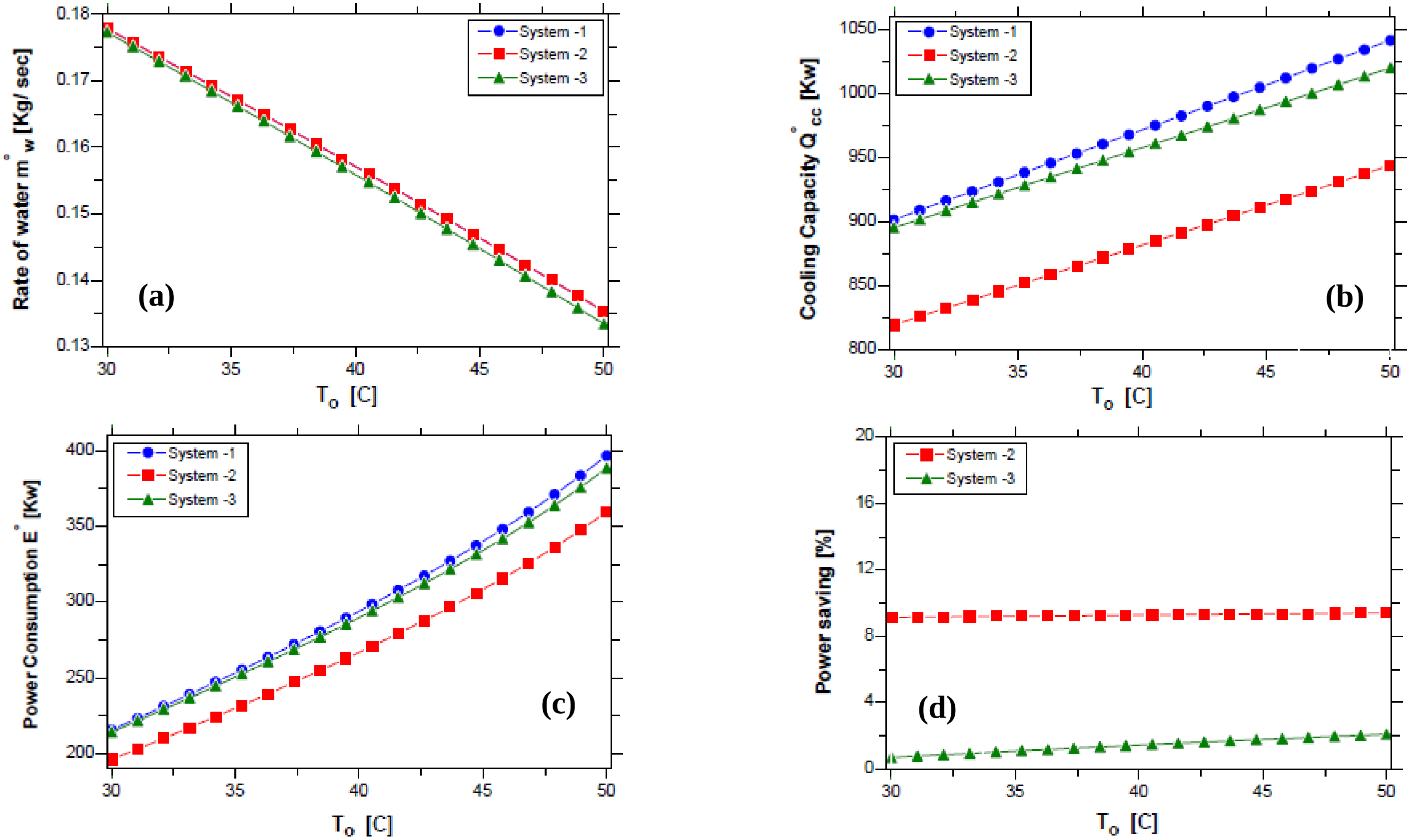

Fig. 3. 4 Effect of ambient air temperature on (a) m°_{w}, (b) Q°_{cc}, (c) E°, and (d) % power saving.

3.4.3 Effects of ambient specific humidity ratio

Fig. 3.5 shows the variation of m°_{w}, E°, Q°_{cc} and the percentage of power saving against ambient specific humidity (ω_o).

Fig. 3.5-a shows the increase of the water production rate with increasing the specific humidity of the outdoor air for the three systems. The reasons for that are the increase both of the humidity of the process air at the entrance of the cooling coil (ω_2) and the air at the inlet of the water-cooled dehumidifier ω_2. This leads to an increase in the water production rate (see Eq. (3.1) to Eq. (3-3)).

Fig. 3.5-b shows the increase of Q°_{cc} with increasing the ambient humidity ω_o. The reason of that is the increase of the enthalpy of the air (latent part) at the inlet of the cooling coil (h_2) with increasing the outdoor specific humidity as shown on the Psychometric charts given in Fig. 3.2. Increasing the enthalpy of air that enters the cooling coil leads to the increase of the cooling capacity as given by Eq. 3.6.

Fig. 3.5-c shows the increase of E° with increasing ω_o. The reason for that is the increase of the compressor power due to the increase of Q°_{cc}.

Fig. 3.5-d shows that the power saving in system-2 and 3 slightly decrease with increasing the specific humidity of the ambient air ωo. The Fig. also shows that system-2 has higher power saving percentage comparable with system-3.

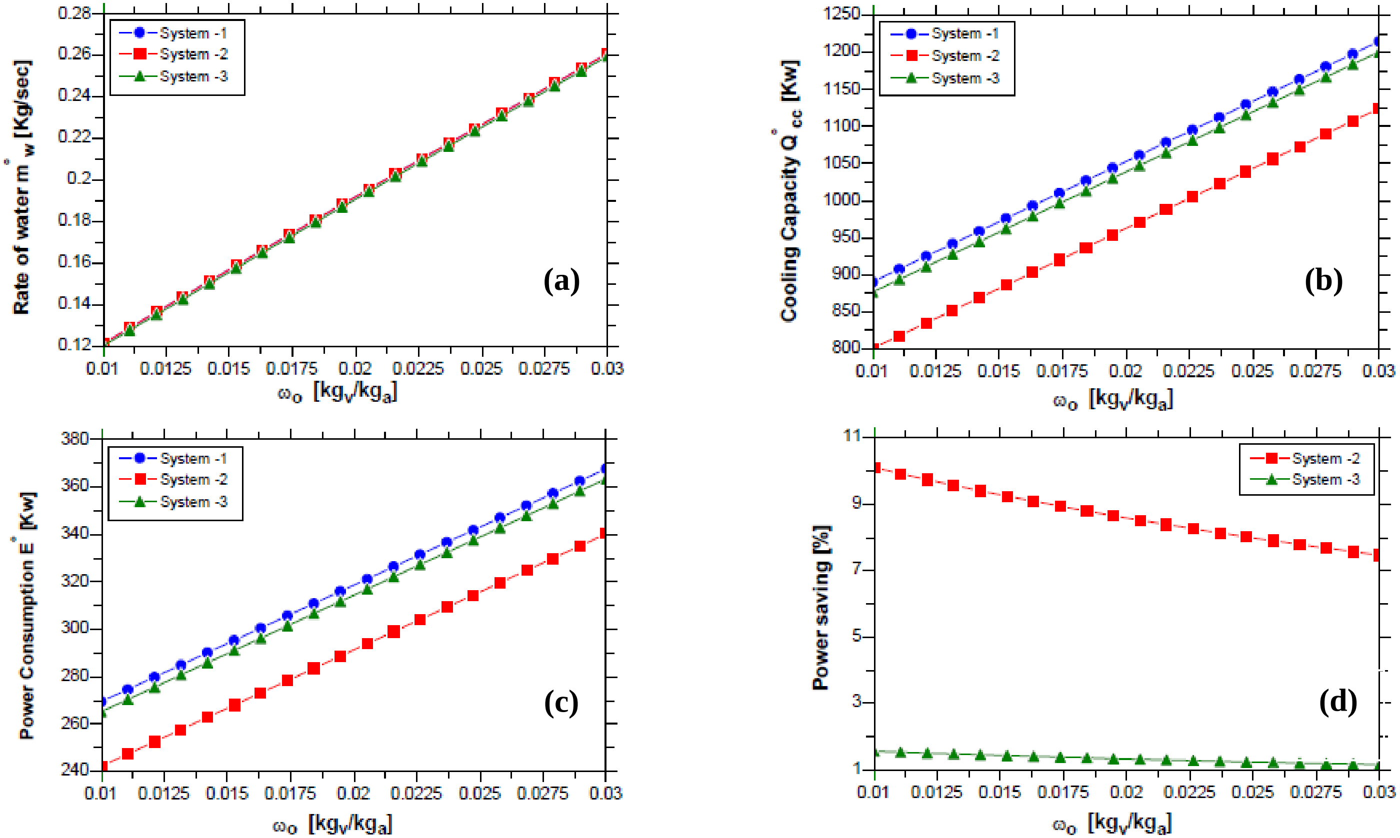

Fig. 3. 5 Effect of ambient specific humidity on (a) m°_{w}, (b) Q°_{cc}, (c) E°, and (d) % power saving.

3.5. Systems comparison and cost analysis

The total saving in cost TSC ($/h) due to power saving and fresh-water productions of systems-2 and 3 can be estimated from:

$$TSC=\dot{m}_w(m^3/hr)\times \text{water unit rate}(\$/m^3)+PS\times ER(\$/kWh) \quad \text{Eq [3.17]}$$

Typical values of potable water and electricity unit rate 2.5 $\$/m^3$ and 0.02 $/ kWh in Gulf cities [16] are considered in this study. The TSC for systems -2 and 3 at different operating parameters are shown in Fig. 3.6.

Fig. 3.6-a shows the increase of TSC of systems-2 with the increase in the outdoor air ratio. The reason for that is clear from Fig. 3.3 where both of the fresh water production rate and the power saving for system-2 and 3 increases with the increase of fresh air ratio.

Fig. 3.6-b shows that for systems 2 and 3, the total saving in costs slightly decreases with the increase of the outdoor temperature. The results show that the trend is the same at all operating parameters. Decreasing TSC with the outdoor air temperature reveals that the decrease of the cost saving due to decrease of the fresh water production rate with increasing of the outdoor temperature (see Fig. 3.4-a) overcomes on the increase of the cost saving due to the increase of the power saving with the outdoor temperature (See Fig. 3.4-d).

Fig. 3.6-c shows the increase in the total cost saving with increasing the outdoor air humidity. The reason for that is the increase of the fresh water production rate and the power saving with the increase of the humidity ratio as shown in Fig. 3.5.

Comparing the total cost saving of systems-2 and 3 that are shown in Fig. 3.6 reports that for all the operating parameters the cost saving of system 2 is higher than that of system 3. This can be attributed to that system 2 always has higher water production rate and power saving as compared to system-3 as shown in Fig. 3.3 to Fig. 3.5.

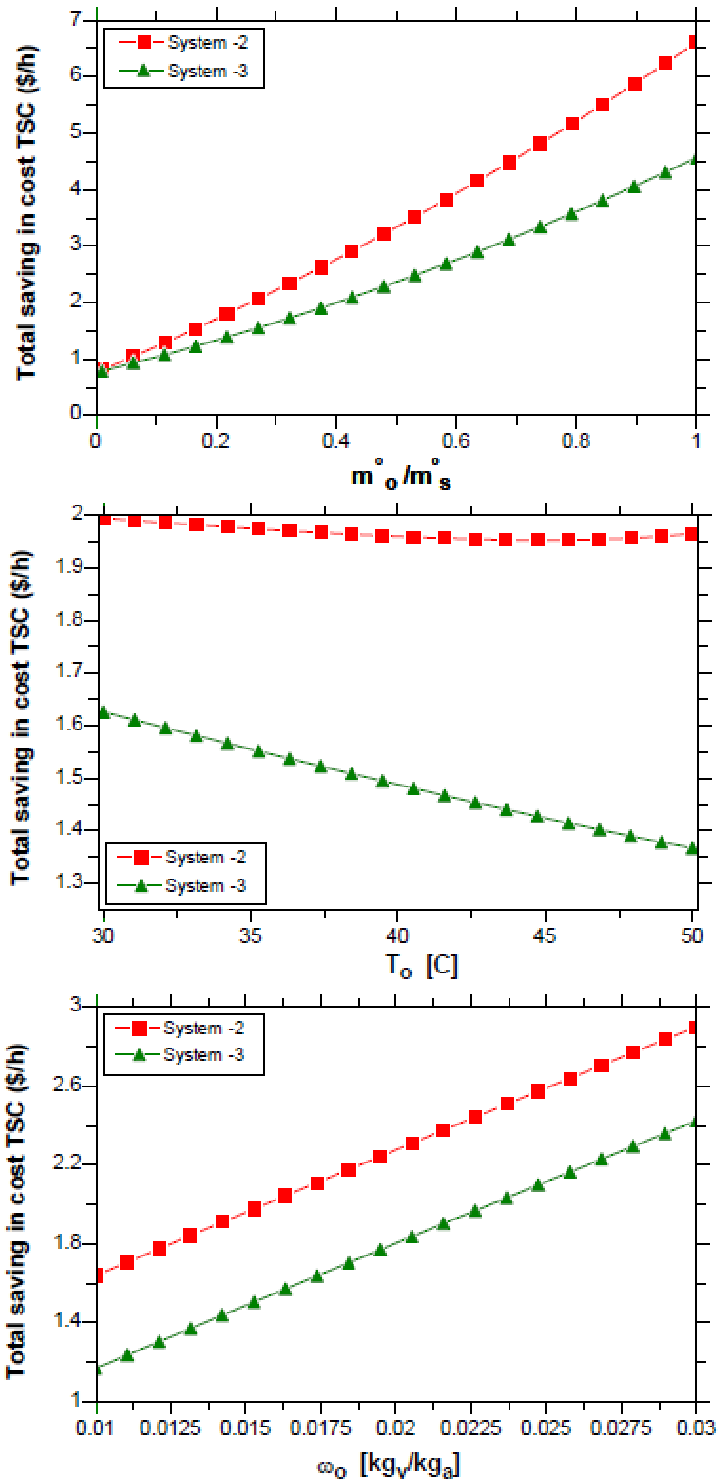

Fig. 3. 6 Effect of the operating parameters on the total cost savings of systems 2, 3

Chapter 4: EXPERIMENTAL FACILITY AND MEASURING INSTRUMENTS

The experimental setup was designed and constructed to study the performance of the humidification dehumidification water desalination system at different operating conditions and geometric design parameters of the dehumidifying coil. The studied operating conditions parameters include air flow rate, air temperature, air humidity, water flow rate to the humidifier and water inlet temperature to the humidifier.

Two geometric design parameters of the dehumidifying coil were tested at different orientations. Two helical coils; one without fins and the other with wire striped fins radially attached to the outer surface of the coil are tested at vertical and horizontal orientations. The setup was constructed to enable carrying out the experiments at different air inlet temperatures, air mass flow rates, water inlet temperatures, and water mass flow rates to the systems. The experiments were conducted at the different operating conditions on the two different helical coils (finned and un-finned coils) at different orientations (vertical and horizontal). The study aims to find the operating conditions, coil type and coil orientation that give maximum performance and water productivity of the system.

4.1. Experimental Setup

The test loop was constructed to (i) study the performance of the humidification dehumidification water desalination system at different operating conditions and geometric design parameters of the dehumidifying coil, and (ii) investigate the heat transfer and vapor condensation characteristics during air dehumidification on the outer surfaces of finned and un-finned helical coils. The apparatus was constructed to enable conducting such investigations at different orientations of the coils and different operating conditions for the air and water.

The test rig is shown schematically in Fig. 4.1. The setup consists of four sections: air duct system, water system for air humidification, condensing unit, and helical coils (test section).

4.1.1 Air Duct System

The air duct section is an open loop section of 3 m length and having a cross section dimension of 390 mm (width) ×335 mm (height). Air flows through the duct using air blower with variable speed. The blower is connected to the duct system through a diverging section as shown in Fig. 4.2. The diverging section is connected in the discharge area of air blower with diverging section had one end of 120×120 mm connected to air blower discharge area and outer end of conical diverging section was 390× 335 mm cross section connected to uniform cross-section part of the air duct, the overall length of this section 620 mm with 11° slope. The air blower (1 Hp, 220-Volt and 50 HZ) is a variable speed fan which connected to varic to control the speed of the fan to required value which needed in experimental work (1 m/sec at 40-Volt and 50 Hz), from experimental work, the amount of air variable by opening and closing air intake area.

The walls of the air duct were thermally insulated using glass wool thermal insulation of thickness 1-inch. The air duct system contains the following sections: electrical heater section, an air mixing section, water humidifier section, and helical coil section.

The air enters to the duct system is firstly passed on the electric heating section where it can be heated to the required temperature. The electrical heater section consists of 3 electric heaters as shown in Fig. 4.3; each one has a power of 3 kW. The heater was made of 3 m of steel bar of a diameter 8.5 mm and formed in the form of serpentine shape that occupies all the cross section of the air duct. The three electrical heaters were placed in the duct in a staggered arrangement to cover the cross-sectional area of the entire duct to assure uniform heating of the air. The electric heaters were connected to a Variac to smoothly control the power input to the heater and accordingly control the temperature of air to the required one.

A mixing section as shown in Fig. 4.4 was placed after the heating section to mix the air and ensure uniform temperature of the air which manufactured from 1 mm thick galvanized sheet steel. It is installed after the electrical heaters section and before water humidifier section. The air is then passing in the humidification section to raise the humidity of the air.

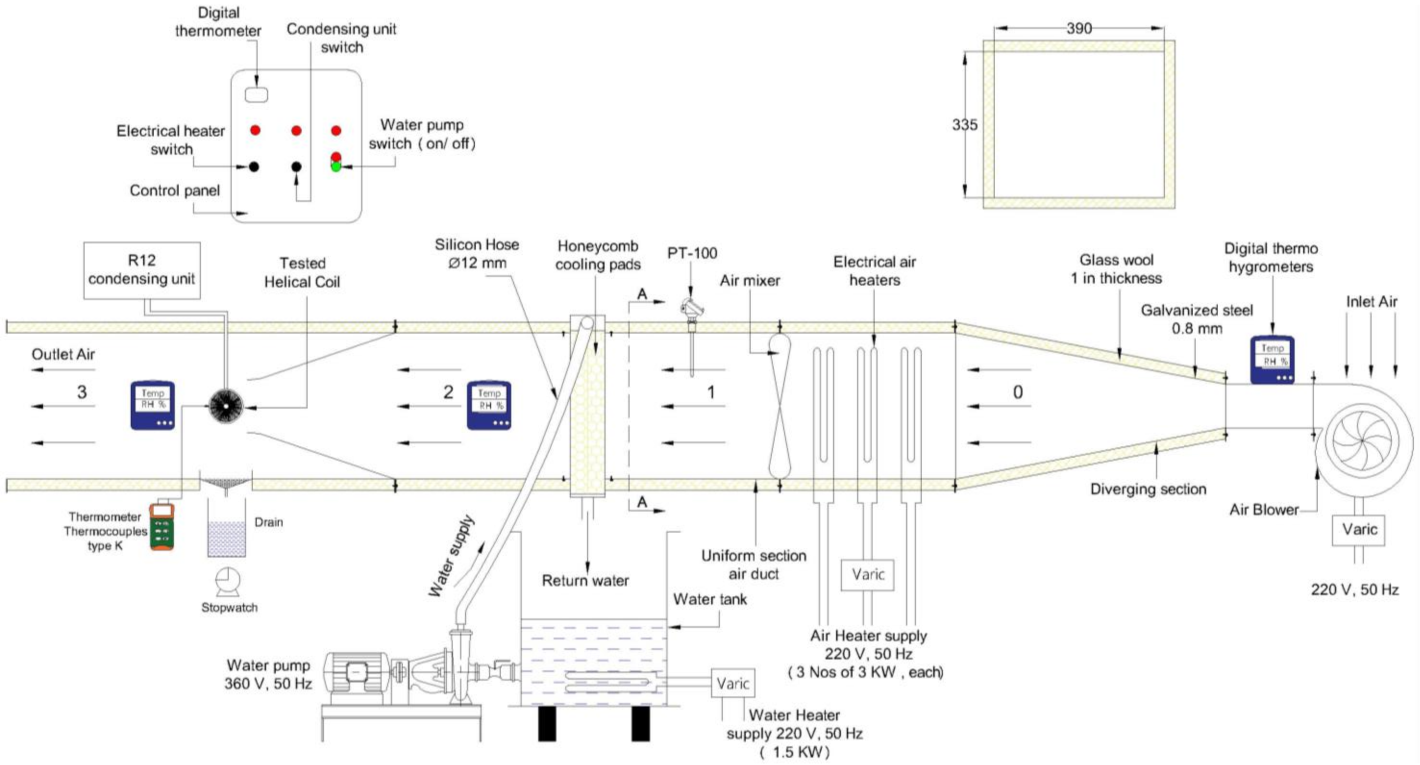

a- Schematic diagram

b- Photograph of the experimental test rig

Fig. 4. 1 Experimental setup

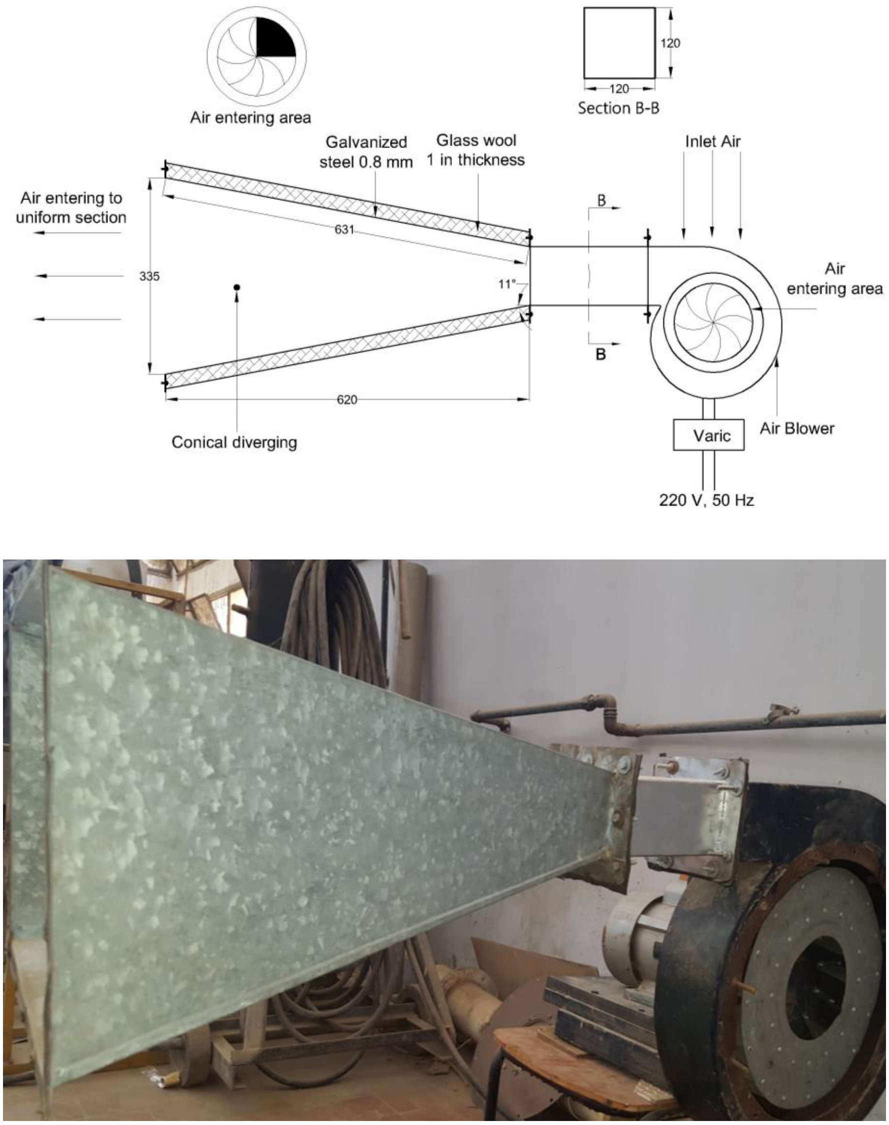

Fig. 4. 2 Air Supply Section

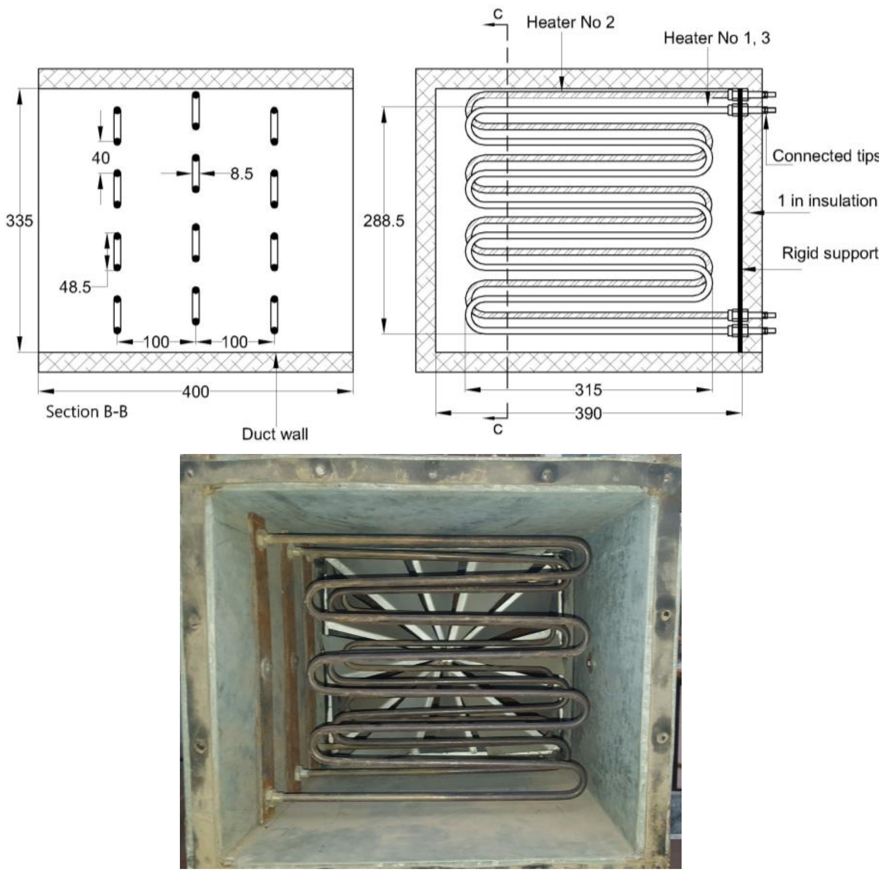

Fig. 4. 3 Full dimensions and arrangements of heaters

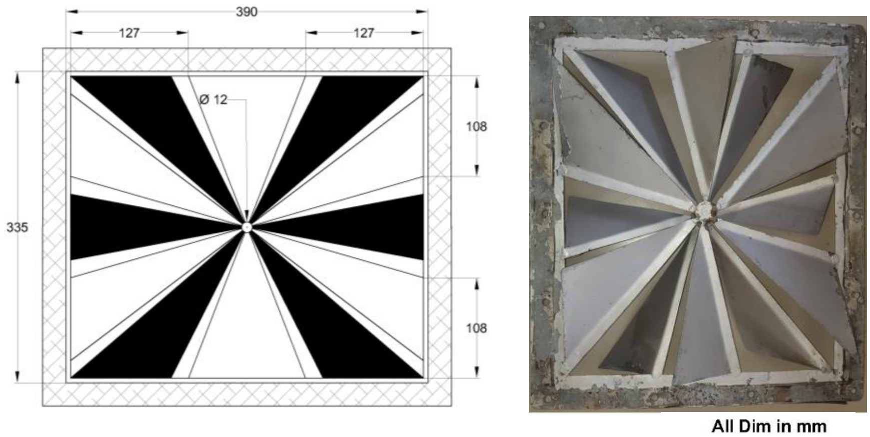

Fig. 4. 4 Air mixer

4.1.2 Air Humidification and Water System

The water humidifier consists of two parts as shown in Fig. 4.5; a honeycomb section and a water distribution section. The honeycomb humidifier pad section consists of two layers of vertical honeycomb pad of thickness 70 mm for increasing the humidity of the air. The cooling pads consists of corrugated sheets of cellulose gathered in an opposite sequence with a beehive “Honeycomb” structure which generates air flow inside the cell.

The specific and geometric dimensions of the honeycomb Pad section are given in Table 4.1 and Fig. 4.7, respectively where appendix B show that the pressure drop across honeycomb cooling pad section at different air flow rate and different water flow rate. The water distribution section is a horizontal stainless-steel distribution water pipe of 1-inch diameter and has 13-holes of 4 mm diameter uniformly distributed across the air duct section to assure uniform feeding of the pad section with water. The honeycomb structure material is uniformly wetted by continuous dripping of water onto the upper edge of the cooling pad and the water flows from top to bottom of the pad.

The humidifier was designed to cover the entire cross-sectional area of the air duct to ensure uniform moisture distribution for air flowing inside the duct. The water system used to supply water to the humidifier section consists of water pump (360-volt, 50 Hz, 10 Lit/min), water mass flow rate flowing through the humidifier was variable by using valve 0.5 inches installed after exiting from the pump to control the quantity of water, water tank (galvanized steel tank of 0.8 mm thickness, 400 mm height × 335 mm width× 390 mm length), electric heater of 1500 Watt connected to a Variac as shown in Fig. 4.6 to heat and control the water to the required temperature and connecting pipes and hose with valves to control the water flow. The air then passes on the helical coil to dehumidify the air by condensing the water vapor on the surface of the coil.

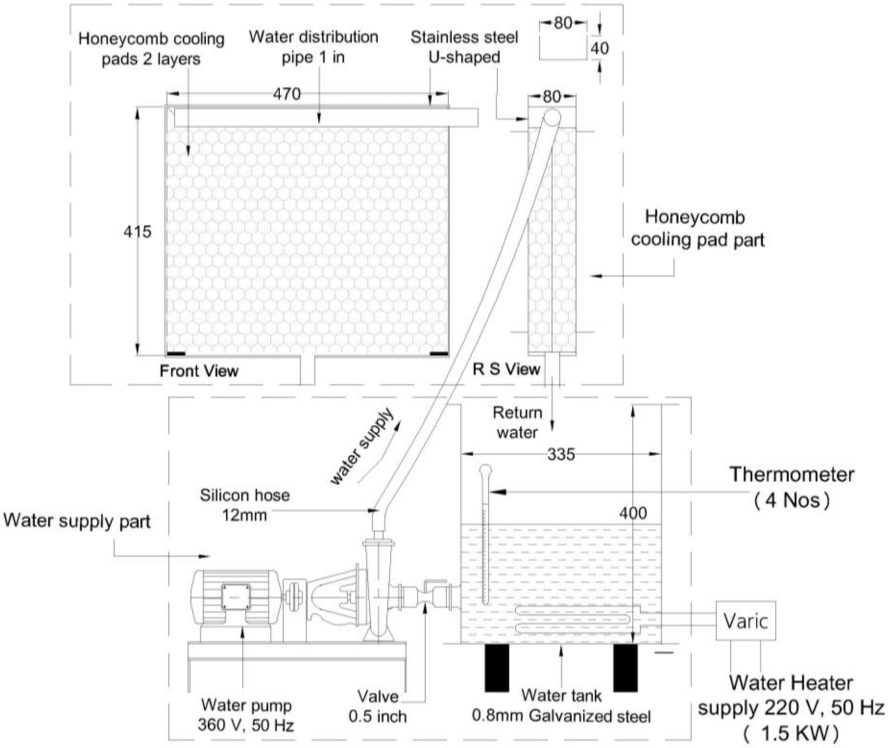

Fig. 4. 5 Water humidifier

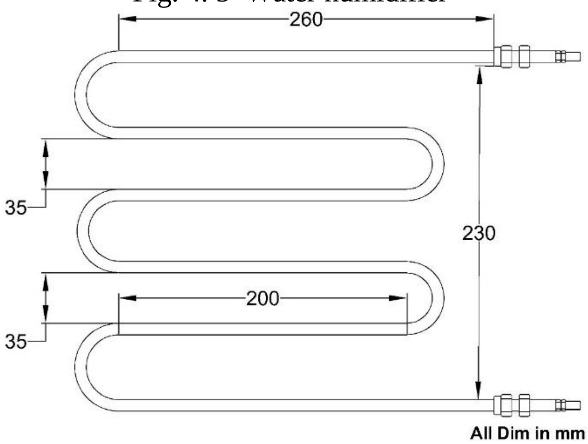

Fig. 4. 6 The electrical heater in a water tank

Table 4.1 Cooling pads specification

<table>
<tr><td>Company</td><td colspan="7">Wadi Group Company in the Arab World, manufacturing cooling pads in Egypt</td></tr>
<tr><td>Cooling Pads material</td><td colspan="7">Corrugated sheets of cellulose.</td></tr>
<tr><td colspan="8">Models and Parameter</td></tr>
<tr><td rowspan="2">Available cooling pads dimensions/Models</td><td>Length “H”</td><td>Width “W”</td><td>Thickness ” D”</td><td>a*</td><td>b*</td><td>Flute size “h”</td><td>Models</td></tr>
<tr><td>90 cm ± 3 mm</td><td>60cm ± 5mm</td><td>3.5cm ±3mm</td><td>45</td><td>45</td><td>3.5, 5, 7 mm</td><td>5090 & 7090</td></tr>
<tr><td>Specification of section used in the current experimental work</td><td>47 cm</td><td>41 cm</td><td>7 cm “two layers”</td><td>45</td><td>45</td><td>7 mm</td><td>7090</td></tr>
</table>

*a, b angle with respect to the air flow direction

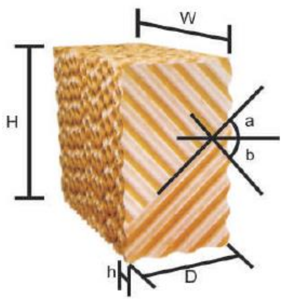

Fig. 4. 7 Honeycomb cooling pads geometric dimensions

4.1.3 Helical Coils Section (Test Section)

DX helical coil with refrigerant R-12 passes inside the helical tube of the coil is used as the test section of the present study. The moist air exits from the humidifier passes on the helical coil to be dehumidified and cooled. The coils are made from thin-aluminum tubes with inner diameter of 8mm and thickness 0.5 mm. The dimensions of the coils as shown in Fig. 4.8-a are: d = 8 mm, Rc = 80 mm, b = 20 mm, and the number of turns = 24. Finned and un-finned coils were tested. The finned coil contains radial ripped fins on the external surface. The fins are in the form of flat aluminum wire strips fins. The wire strips dimensions are 30 mm × 2 mm × 0.5mm (length × width × thickness) with spacing distance between wires of 0.7 mm. Fig. 4.8-b shows the geometric dimensions of the helical coils without fins and with ripped wired fins. The test section was designed to enable placing the helical coil at horizontal or vertical orientations to conduct separate tests were conducted at coil horizontal and vertical orientations.

Un-finned helical coil

Finned-helical coil

a-Photos of tested helical coils

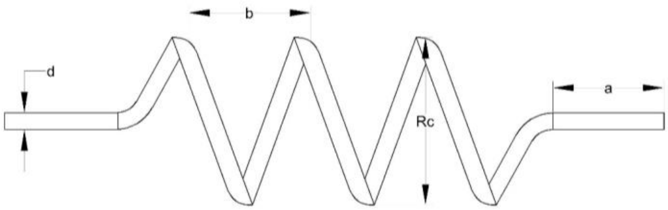

b- Dimensions of helical coil

Fig. 4. 8 Helical coil

4.1.4 Condensing Unit Section

A condensing unit as shown in Fig. 4.9 was used to supply refrigerant R-12 to the helical coil to remove the coil cooling load and maintain the outside surface temperature of the coils at the required low temperature. The model of the unit is Optyma™ Danfoss condensing unit. The main components of the condensing unit are compressor (model SC15G- 104G8525), air cooled condenser (Model BG- 4/5-118U0031) and filter drier. The helical coil (test section) was connected to the condensing unit and worked as DX coil. Refrigerant R-12 passes inside the condensing unit circuit and the test coil, while the moist air passes over the surface of the helical coil. A basin was placing underneath the helical coil to collect the water condensed on the coil surface. The basin was connected to a beaker to collect and measure the rate of water condensation.

Fig. 4. 9 Condensing unit (Optyma™ Danfoss)

4.2. Measuring Instruments

Measuring instruments are used to measure the physical quantities necessary to study the performance of the humidification-dehumidification water desalination system as well as the performance of the dehumidifying coil. The measuring instruments used in this study to measure these physical quantities are hygro-thermometer, PT-100, digital thermometer, Beakers 100, 250 ml, Stop watch, and Pitot Tube Anemometer.

4.2.1 Hygro- thermometer

Three hygro-thermometers are used to measure the relative humidity at different locations in the circuit. A photograph of the hygro-thermometer is shown in Fig. 4.10. The hygro-thermometer is an instrument that combines a hygrometer and a thermometer. The hygrometer portion of the instrument is used to measure the moisture content and then calculate the relative humidity of the air. The warmer the air is the more humidity it can absorb until it is saturated. Relative humidity is the measurement of the saturation level relative to the current air temperature.

Hygro-thermometer uses the thermometer portion of the instrument to make the air temperature measurement to determine the relative humidity of the air. The handheld hygro thermometer's large LCD shows both the relative humidity and temperature readings at the same time. Two Digital hygro-thermometers are used to indicate the relative humidity of the air across the cooling coil.

The two hygro-thermometer are of model HTC-1 of measuring range (temperature -10 °C ~ +50°C, accuracy ± 1°C, temperature resolution ± 0.1 °C, and humidity range 10% ~ 99% RH, with accuracy ±5 %RH, humidity resolution 1%.). The third digital hygro-thermometer is used to indicate the relative humidity of the air at ambient condition in the laboratory.

The third one is of model SH-109 and has measuring range (temperature indoor -10 °C ~ +50°C, temperature outdoor -50 °C ~ +70°C, accuracy ± 1°C, temperature resolution ± 0.1 °C, and humidity range 20% ~ 99% RH, with accuracy ±5 %RH, humidity resolution 1%).

Fig. 4. 10 Hygro-thermometer

4.2.2 PT-100 Temperature sensor

Pt-100 sensors (platinum resistance thermometers) are used to measure the air temperature after the heating section. Pt refers to that the sensor is made from Platinum (Pt), 100 refers to that at 0°C sensor has a resistance of 100 ohms (Ω). PT100 is connected to a digital thermometer (model TC4Y; see Fig. 4.11) to record the measured temperature.

Fig. 4. 11 PT-100 Dimension

4.2.3 Digital thermometer

Three 3 thermocouples (type K) are used for measuring the surface temperature for the helical coil. The thermocouples wires are connected to a digital thermometer of a measuring range -200: + 1370 °C, accuracy ±0.1% +0.7 C (see Fig. 4.12) for recording the thermocouples readings.

Fig. 4. 12 Digital thermometer

4.2.4 Pitot Tube Anemometer

As shown in Fig. 4.13, Pitot tube anemometer is used to measures the air velocity and airflow rate in the air duct. The model of the Anemometer is Extech HD350 and has a velocity measuring range of 1-80 m/sec with a basic accuracy ± 1% and a max resolution 0.01.

Fig. 4. 13 Pitot tube anemometer

4.2.5 Water Flow rate measuring

Finally, a graduated beaker is used to measure the water and condensate flow rate by collecting a certain amount of water in a certain period of time. The graduated cylinder is of volume 2 liter with a graduated scale division of 10 ml. The used stop watch is of error 0.1 second. Fig. 4.14 shows the picture of the graduated beaker and the stop watch.

Fig. 4. 14 Beaker and stop watch to measure rate of water condensation

4.3. Experimental work Procedure

The procedure of the experimental used in this study can be described in three sections: preparation of the experiment, achievement of steady-state conditions, and conducting collected measurements.

4.3.1 Preparation for Experiments

Before starting any experiments, the following steps should be conducted to ensure the accuracy of the data collected.

1. The electric wire connections for the air blower, Pt-100, water pump, air heaters, condensing unit, and control panel are checked.
2. The water level in the water tank which supplies water to humidification section was maintained.
3. Adjust control valve before water pump.
4. Turn on the main switch for water pump.
5. Main input switch for both of air blower and air heater was turned on.
6. Finally, the main switch for the condensing section was turned on.

4.3.2 Achievement of steady state condition

After running the air blower, air heater, and water pump, the readings of temperature and relative humidity have been monitored and recorded to assure that steady state condition was maintained. To be sure of steady state condition, the following precautions are taken into account.

1. Air blower flow rate is maintained at a constant value which is the specific required value.
2. Air heater temperature was maintained at a constant value which is the specific required value.
3. Water pump flow rate was maintained at a constant value which is the specific required value.
4. The water temperature is constant at the specific required value.
5. All the temperatures measurements were maintained constants.
6. All relative humidity measurements were maintained constants.

The above precautions are carefully considered through a period of time not less than 30-40 minutes, after which measurements have been recorded.

4.3.3 Measurements

After the achievement of steady state condition, the following measurements were recorded in each experiment:

1. Hygro-thermometer (model SH-109) measuring the ambient condition (temperature, relative humidity).
2. The Pt-100 reading measuring the air-dry bulb temperature after the air heaters.
3. Two Digital hygro-thermometers (model HTC-1) for measuring the relative humidity of the air at the inlet and exit of the dehumidifying coil.
4. Digital thermometer (dual input model AZ8852) for the measurements of the thermocouple's readings.
5. Water thermometer for the measurements of the temperature of water in the water tank.
6. Stopwatch and graduated cylinder to measure water condensation rate across the dehumidifying coils.
7. Pitot tube anemometer used to measure air velocity and airflow rate in air duct.

4.4. Experimental Conditions

The experiments were conducted at different operating parameters to study the effects of these parameters on the freshwater production rate of the system and on the performance of the helical fined and un-finned dehumidifying coils at different orientations. The studied parameters and ranges are given below:

▪ Airflow rate $\mathring{m}_{air}$	0.0424, 0.085, 0.127, 0.169 Kg/sec.
▪ Water flow rate $\mathring{m}_{w, hum}$	0.0465, 0.0952, 0.1176, 0.1667 Kg/sec.
▪ Air temperature $T_{1, air}$	55, 60, 65, 70, 75 °C
▪ Water temperature $T_{w, hum}$	31, 33, 35, 37 °C
▪ Coil surface geometry	Finned / Un-finned
▪ Orientation of the coil	Vertical / Horizontal

4.5. Experimental Procedure

The experimental procedure was as follow:

1. Set the orientation of the dehumidifying coil (finned or un-finned coil) at the required orientation (Horizontal or vertical).
2. Measure the ambient air relative humidity and temperature.
3. The water level in the tank which supplies water to humidifying section was maintained.
4. The main input switch for both of air blower, water pump, and air heater was turned on.
5. Adjusting the air frontal velocity to achieve the required mass flow rate m°_{air}.
6. Adjusting the air exit temperature from the heating section to the required value $T_{1, air}$, heater.
7. Adjust control valve before water pump to required value $m^{\circ}_{w, hum}$.
8. Adjust water temperature in a tank of humidifier section to required value $T_{w, hum}$.
9. Finally, the main switch for the condensing unit turned on.
10. Waiting until a steady state was achieved. It was found that this takes about to 40 min depending on the air velocity.
11. Collect water condensation across helical coil in graduated cylinder.
12. The readings have been recorded after a steady state condition was maintained (i.e. at constant values).
13. Repeating the above steps once when using finned coil at a horizontal orientation, and again using un-finned coil at a horizontal orientation, with different operating conditions according to the following ranges:
    - Frontal air velocity 1 m/sec which m°_{air} change by closing air inlet area to value m°_{air} = 0.0424, 0.085, 0.127, 0.169 Kg/sec
    - The temperature of air exit from the heating section to value $T_{1, air}$ = 55, 60, 65, 70, 75 °C.
    - The temperature of water exits from the pump to value $T_{w, hum}$ = 31, 33, 35, 37 °C.
    - Water mass flow rate supply to humidifier to value $m^{\circ}_{w, hum}$ = 0.0465, 0.0952, 0.1176, 0.1667 Kg/sec.

14. Repeating step 13 at Vertical orientation of the coil

4.6. Data Reduction

The rate of vapor condensation on the coil surface, sensible and latent heat transfer between the air and the coil, heat transfer coefficient between the air and the coil and coil efficiency were calculated for each experiment from the measurements of each experiment. Equations (4.1) to (4.7) are used to calculate these quantities for each experiment. The performance of the coil and the heat transfer characteristics of the helical coil were investigated by studying and solving these equations (Eq. (4.1) to Eq. (4.7)) using EES (Engineering Equation Solver, commercial version 6.883-3D) software. The rate of vapor condensation from the air on the surface of the coil was calculated by measuring the amount of water condensed on the coil surface during a period of time. The water condensation rate can be also calculated for check from the different measurements using Eq. 4.1.

$$\dot{m}_{water} = \dot{m}_{air} \times (\omega_{i,\,coil} - \omega_{e,\,coil}) \tag{4.1}$$

The sensible, latent and total heat transfer rate between the air and the coil surface were calculated from eq. 4.2, 4.3 and 4.4, respectively

$$Q_s = \dot{m}_{air} \times Cp_{air} (T_{i,\,coil} - T_{e,\,coil}) \tag{4.2}$$

$$Q_l = \dot{m}_{water,\,condensation} \times h_{fg} \tag{4.3}$$

$$Q_t = Q_s + Q_l \tag{4.4}$$

The condensation heat transfer coefficient was calculated from Eqs. 4.5, 4.6.

$$h_s = Q_s / [A_c \times (T_{i,\,coil} - T_{surface\ coil})] \tag{4.5}$$

$$h_T = Q_T / [A_c \times (T_{i,\,coil} - T_{surface\ coil})] \tag{4.6}$$

where Ac is the surface area of the helical coil (π d L) where d is the diameter of helical coil, and L is the tube length.

The helical coil effectiveness (η_{eff}) is calculated from Eq.4.7

$$\eta_{eff,\,coil} = (T_{i,\,coil} - T_{e,\,coil}) / (T_{i,\,coil} - T_{surface\ coil}) \tag{4.7}$$

4.7. Uncertainty Analysis

The measurement errors of these parameters are ±0.2 for any temperature measurements, ±0.5% for any humidity measurements, ±0.01 liter for measurements of volume of condensate water, ±0.1 seconds for time measurements and ± 0.0005 kg/s for measurements of air mass flow rate. The uncertainty in the calculation of y due to the different errors in the measurements of the different physical quantities $(x_1, x_2, x_3, \ldots\ldots x_n)$ can be calculated from Eq. 4.8. [69]

$$\frac{\Delta y}{y} = \left[\left(\frac{\partial y}{\partial x_1}\frac{\Delta x_1}{y}\right)^2 + \left(\frac{\partial y}{\partial x_2}\frac{\Delta x_2}{y}\right)^2 + \cdots + \left(\frac{\partial y}{\partial x_{n1}}\frac{\Delta x_n}{y}\right)^2\right]^{1/2} \tag{4.8}$$

Where $\frac{\partial y}{\partial x_i}$ was calculated by analytical differentiation at the measurement's values. The minimum and maximum uncertainty in calculating the condensate mass flow rate, the heat transfer rate, the heat transfer coefficient and the coil effectiveness were calculated to be (1.9 and 2.3%), (3.05, 4.34%), (3.45% and 5.03%) and (2.7 and 3.65%), respectively.

Chapter 5: RESULTS AND DESCUSSIONS

The results of the experimental work were presented to investigate the performance and characteristics of the HDH system with honeycomb humidifier pad section and finned and un-finned helical dehumidification coils at different operating conditions. The results also investigate and compare the heat transfer characteristics and the air dehumidification/water condensation rates of the finned and the un-finned helical coils at the vertical and horizontal orientations. The coil performance was measured in terms of the heat transfer rate, heat transfer coefficient, the water condensation rate and the coil effectiveness.

The investigation and comparisons are conducted for different operating conditions: air flow rates, air temperatures, air humidity, water temperatures and water flow rates. For the sake of the investigation and comparison studies, the effects of the different parameters such as air temperature, air humidity, air flow rate, the helical coil orientations and the existence of the fins on the entire system performance as well as on the helical coils performance were presented in details.

5.1. Effect of operating parameters on the system productivity

5.1.1 Effect of air flow rate

Fig. 5.1 shows the effect of the air flow rate on the fresh water productivity of the system for different coil geometries and orientations and at different air inlet temperatures. The figure shows that for the finned and un-finned coils at the horizontal and vertical orientations, the water condensation rate increases with the increase of the air flow rate. The trend of the variation was noticed to be the same for any air temperature. The increase of the water production rate with the increase of the air flow rate can be attributed to (i) the increase of the vapor content in the air with increasing the air flow due to the increase of the humidification rate in the humidifier, (ii) the increase of the heat and mass transfer rates between the air and the coil surface with increasing the air flow rate, (iii) the increase of the process of renew of air that in contact with the coil surface with increasing the air flow rate, and (iv) increasing the air flow rate increases the water condensation rate on the coil surface as per Eq. 4.1. This trend of variation is the same trend obtained by Huzayyin et al. [70] for air cooling and dehumidification on a wavy-finned straight tubes coil.

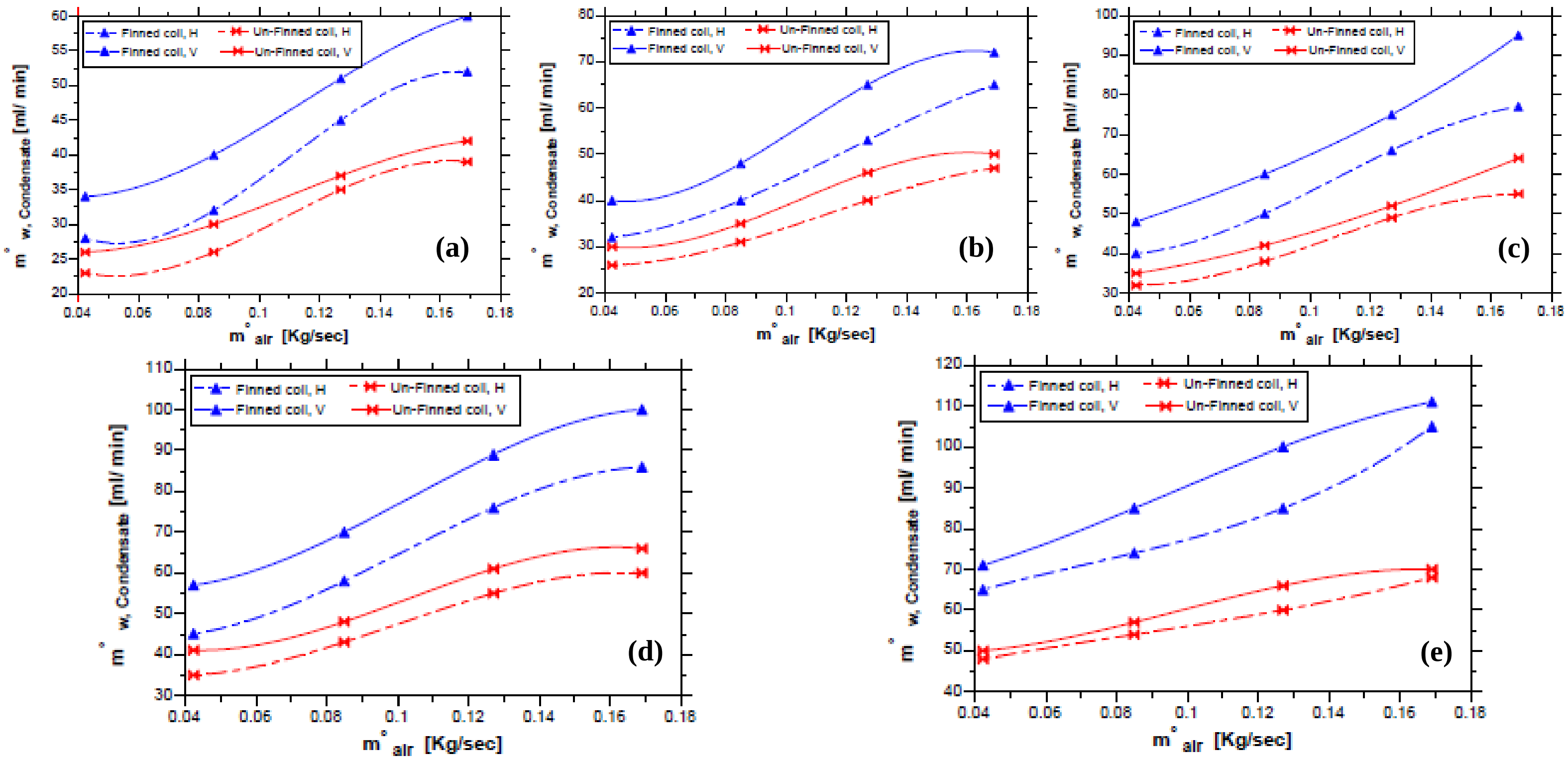

Fig. 5. 1 Effect of air flow rate on the dehumidification capacity of the finned and un-finned coils at the horizontal and vertical orientations at $T_{1,\,air}$ = (a) 55, (b) 60, (c) 65, (d) 70, (e) 75°C

5.1.2 Effect of air Temperature

Fig. 5.2 shows the effect of the air temperature at the exit of the heating coil on the fresh water productivity of the system for different coil geometries and orientations and at different air flow rates ($\mathring{m}_{air}$ = 0.0424, 0.085, 0.127, 0.169 Kg/sec).

The figure shows that for the finned and un-finned coils at the horizontal and vertical orientations, the fresh water production rate increases with the increase of the air temperature. The trend of the variation was noticed to be the same for any air flow rate.

Fig. 5.2 shows the increase of the fresh water production rate with the increase of the temperature of air at exit of heating coil. This can be attributed to that:

(i) increasing the air temperature at the inlet of the humidifier section decreases the vapor pressure of the air and this increases the ability of the air to carry more vapor in the humidifier; i.e. increasing the humidification capacity, which leads to more vapor to be condensed on the dehumidification coil.

(ii) increasing the air temperature at the exit of the heating coil leads to the increase of the air temperature at the inlet of the dehumidifying coil which causes the increase of the heat transfer rate from the coil to the air with increasing the temperature difference between the coil surface and the air. Increasing the heat transfer rate leads to the increase of water condensation rate on the coil surface, and (iii) increasing the air temperature means the increase of water vapor content in the air for the same relative humidity which leads to higher dehumidification rate on the cooling coil.

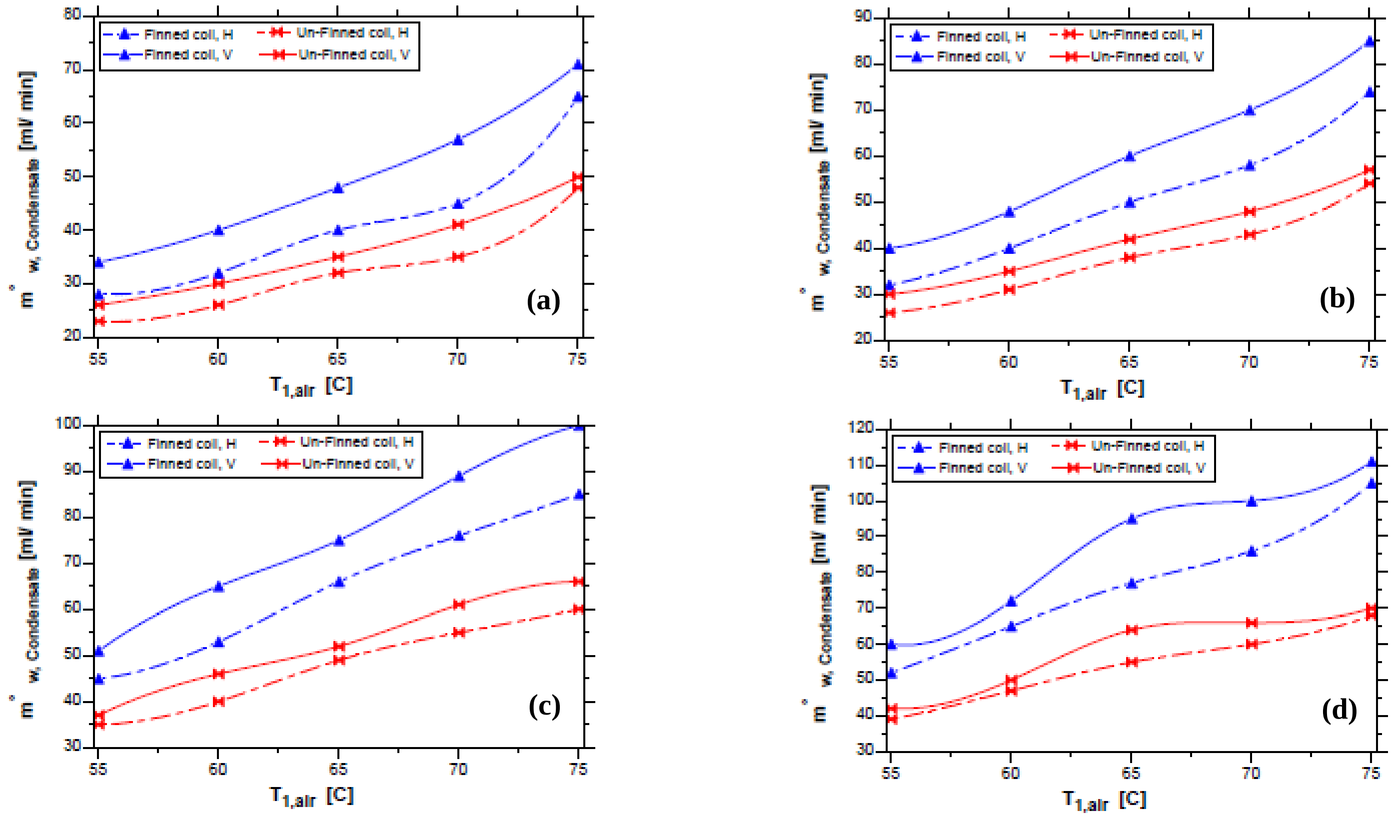

Fig. 5. 2 Effect air temperature on the fresh water production at m°_{air}= (a) 0.0424, (b) 0.085, (c) 0.127, (d) 0.169 Kg/s

5.1.3 Effect of water flow rate to humidifier

Fig. 5.3 shows the effect of the water flow in the humidifier on the fresh water production rate for the finned and un-finned coils at the vertical and horizontal orientation of the coil for different air temperatures. The air flow rate and water inlet temperature are maintained constants during the experiments.

As shown in the figure at any air temperature $T_{1,\ air}$ the rate of fresh water production rate ($m^{\circ}_{water,\ condensate}$) increases with increasing the water mass flow rate ($m^{\circ}_{w,\ hum}$,) to the humidifier. The trend was the same for all the air temperatures, air flow rate and water temperatures at the humidifier inlet.

The increase of the fresh water production rate with the increase of the water flow rate can be attributed to that increasing the rate of water increases the capacity of the humidifier to moisturize the largest area of honeycomb cooling pads which leads to the increase of the humidification capacity of the hot dry air passes through honeycomb cooling pads.

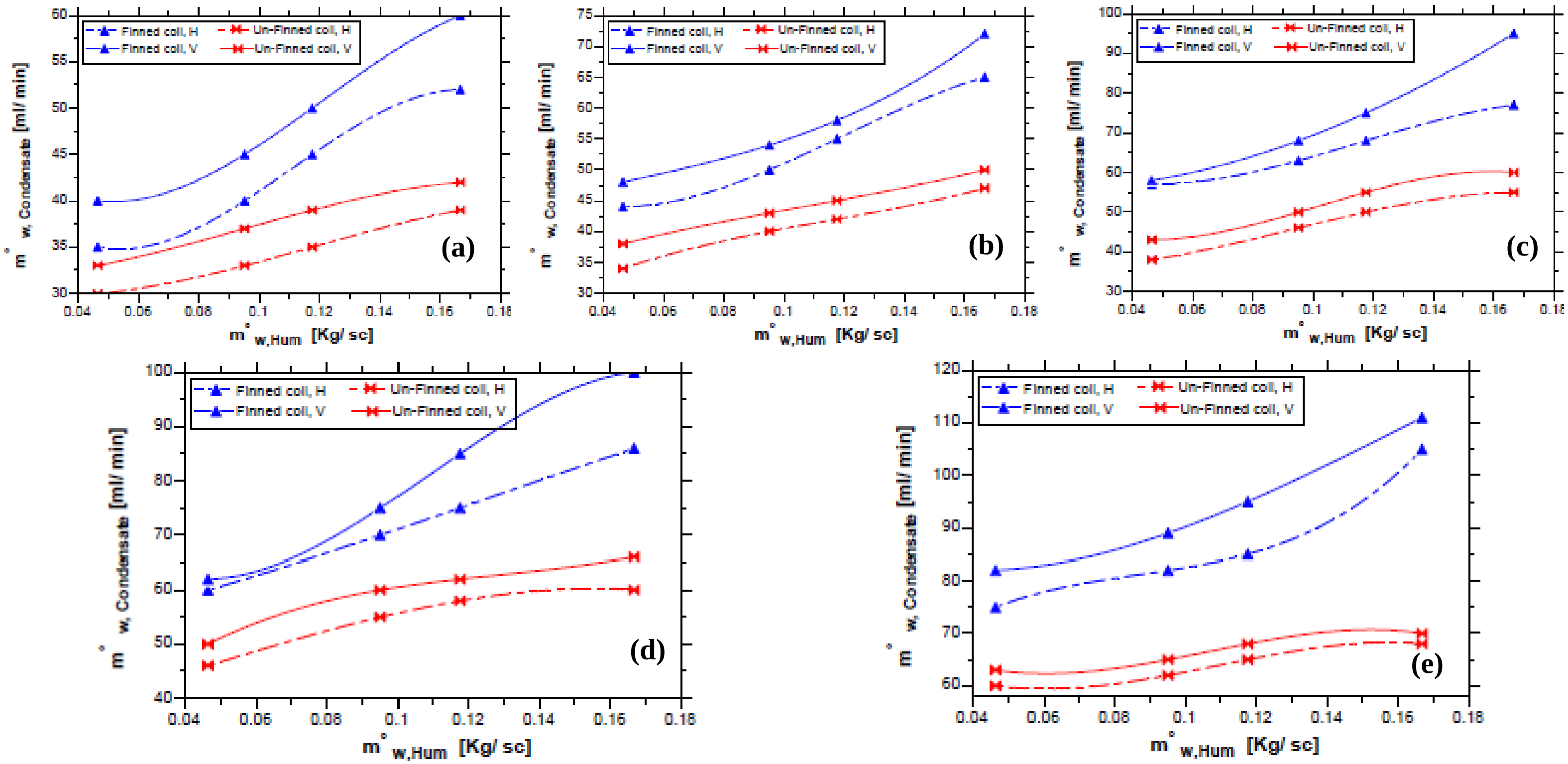

Fig. 5. 3 Effect of water flow rate to humidifier on the fresh water condensation rate across the finned and un-finned coils at: $T_{1,\,air}$ = (a) 55, (b) 60, (c) 65, (d) 70, (e) 75˚C

5.1.4 Effect of water temperature to the humidifier

Fig. 5.4 shows the effect of the water temperature to the humidifier on the fresh water production rate for the finned and un-finned coils at the vertical and horizontal orientation of the coil for different air temperatures. The air flow rate and water flow rate are maintained constants during the experiments.

As shown in the figure at any air temperature $T_{1,\ air,}$ the rate of fresh water production rate ($m^{\circ}_{water,\ condensate}$) increases with increasing the water temperature at the inlet of the humidifier. The trend is the same for all air temperatures, air flow rates, and water flow rates.

The increase of the fresh water production rate with the increase of the water temperature can be attributed to the increase of the humidification capacity of the air with increasing the water temperature due to the increase of the water evaporation rate with the water temperature.

Increasing the water evaporation rate mean that the air can carry the largest amount of water vapor from the cooling pad which leads to the decrease of its temperature and the increase of its relative humidity of air $RH_{2,\ air}$ and both leads to the increase of the dehumidification capacity of the air on the cooling and dehumidifying coil.

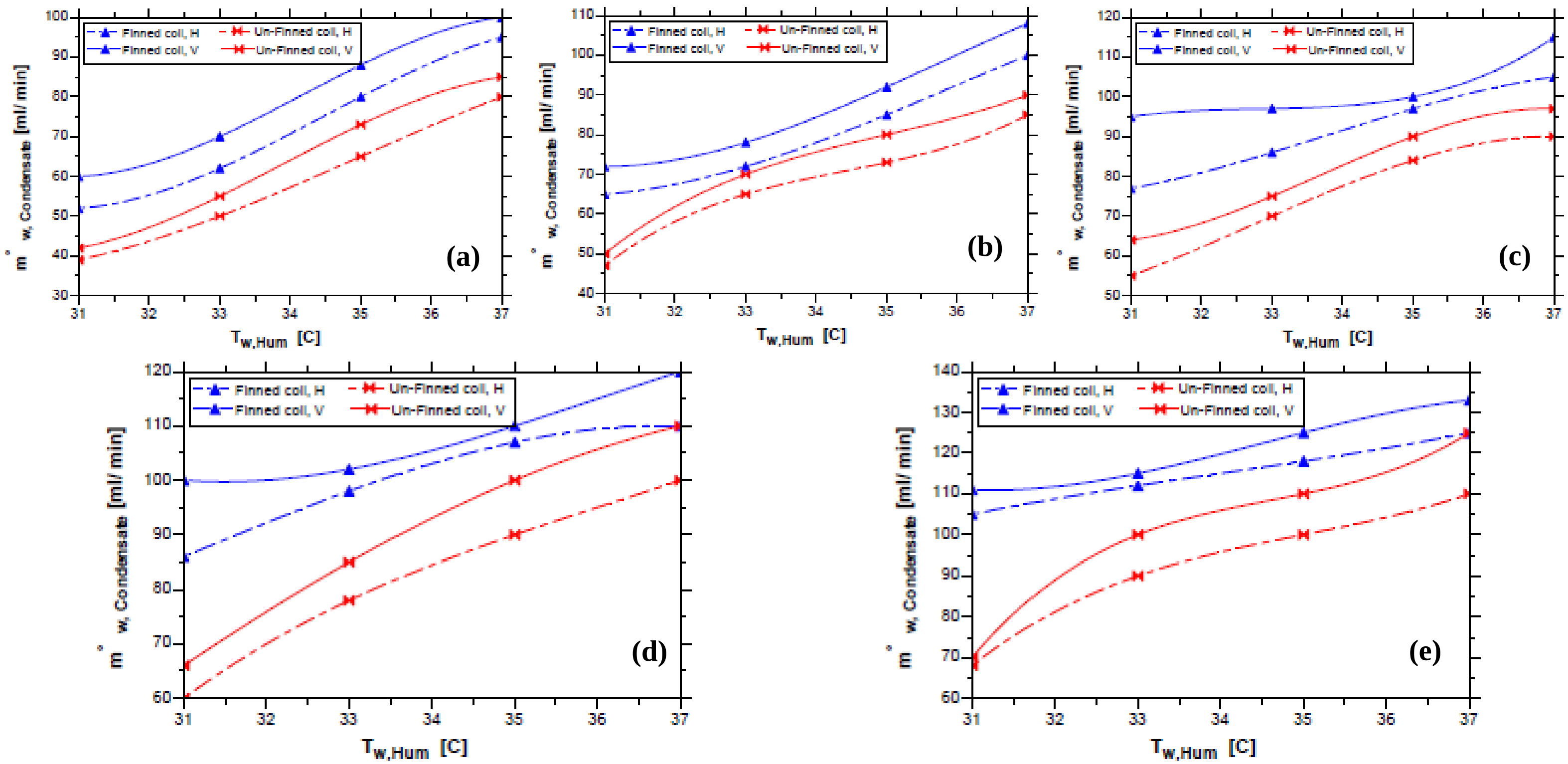

Fig. 5. 4 Effect water temperature on the fresh water production rate at: $T_{1\ air}$ = (a) 55, (b) 60, (c) 65, (d) 70, (e) 75˚C

5.2. Performance of the dehumidifying helical coils

Experimental work was also conducted to study the performance of the dehumidifying helical coils for different geometric conditions and orientations. The experiments were also conducted to study the effects of the air flow rates and the air temperatures and humidity at the inlet of the coils on the coils performance. The results of this work are presented to investigate and compare the heat transfer and the air dehumidification/water condensation characteristics for the finned and the un-finned helical coils placed at different (vertical and horizontal) orientations. The investigation and comparisons are conducted for different operating conditions: air flow rates, air inlet temperature and air inlet humidity. The coil performance was measured in terms of the heat transfer rate, heat transfer coefficient, water dehumidification/condensation rate and coil effectiveness.

5.2.1 Effect of air flow rate

Figs. 5.5 to 5.8 show the effect of the air flow rate on the coils performance: water condensation rate, heat transfer rate, heat transfer coefficient and coil effectiveness, respectively for the finned and un-finned coils at the vertical and horizontal orientations of the coil at different air temperatures 55, 60, 65, 70, 75 °C.

Fig. 5.5 shows that for the finned and un-finned coils at the horizontal and vertical orientations, the water condensation rate increases with the increase of the air flow rate. The trend of the variation was noticed to be the same for any inlet air temperature and inlet air humidity. The trend of this variation is attributed to:

- **(i)** The increase of the heat and mass transfer rates between the air and the coil surface with increasing the air flow rate.
- **(ii)** The increase of the process of renew of air that in contact with the coil surface with increasing the air flow rate.
- **(iii)** Increasing the air flow rate increases the water condensation rate on the coil surface as per Eq. 4.1.

trend of variation is the same trend obtained by Huzayyin et al. [41] for air cooling and dehumidification on a wavy-finned straight tubes coil.

Figs. 5.6 and 5.7 show the increase of the heat transfer rates and the heat transfer coefficient with increasing the air flow rate.

The trend is the same for the finned and un-finned coils and at any coil orientation and air inlet temperature.

The increase of the heat transfer with the air flow rate is attributed to:

(i) the increase of the air velocity and air Reynolds number that leads to the increase of the air turbulence level around the coil.

(ii) The increase of the water condensation rate with the air flow rate as shown in Fig. 5.5. which leads to the increase of the heat transfer rate as illustrated in Eq. 4.6.

Fig. 5.8 shows the increase of the coil effectiveness with the flow rate of air. This can be attributed to the increase of the heat transfer coefficient which leads to the increase of the heat transfer rate which causes more reduction of the air outlet temperature and consequently the increase of the coil effectiveness as given by Eq. 4.7.

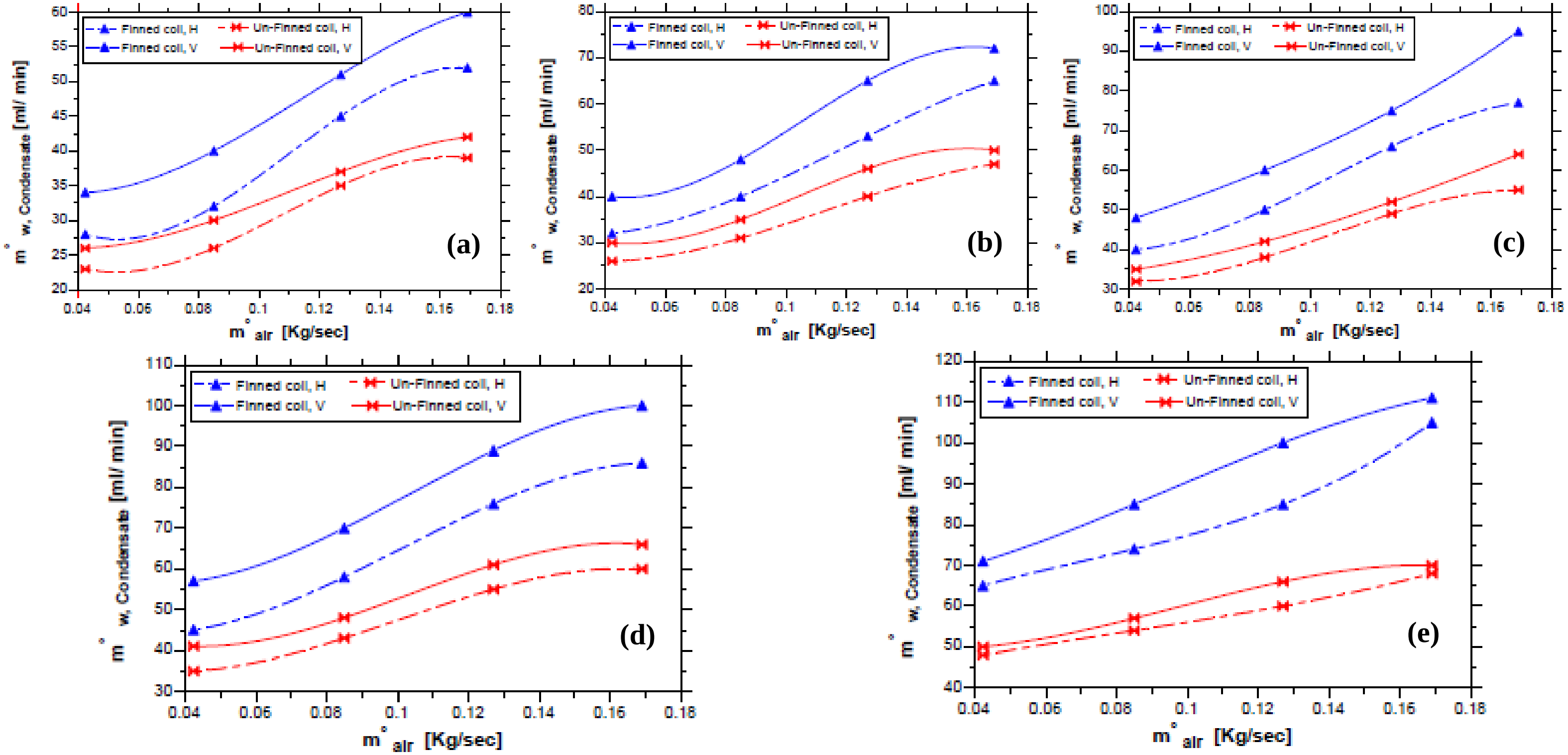

Fig. 5. 5 Effect of air flow rate on the dehumidification capacity of the finned and un-finned coils at the horizontal and vertical orientations at: $T_{1,\,air}$ = (a) 55, (b) 60, (c) 65, (d) 70, (e) 75˚C

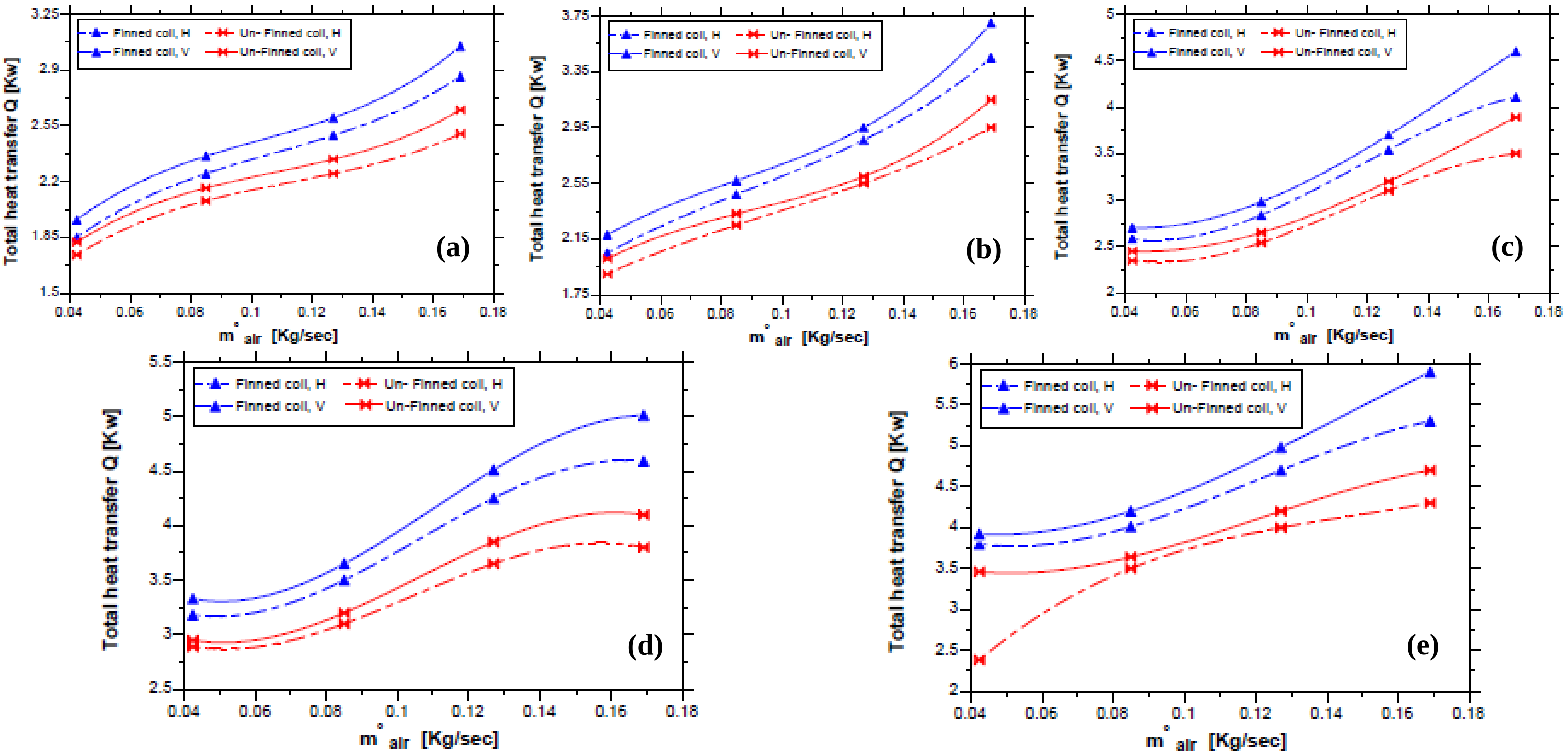

Fig. 5. 6 Effect of air flow rate on the heat transfer rates of the finned and un-finned coils at the horizontal and vertical orientations at $T_{1,\,air}$ = (a) 55, (b) 60, (c) 65, (d) 70, (e) 75°C

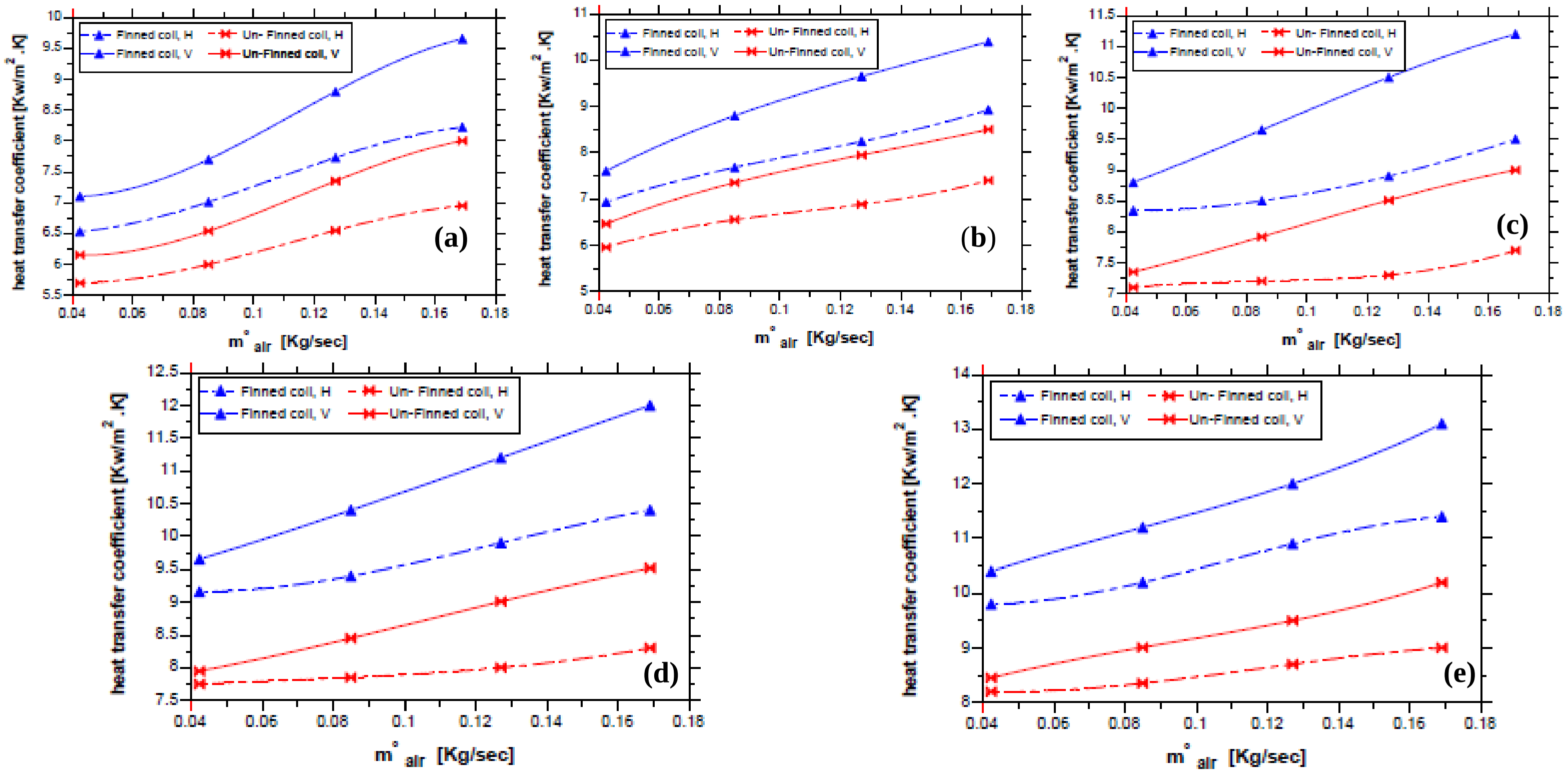

Fig. 5. 7 Effect of air flow rate on the heat transfer coefficients of the finned and un-finned coils at the horizontal and vertical orientations at $T_{1,\,air}$ = (a) 55, (b) 60, (c) 65, (d) 70, (e) 75°C

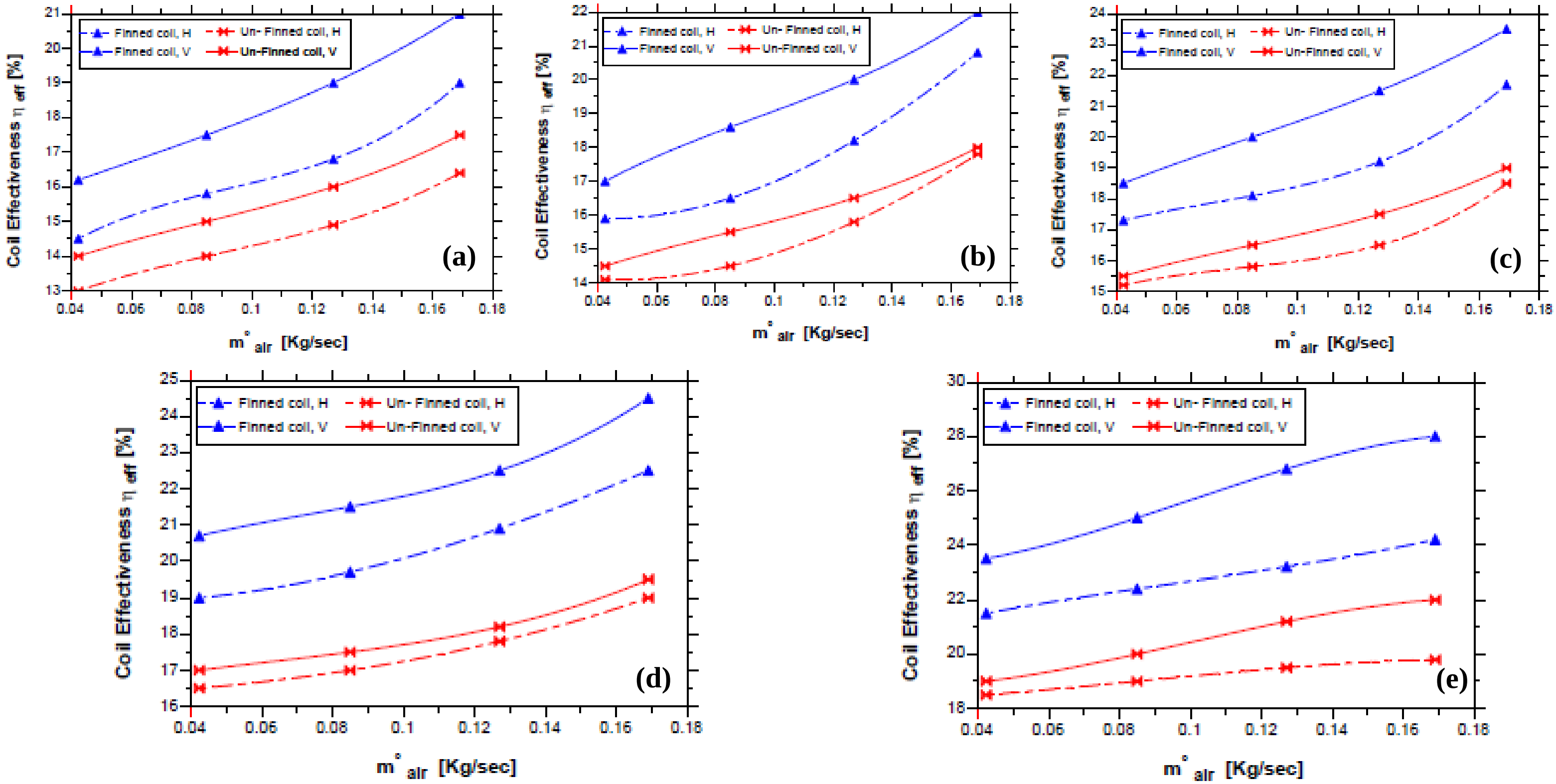

Fig. 5. 8 Effect of air flow rate on the coil effectiveness of the finned and un-finned coils at the horizontal and vertical orientations at $T_{1,\,air}$ = (a) 55, (b) 60, (c) 65, (d) 70, (e) 75°C

Fig. 5.9 compares the rates of the sensible and latent heat transfers for the un-finned as an example at air inlet temperature of 55° C and different air flow rate and coil orientations. The comparison result is the same for the finned and un-finned coils at the vertical and horizontal orientations and at any air. The figure shows that the sensible heat transfer is relatively low compared to the latent heat. This may be attributed to the wet condition of the coil surface and the high condensation rate on the coil surface which leads to covering the coil surface with thick condensate film which make as a resistance of sensible heat transfer. Fig. 5.9 also shows that the sensible heat is approximately constant with the air flow rate. This can be attributed to the bypass and contact factor of the coil. The amount of air that in contact with the coil surface is approximately constant whatever the air flow rate and the extra air is bypassed across the coil.

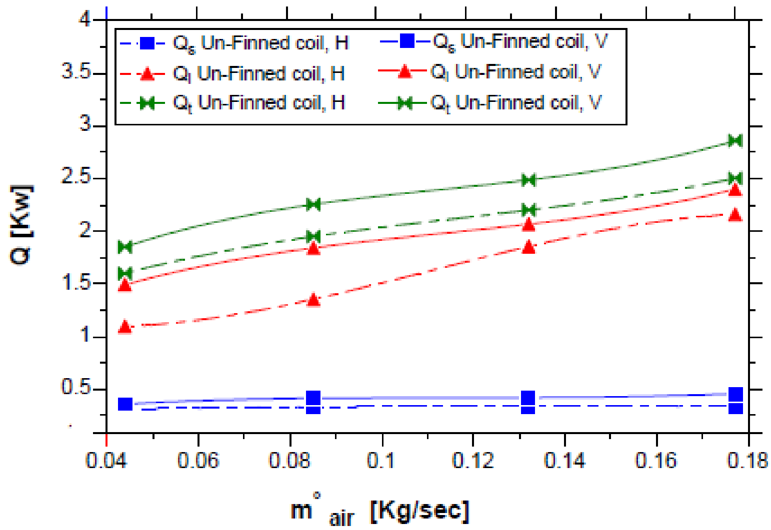

Fig. 5. 9 Comparison between sensible and latent heat transfers at the horizontal and vertical coil orientations

5.2.2 Effect of air temperature at coil entrance

The effect of the air temperature at the coil entrance on the coil performance: Water condensation rate, heat transfer rate, heat transfer coefficient and the coil effectiveness are shown in Fig. 5.10 to 5.12 for the finned and un-finned coils at different coil orientations and different rates of air flow.

Fig. 5.10 shows that the water condensation rate increases with increasing the air temperature at coil entrance. This increase may be attributed to:

- **(i)** the rise of the water vapor pressure in the air with the increase of air temperature which cause the increase of the potential difference of the mass transfer leading to the increase of the vapor mass transfer from the air to the cooling coil surface.
- **(ii)** The increase of the air humidity at the saturation condition of the air with increasing the air temperature which leads to high vapor transfer from the air to the coil surface.
- **(iii)** The increase of the heat transfer rate from the coil to the air with increasing the temperature difference between the coil surface and the air; increasing the heat transfer rate leads to the increase of water condensation rate on the coil surface.

Figs. 5.11 and 5.12 show that the heat transfer rate and the heat transfer coefficient increase with the increase of the air temperature. This may be attributed to:

- **(i)** increasing the temperature difference between the air and the coil surface with increasing the air inlet temperature which leads to the increase of the heat transfer rate and consequently the heat transfer coefficient.
- **(ii)** The increase of the water condensation rate with increasing the air inlet temperature as shown in Fig. 5.10 and this leads to the increase of the latent heat transfer.

Fig. 5.13 shows that the coil effectiveness increases with increasing the air temperature and this can be attributed to the increase of the heat transfer rate and heat transfer coefficient which leads to lower air temperature reduction across the cooling coil which means the increase of the coil effectiveness.

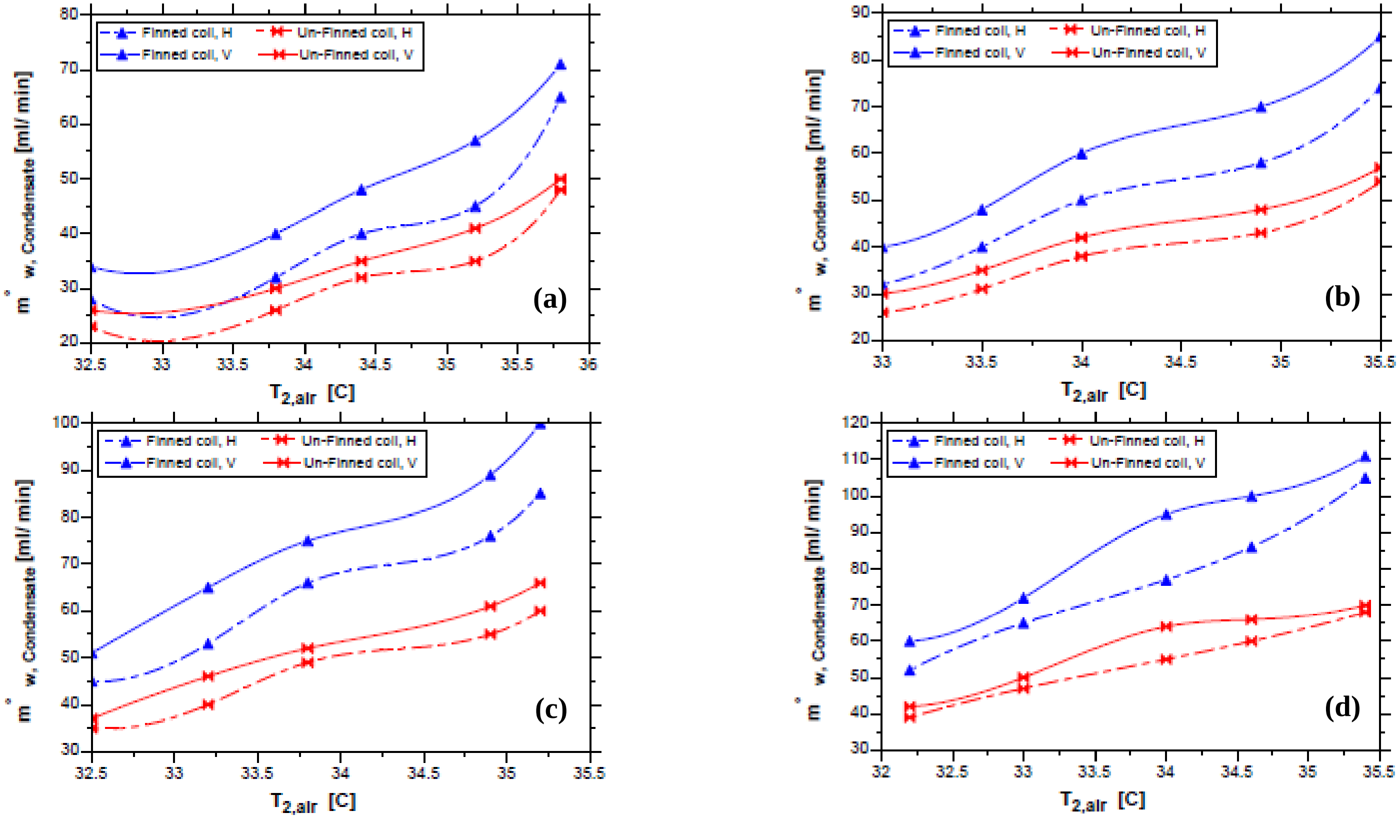

Fig. 5. 10 Effect of air temperature on the dehumidifying capacity of the finned and un-finned coils at the horizontal and vertical orientations at m°_{air}= (a) 0.0424, (b) 0.085, (c) 0.127, (d) 0.169 Kg/sec

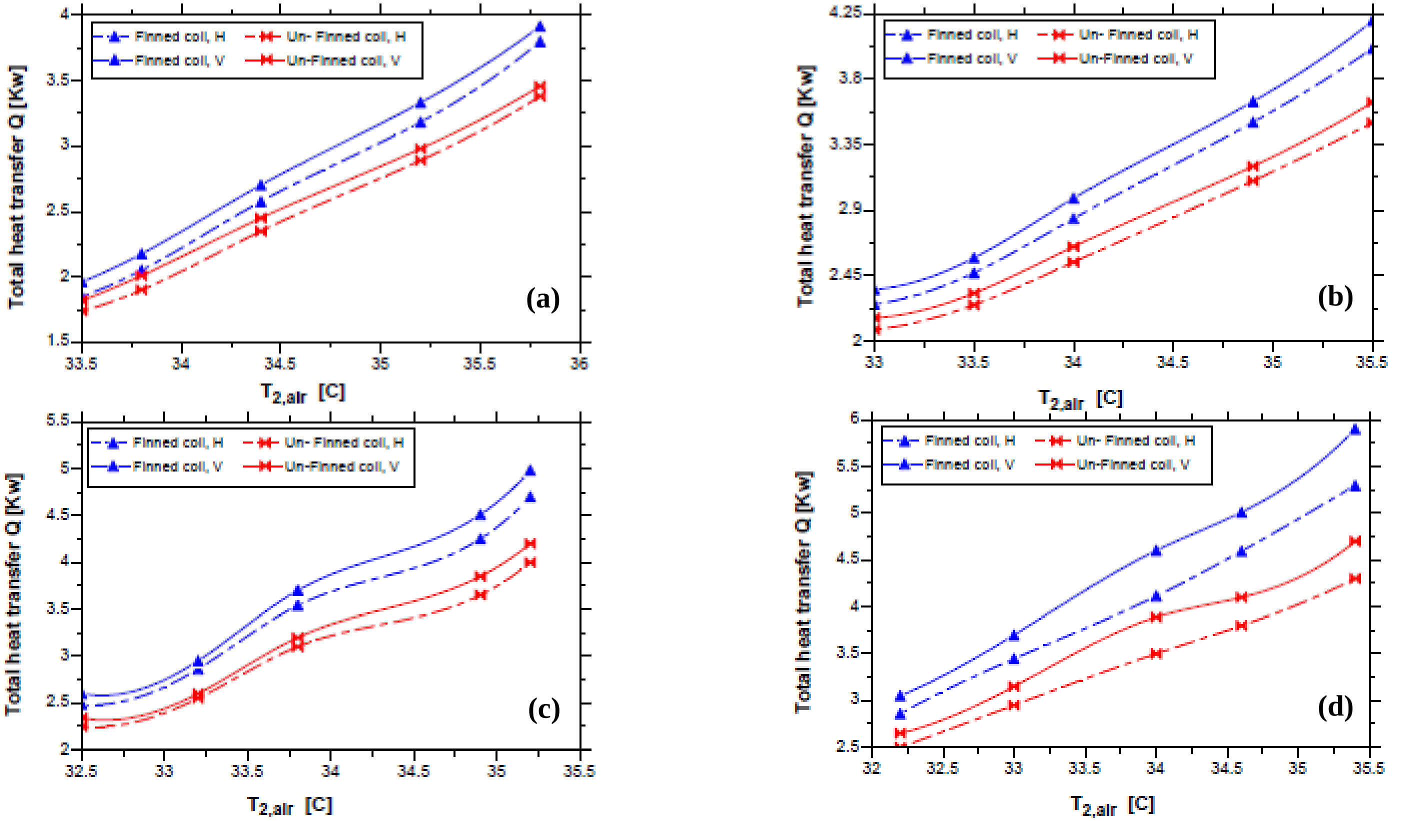

Fig. 5. 11 Effect of air temperature on the heat transfer rates of the finned and un-finned coils at the horizontal and vertical orientations at $\dot{m}_{air}$= (a) 0.0424, (b) 0.085, (c) 0.127, (d) 0.169 Kg/sec

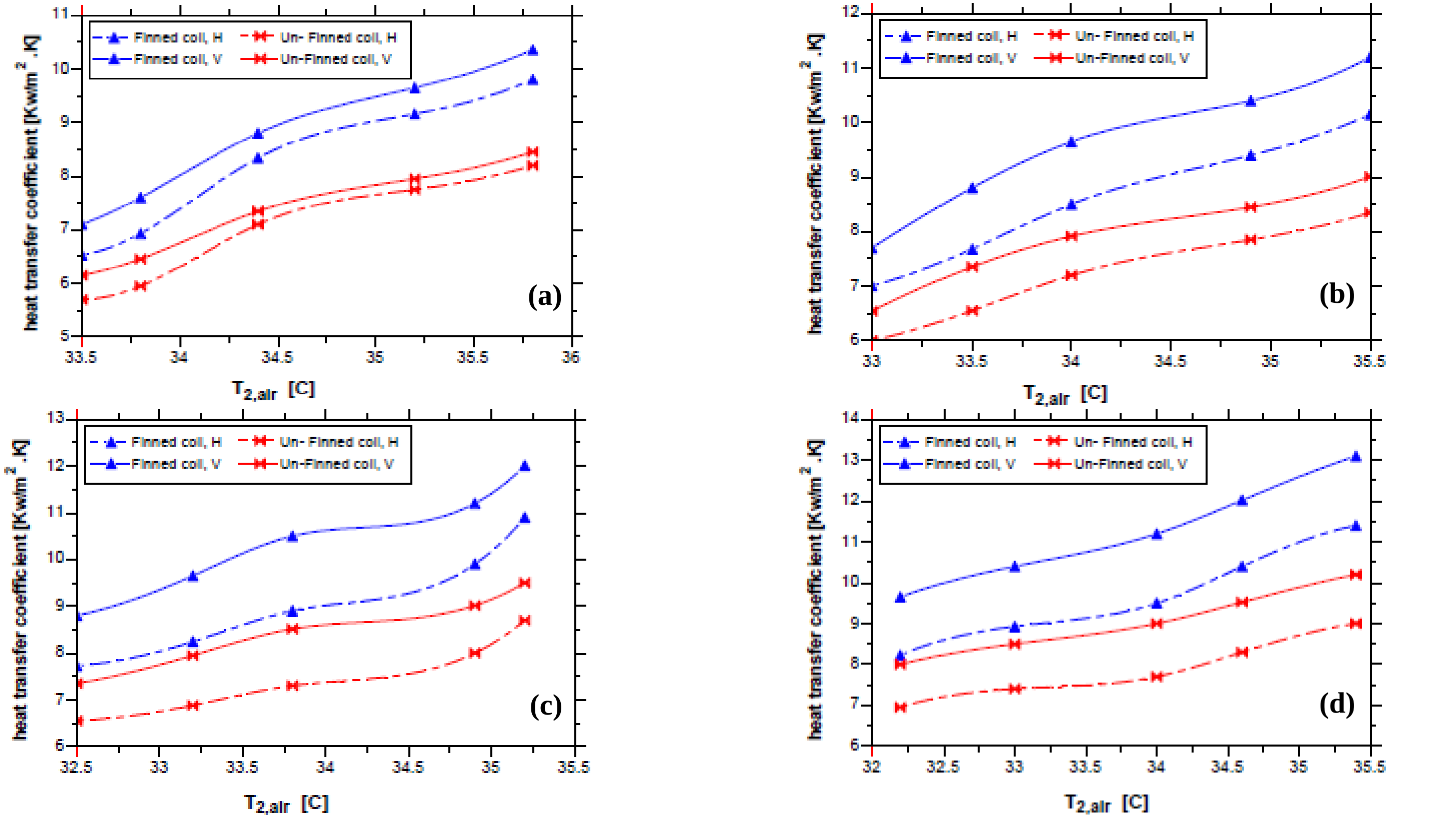

Fig. 5. 12 Effect air temperature on the heat transfer coefficient of the finned and un-finned coils at the horizontal and vertical orientations at m°_{air} = (a) 0.0424, (b) 0.085, (c) 0.127, (d) 0.169 Kg/sec

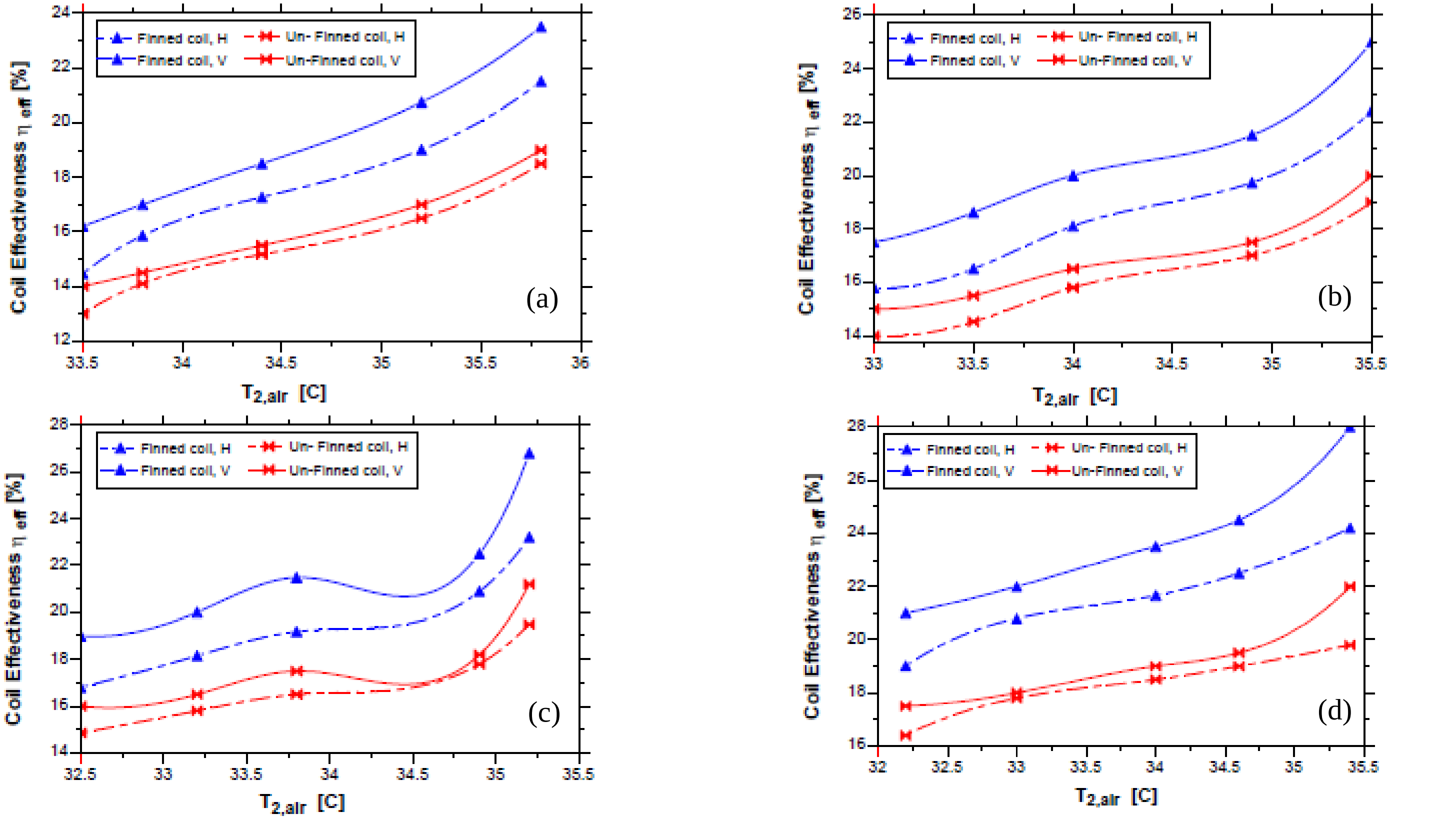

Fig. 5. 13 Effect of air temperature on the effectiveness of the finned and un-finned coils at the horizontal and vertical orientations at m°_{air} = (a) 0.0424, (b) 0.085, (c) 0.127, (d) 0.169 Kg/sec

5.2.3 Effect of air humidity at coil entrance

Figs. 5.14 to 5.18 demonstrate the effect of humidity of air on the coil performance; namely the dehumidification capacity, heat transfer rate, heat transfer coefficient, and the coil effectiveness.

As shown in Fig. 5.14, increasing the air humidity of the air increases the dehumidification capacity of the finned and un-finned coil. The trend of the effect is the same whatever the coils orientation, the air flow rate and air temperature. The increase of the dehumidification capacity with increasing humidity of air is attributed to the vapor pressure that increases with the increase of the humidity which leads to the tendency of the vapor to transfer from the air to the coil surface leading to more water condensation rate.

Figs. 5.15 to 5.17 show the increase of the heat transfer rate, heat transfer coefficient and the coil effectiveness with the increase of the air humidity. The trend is the same for all coils at the vertical and horizontal orientations and at all air flow rates and air temperatures. This trend of variation can be attributed to the high-water condensation rate with the high air humidity which leads to the increase of the latent and total heat transfer and the heat transfer rate and the coil effectiveness.

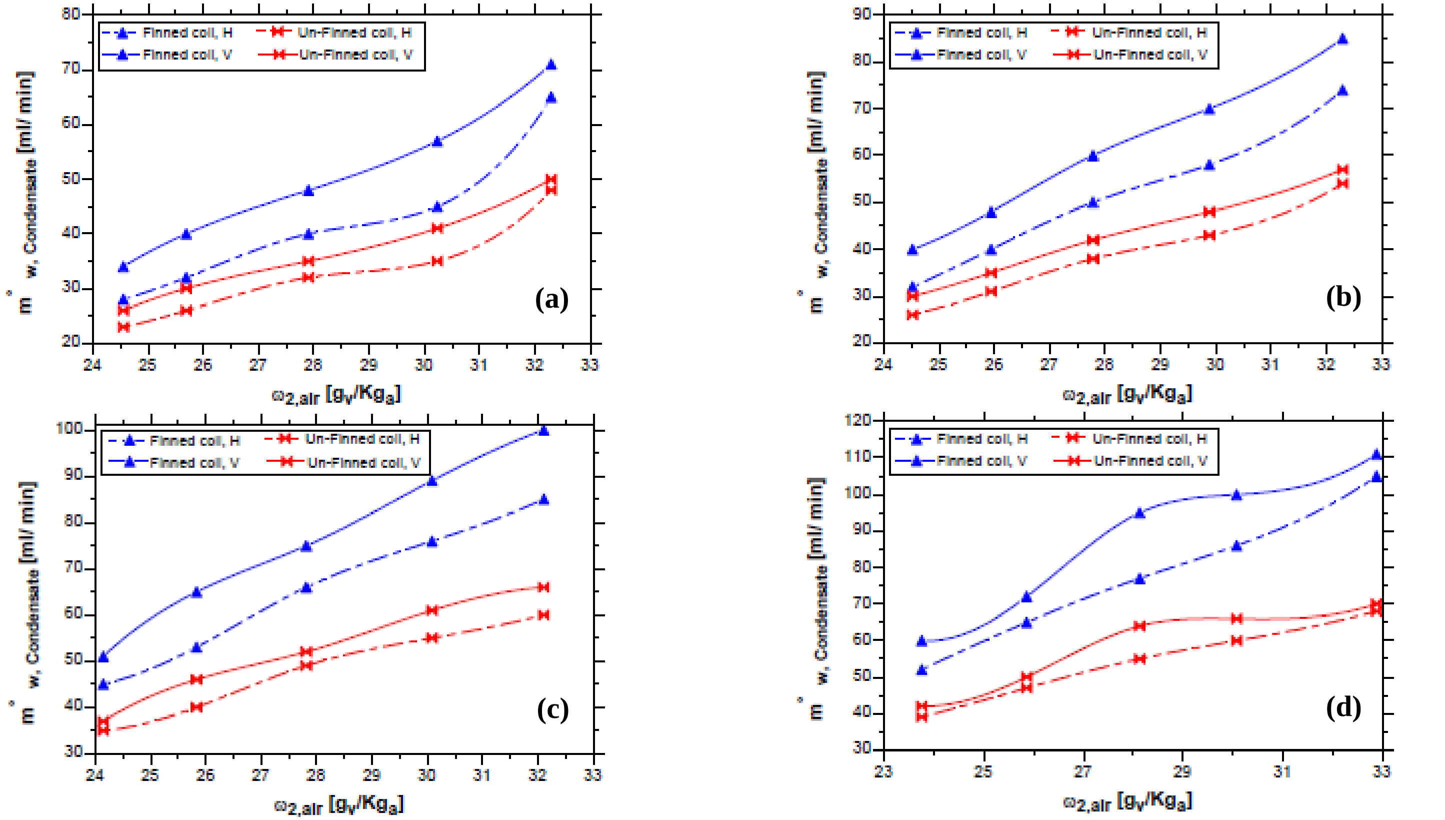

Fig. 5. 14 Effect air humidity on the dehumidifying capacity of the finned and un-finned coils at the horizontal and vertical orientations at m°_{air} = (a) 0.0424, (b) 0.085, (c) 0.127, (d) 0.169 Kg/sec

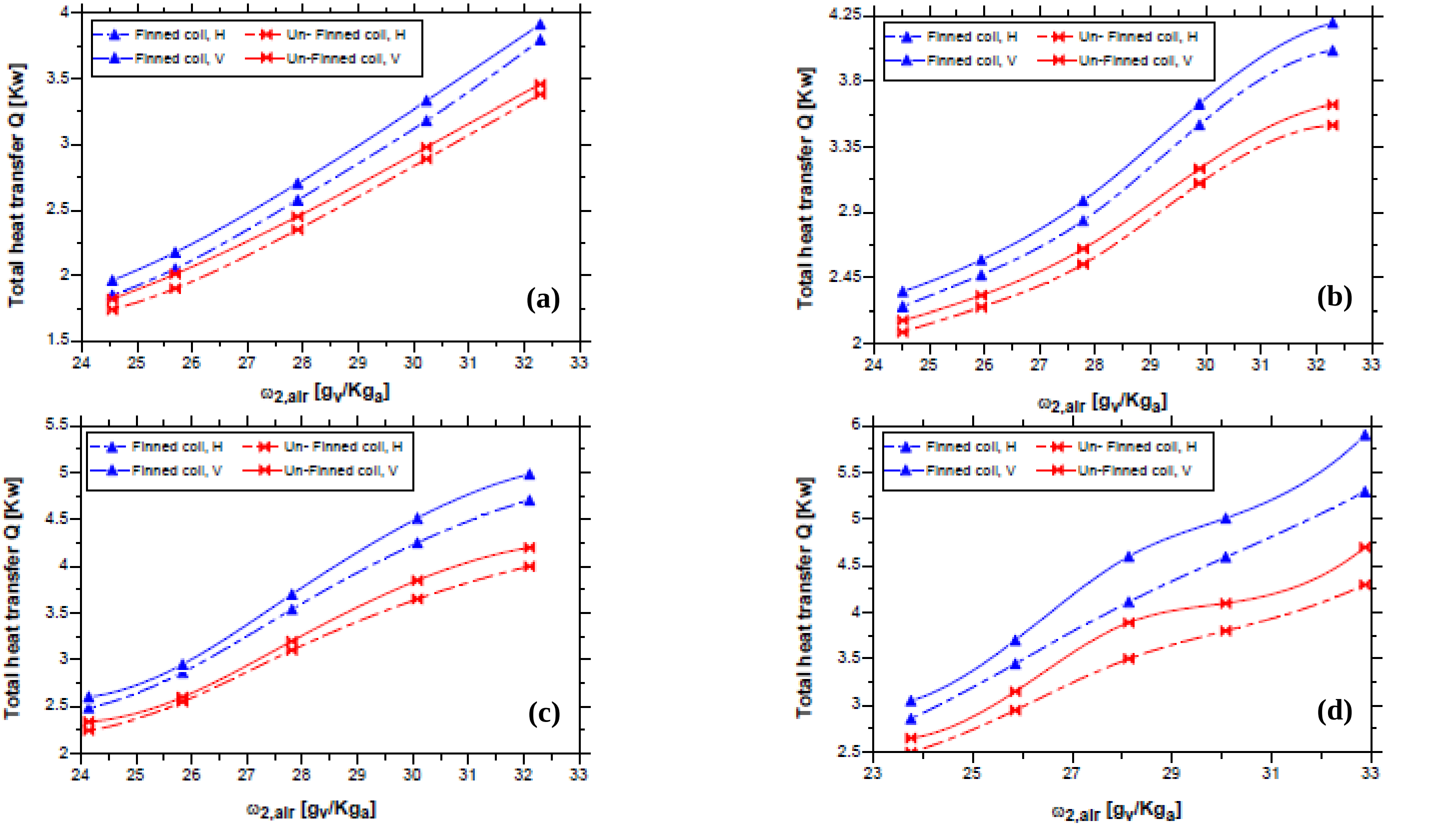

Fig. 5. 15 Effect air humidity on heat transfer rate of the finned and un finned coils at horizontal and vertical orientations at $\dot{m}_{air}$ = (a) 0.0424, (b) 0.085, (c) 0.127, (d) 0.169 Kg/sec

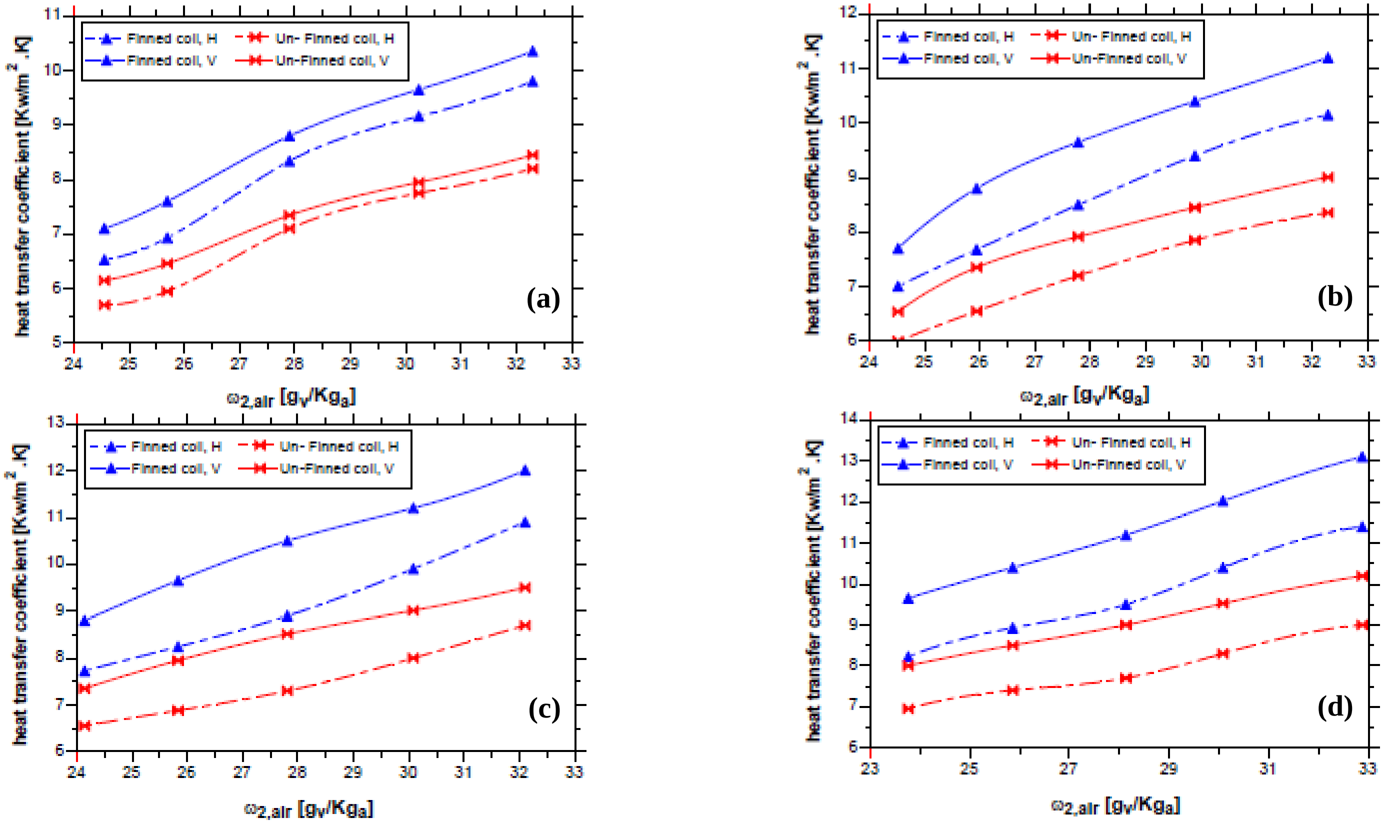

Fig. 5. 16 Effect air humidity on heat transfer coefficient of the finned and un-finned coils at horizontal and vertical orientations at $\dot{m}_{air}$ = (a) 0.0424, (b) 0.085, (c) 0.127, (d) 0.169 Kg/sec

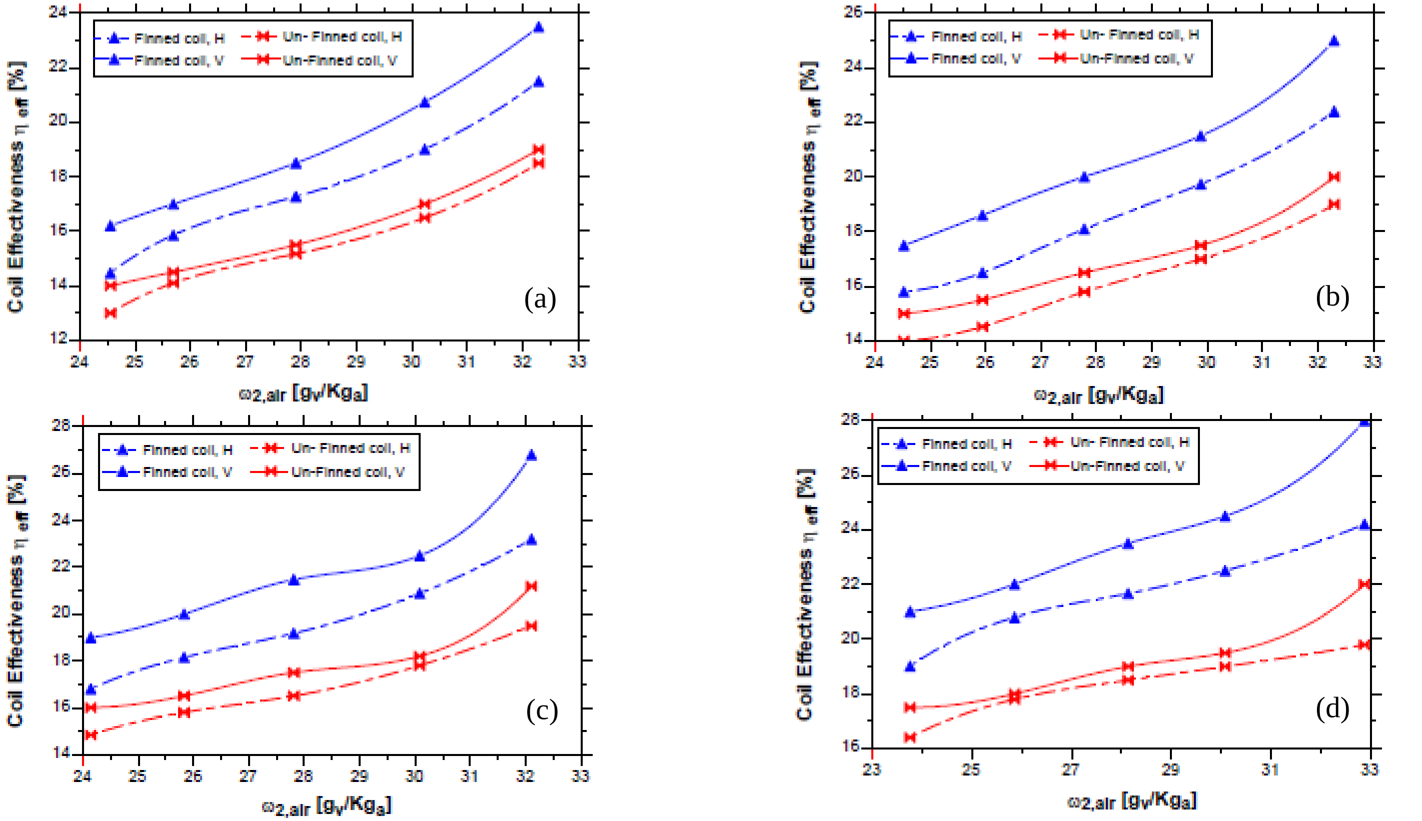

Fig. 5. 17 Effect air humidity on coil effectiveness of the finned and un-finned coils at horizontal and vertical orientations at m°_{air} = (a) 0.0424, (b) 0.085, (c) 0.127, (d) 0.169 Kg/sec

5.3. Comparison between the finned and un-finned helical coils

Figs. 5.1 - 5.17 compare between the performance of the finned and un-finned helical coils for different coil orientations and at different air flow rates, air temperatures, temperatures and flow rate of water inlet to the humidifier and air humidity and temperatures at coil entrance.

Figs. 5.1 - 5.5, 5.10 and 5.14 show that the finned helical coil gives higher water dehumidification /condensation rate than the un-finned helical coil. The trend is the same whatever the coil was vertically or horizontally oriented and whatever the air inlet temperatures and air flow rates. For example, the existence of the fins increases the water condensate rate from 70 ml/ min to 111 ml/min in case of the vertical coil at the air flow rate and the air temperature of 0.169 kg/sec and 75°C, respectively.

The higher dehumidification capacity of the finned helical coil compared to the un-finned coil can be returned to:

- **(i)** The existence of fins on the coil surface increases the heat and mass transfer surface areas which leads to higher heat transfer rates and water condensation rates.
- **(ii)** The existence of the wire strips fins on the coil surface increase the drainage rate of water droplets from the coil surface and this decreases the condensate film thickness on the coil surface which leads to the increase of the heat transfer rate and consequently the water condensate rate.

Figs. 5.6, 5.11, 5.15, 5.7, 5.12, and 5.16 show that the existence of fins on the coil surface increases that rate of the heat transfer and the heat transfer coefficient where the figures show that the finned coil has higher heat transfer rates and heat transfer coefficient compared to the un-finned coil. For example, the total heat transfer rate increased by 20.4 % and the heat transfer coefficient increased by 22.13 % due to the existence of fins in case of vertical orientation and at air flow rate and air temperature of 0.169 Kg/sec and 75°C. The trend is the same for the different coil orientation and air flow rates and air temperatures.

The increase of the heat transfer rates and the heat transfer coefficient due to the existence of the fins can be attributed to:

(i) the increase of the heat transfer and water condensation surface area with the existence of fins.

(ii) The decrease of the resistance of heat transfer as the fins leads to higher water drainage rate from the coil surface which leads to lower thickness of the condensate film on the coil surface.

(iii) The existence of fins increases the turbulence level around the coil surface which leads to higher heat transfer rates.

Figs. 5.7, 5.12 and 5.16 compare the coil effectiveness for the finned and un-finned coils for the different coil orientations and different air flow rates and air temperature. The Figures show that for the vertical and horizontal coil orientations and at any air flow rates and air temperatures, the effectiveness of the finned coil is always higher than that of the un-finned coil. For example, in the case of the vertical orientation and at the air flow rate and the air temperature of 0.169 kg/s and 75°C respectively, the coil effectiveness increases by 21.5 % the increase of the coil effectiveness with the existence of fins can be attributed to the increase of the dehumidification rate, heat transfer rate and the heat transfer coefficients which lead to higher air temperature drop across the coil.

The percentage of increase of the water condensation rate, heat transfer rate, heat transfer coefficient and coil effectiveness due to the presence of fins on the coil surface is shown on Figs. 5.18 - 5.20, respectively for vertical and horizontal orientations of the coil at different air flow rates and air temperatures. As shown in the Figures, the percentage of the water condensation rate, heat transfer rate, heat transfer coefficient and coil effectiveness increase with increasing the air flow rate and air temperature. This can be attributed to that the high air flow rate and air temperature need high surface areas of the coil to condense more water and transfer more heat.

Figs. 5.18 - 5.20 also shows that the existence of fins on the coil surface is more effective in vertical orientation than that of horizontal orientation where the percentage of increase of the water condensation rate, heat transfer rate, heat transfer coefficient and coil effectiveness due to using fins in case of vertical orientation is higher than those of the horizontal orientation. This can be attributed to that in vertical orientation the presence of fins makes the water droplets to fall down directly without sliding on the coil tube and this reduces the condensate film thickness on the coil surface which reduces heat and mass transfer resistance and increases the heat transfer and the water condensation rate.

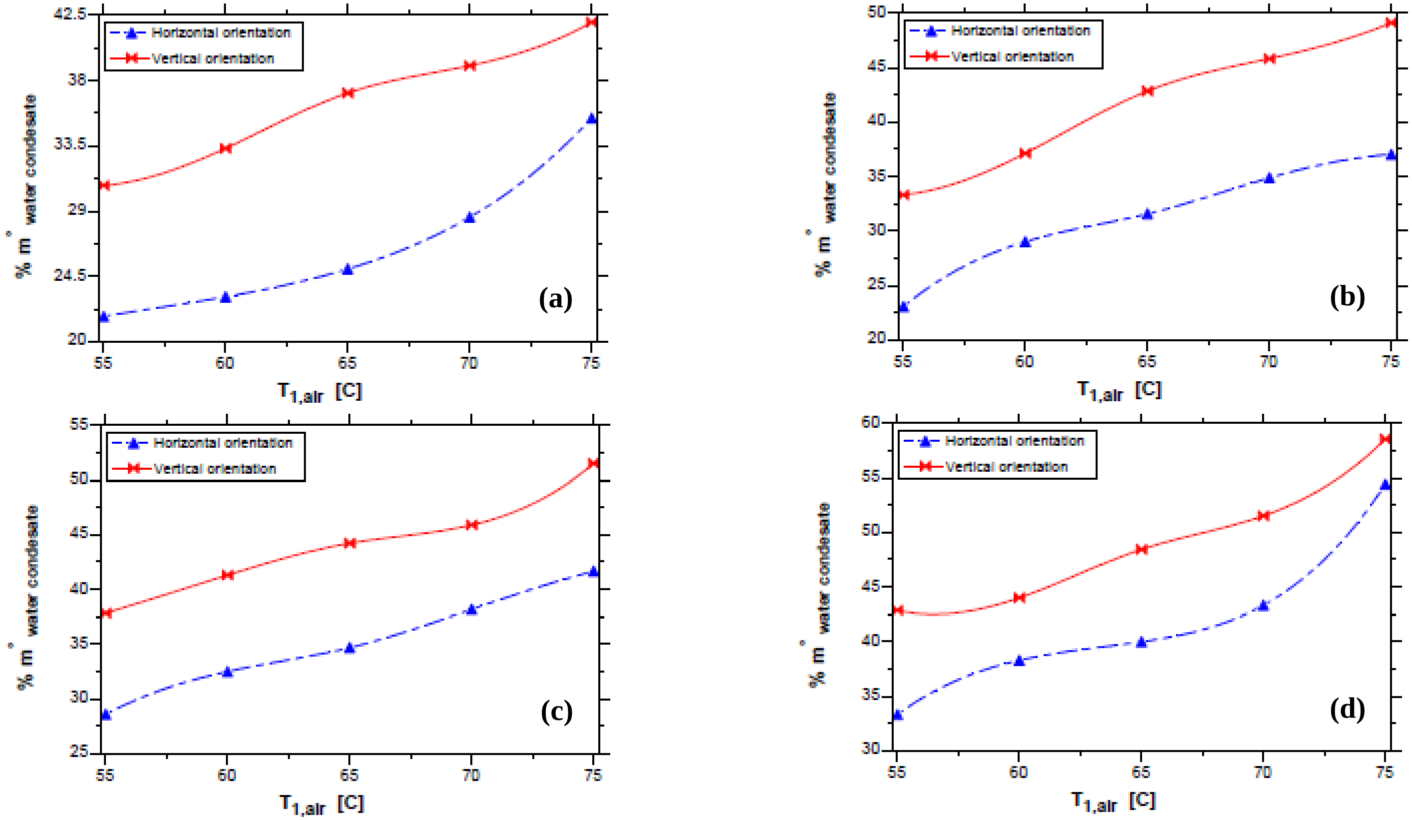

Fig. 5. 18 The percentage of increase of water condensate due to the presence of fins at
m°_{air} = (a) 0.0424, (b) 0.085, (c) 0.127, (d) 0.169 Kg/sec

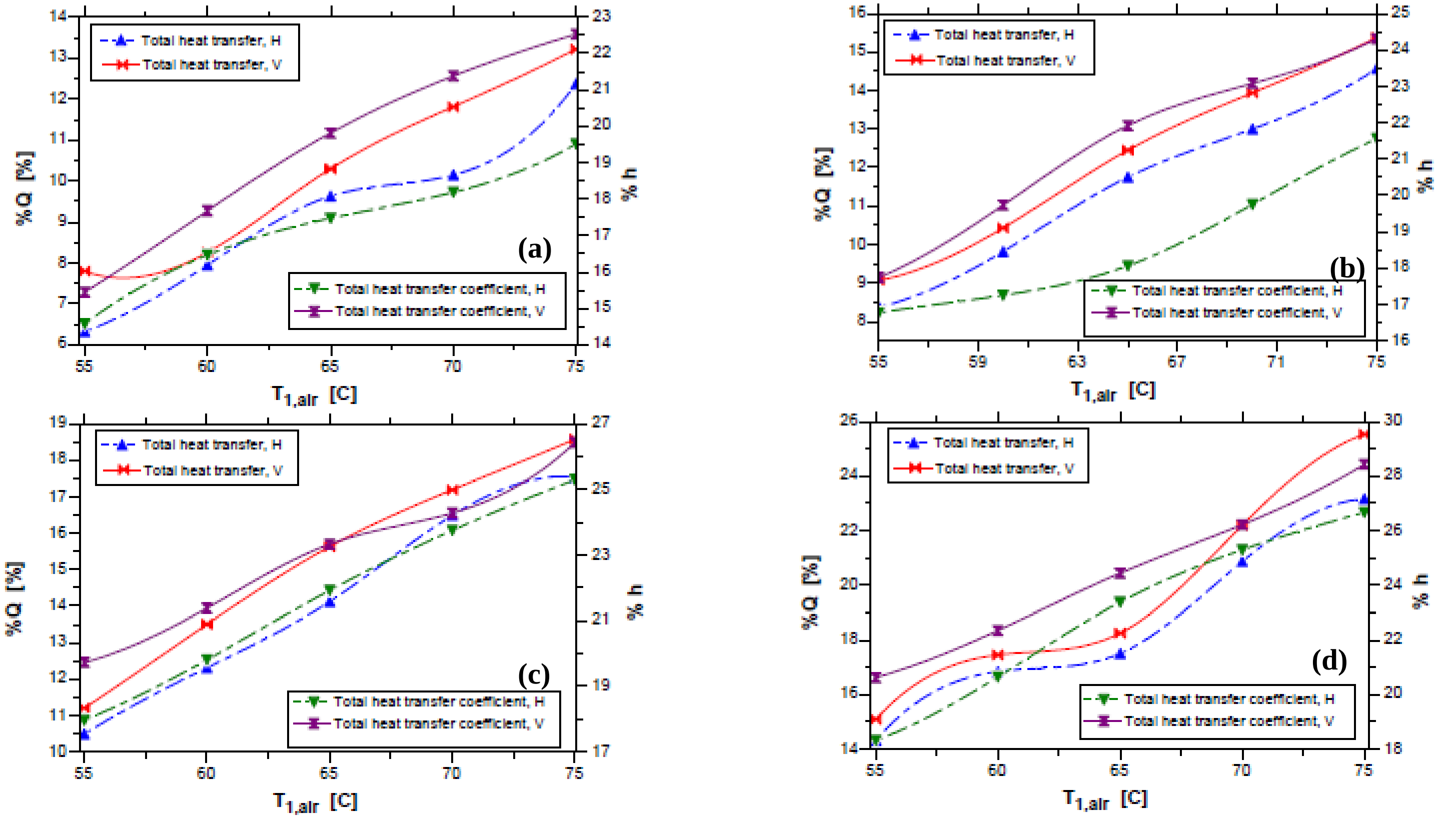

Fig. 5. 19 The percentage of increase of the heat transfer rate and heat transfer coefficient due to using fins at m°_{air} = (a) 0.0424, (b) 0.085, (c) 0.127, (d) 0.169 Kg/sec

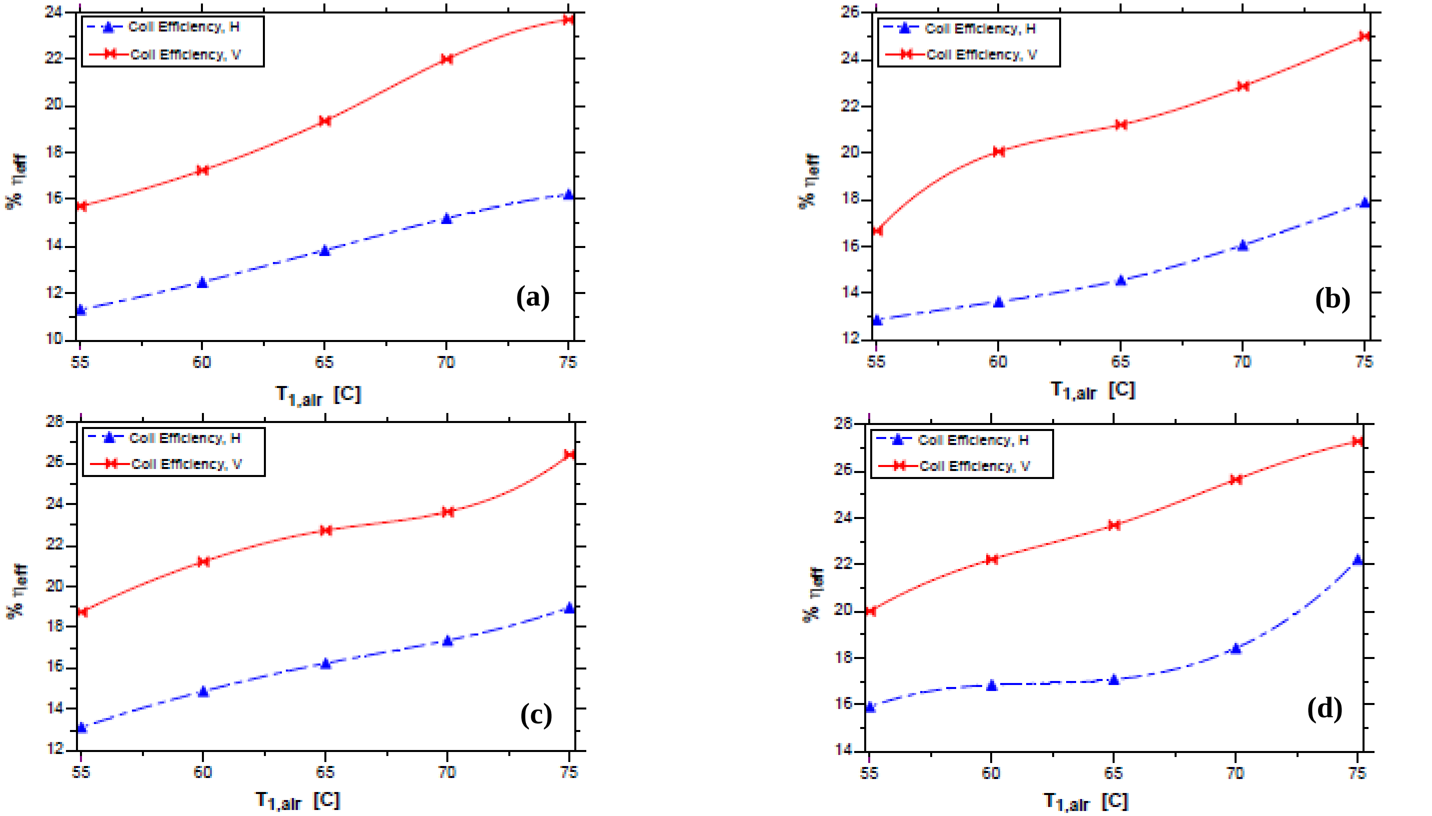

Fig. 5. 20 The percentage of increase of coil effectiveness due to using fins at $\dot{m}_{air}$ = (a) 0.0424, (b) 0.085, (c) 0.127, (d) 0.169 Kg/sec

5.4. Effect of Coil Orientation.

Figs. 5.1-5.17 shows the effect of the coil orientation on the performance of the finned and un-finned helical coils for the different air flow rates and temperatures.

Figs. 5.1-5.5, 5.10 and 5.14 show that the vertical orientation of the coil always gives higher water condensation rate compared to the horizontal orientation. The trend is the same whatever the coil was fined or un-finned and at all air inlet temperatures and flow rates. For example, the water condensation rate increased 14.3% and 5.5 % when the orientation of the un-finned and finned coils changed from the horizontal and vertical orientation respectively at air flow rate and air temperature of 0.169 kg/sec and 75°C.

The higher dehumidification capacity of the vertical orientation of the helical coil can be attributed to the length of the path of the condensate film/droplets until it separates the coil surface. In the vertical position the droplet moves vertically downward without slides along the longitudinal direction of the coil tube; so, the longest path of the condensate droplet is $\pi D/2$. In the horizontal orientation of the coil, the condensate droplets can slide along the longitudinal direction of the coil tube during its vertical movement; so, the longest path of the condensate droplet, in this case, is $\pi D/2$.

This means that the vertical orientation of the coil has the shortest condensate droplet path until its separation from the coil surface. This makes the rate of condensate removal from the coil surface in case of the vertical coil is higher than the horizontal coil. Moreover, the shorter of the condensate path of the vertical orientation means thinner condensate film thickness on the coil surface which leads to higher heat transfer rate and higher condensation rate.

Figs. 5.6, 5.7, 5.11, 5.12, 5.15 and 5.16 show that the vertical orientation of the coil has a higher heat transfer rate and heat transfer coefficient comparing the horizontal orientation of the coil. The trend is the same for the finned and un-finned coil and for the different the air flow rates and air temperatures. For example, the total heat transfer rate and the heat transfer coefficient for the finned coil increases by 11 % and 12.2 % due to changing the coil orientation from horizontal to vertical orientation at an air flow rate and an air temperature of 0.169 kg/s and 75°C.

The increase of the heat transfer rate and the heat transfer coefficient with changing the coil orientation from the horizontal to the vertical can be attributed to the shorter condensate film path and the thinner condensate film on the coil surface in case of vertical orientation of the coil which reduces the heat transfer resistance and increases the heat transfer rate and the heat transfer coefficient.

Figs. 5.8, 5.13 and .517 compare the coil effectiveness for the vertical and horizontal orientations of the finned and un-finned coils for the different air flow rates and air temperatures. The Figures show that the vertical orientation has higher efficiency than the horizontal orientations for the finned and un-finned coil and at any air flow rates and air temperatures. For example, at an air flow rate and an air temperature of 0.169 kg/s and 75 °C, the coil effectiveness of the finned and un-finned coils increases by 13.5 % and 10 %, respectively when the orientation of the coil changed from horizontal to vertical orientation. The increase of the coil effectiveness in case of vertical orientation can be attributed to the increase of the heat transfer rates and the heat transfer coefficients which lead to higher air temperature drop across the coil.

Chapter 6: SUMMARY AND CONCLUSIONS

6.1. Conclusions

Proposed mathematical models for integrative air conditioning (air-cooled chiller unit) and desiccant cooling systems (DCS) for freshwater production at low humidity applications are presented, investigated, evaluated and compared. The effects of the fresh air ratio, outdoor air temperature and humidity on the performance of the proposed systems are investigated.

The results revealed from the theoretical analysis show that:

1. The fresh water production rate and the cooling coil capacity of the air conditioning system increase with increasing the fresh air ratio and outdoor humidity and decrease with increasing the ambient air temperature
2. The saving in power consumption due to using energy recovery in enhanced systems remarkably noticed with increasing the outdoor air ratio,
3. The system with energy recovery located after the desiccant wheel is operating more efficiently and economically compared to the other systems.

An experimental investigation for the HDH system using honeycomb humidifier pad section and finned and un-finned helical dehumidification coils is conducted at different operating conditions. The investigation aimed also to test the un-finned and strips wired finned cooling and dehumidifying helical coils placed at vertical and horizontal orientations. The investigations were conducted at a wide range of air flow rates, air temperatures, water temperature, water flow rate and air humidity. The HDH system productivity and coil performance were tested, measured and evaluated in terms of the fresh water productivity, coil dehumidification capacity, coil heat transfer rate and heat transfer coefficient and the coil effectiveness. The results of the experimental work show that:

1. The HDH system productivity, coil dehumidification capacity and the coil performances increase with the increase of the air

flow rate, air temperature, and air humidity. The trend is the same for finned and un-finned coils at the vertical and horizontal orientations.

2. The performance (dehumidifying capacity, heat transfer rate, heat transfer coefficient, and coil effectiveness) of the helical coil with strips wire fins is higher than that of the un-finned coils at all coil orientations, air flow rates, and air properties.
3. The vertical orientation of the helical coils (finned or un-finned coils) enhances the coil performance and the system productivity compared with the horizontal orientation for the entire range of the air flow rate and air properties.
4. The percentage of increase in the coil performance due to using fins increases with increasing the air flow rate and the air temperature
5. The effect of using strip fins on the coil surface is more dominant in the case of the horizontal orientation of the coil compared to the vertical orientation.

6.2. Future Work

1. Study the possibility of using solar thermal energy in the heating section for energy saving.
2. Studying the effect of the geometric and characteristics parameters of the honeycomb cooling pads section on the fresh water productivity and the system characteristics.
3. Cost analysis of the presented experimental HDH system.

REFERENCES

1. Aly NH, El-Figi AK. Mechanical vapor compression desalination systems - A case study. Desalination. 2003; 158(1) :143-150.
   doi: https://doi.org/10.1016/S0011-9164(03)00444-2
2. Ghalavand Y, Hatamipour MS, Rahimi A. Humidification compression desalination. Desalination. 2014; 341:120-125.
   doi: https://doi.org/10.1016/j.desal.2014.02.039
3. Nada SA, Elattar HF, Fouda A. Performance analysis of proposed hybrid air conditioning and humidification-dehumidification systems for energy saving and water production in hot and dry climatic regions. Energy Conversion Management . 2015; 96:208-227.
   doi: http://dx.doi.org/10.1016/j.enconman.2015.02.082
4. Nada SA, Elattar HF, Fouda A. Experimental study for hybrid humidification–dehumidification water desalination and air conditioning system. Desalination. 2015; 363:112-125. doi: https://doi.org/10.1016/j.desal.2015.01.032
5. Al-Enezi G, Ettouney H, Fawzy N. Low temperature humidification dehumidification desalination process. Energy Conversion Management . 2006; 47(4): 470-484. doi: https://doi.org/10.1016/j.enconman.2005.04.010
6. Mohamed AMI, El-Minshawy NA. Theoretical investigation of solar humidification–dehumidification desalination system using parabolic trough concentrators. Energy Conversion Management 2011; 52(10): 3112 3119.
   doi:https://doi.org/10.1016/j.enconman.2011.04.026
7. Ghazal MT, Atikol U, Egelioglu F. An experimental study of a solar humidifier for HDD systems. Energy Conversion Management. 2014; 82:250-258.
   doi: https://doi.org/10.1016/j.enconman.2014.03.019
8. Nafey AS, Fath HES, El-Helaby SO, Soliman AM. Solar desalination using humidification dehumidification processes. Part I. A numerical investigation. Energy Conversion Management. 2004; 45(7):1243-1261.
   doi: https://doi.org/10.1016/S0196-8904(03)00151-1
9. Nafey AS, Fath HES, El-Helaby SO, Soliman A. Solar desalination using humidification–dehumidification processes.

Part II. An experimental investigation. Energy Conversion Management. 2004; 45(7): 1263-1277.
doi: https://doi.org/10.1016/S0196-8904(03)00152-3

10. Fouda A, Nada SA, Elattar HF. An integrated A/C and HDH water desalination system assisted by solar energy: Transient analysis and economical study. Applied Thermal Engineering.2016; 108:1320-1335.
doi: 10.1016/j.applthermaleng.2016.08.026.

11. Elattar HF, Fouda A, Nada SA. Performance investigation of a novel solar hybrid air conditioning and humidification-dehumidification water desalination system. Desalination. 2016; 382 :28-42. doi:10.1016/j.desal.2015.12.023

12. Dayem AMA, Fatouh M. Experimental and numerical investigation of humidification/dehumidification solar water desalination systems. Desalination. 2009; 247(1) :594-609. doi: https://doi.org/10.1016/j.desal.2008.12.039

13. Giwa A, Fath H, Hasan S. Humidification–dehumidification desalination process driven by photovoltaic thermal energy recovery (PV-HDH) for small-scale sustainable water and power production. Desalination. 2016; 377:163-171. doi:10.1016/j.desal.2015.09.018.

14. Kabeel AE, El-Said EMS. A hybrid solar desalination system of air humidification dehumidification and water flashing evaporation:A comparison among different configurations. Desalination.2013; 330 :79-89.
doi: https://doi.org/10.1016/j.desal.2013.10.004

15. Yıldırım C, Solmuş İ. A parametric study on a humidification–dehumidification (HDH) desalination unit powered by solar air and water heaters. Energy Conversion Management . 2014; 86:568-575.
doi: https://doi.org/10.1016/j.enconman.2014.06.016

16. Sharshir SW, Peng G, Yang N, El-Samadony MOA, Kabeel AE. A continuous desalination system using humidification – dehumidification and a solar still with an evacuated solar water heater. Applied Thermal Engineering. 2016; 104:734-742.
doi: https://doi.org/10.1016/j.applthermaleng.2016.05.120

17. Suyono T, Sohif M, Yahya M, Ruslan MH, Zaharim A, Sopian K. Theoretical and experimental analysis of desiccant wheel performance for low humidity drying system. Conference:

Proceedings of the 10th WSEAS international conference on System science and simulation in engineering; 2011:132-137. doi: http://dl.acm.org/citation.cfm?id=2051292.2051314

18. Avadhesh Yadav, V.K. Bajpai. "Optimization of Operating Parameters of Desiccant Wheel for Rotation Speed. international Journal of Advanced Science and Technology. 2011; 32: 109-116. https://www.earticle.net/Article/A15352

19. Dai Y, Wang RZ, Zhang HF, Yu JD. Use of desiccant cooling to improve the performance of vapour compression air conditioning. Applied Thermal Engineering. 2001;21:1185-1202. doi:10.1016/S1359-4311(01)00002-3

20. Mandegari MA, Pahlavanzadeh H. Introduction of a new definition for effectiveness of desiccant wheels. Energy. 2009; 34(6): 797-803. doi: https://doi.org/10.1016/j.energy.2009.03.001

21. Mohamed Kamar H, Kamsah N, Alhamid M, Sumeru K. Effect of Regenaration Air Temperature on Desiccant Wheel Performance. International Journal of Technology. 2016; 7: 281. doi: https://doi.org/10.14716/ijtech.v7i2.2971

22. Alireza Zendehboudi, Ramin Hashemi and Abbas zendehboudi "Performance assessment of a Solid Desiccant Based on Dehumidifier System Coupled with Air Conditioning System in a Tropical Climate" International Journal of Science and Technology. 2014; 7: 167-178. doi. https://www.earticle.net/Article/A231100

23. Daou K, Wang RZ, Xia ZZ. Desiccant cooling air conditioning: a review. Renew Sustain Energy Rev. 2006; 10(2) :55-77. doi: https://doi.org/10.1016/j.rser.2004.09.010

24. Al-Enezi G, Ettouney H, Fawzy N. Low temperature humidification dehumidification desalination process. Energy Conversion Management. 2006; 47 (4): 470-484. doi:https://doi.org/10.1016/j.enconman.2005.04.010

25. Yuan G, Zhang L, Zhang H. Experimental research of an integrative unit for air-conditioning and desalination. Desalination. 2005; 182(1) :511-516. doi: https://doi.org/10.1016/j.desal.2005.02.040

26. Gao P, Zhang L, Zhang H. Performance analysis of a new type desalination unit of heat pump with humidification and dehumidification. Desalination. 2008; 220(1): 531-537. doi: https://doi.org/10.1016/j.desal.2007.01.053

27. Mehrgoo M, Amidpour M. Constructal design and optimization of a direct contact humidification–dehumidification desalination unit. Desalination. 2012; 293: 69-77. doi: https://doi.org/10.1016/j.desal.2012.02.025
28. Prabhanjan DG, Raghavan GS V, Rennie TJ. Comparison of heat transfer rates between a straight tube heat exchanger and a helically coiled heat exchanger. International Communications Heat Mass Transfer. 2002; 29(2): 185-191. doi: https://doi.org/10.1016/S0735-1933(02)00309-3
29. Coronel P, Sandeep K. Heat Transfer Coefficient in Helical Heat Exchangers under Turbulent Flow Conditions. International Journal of Food Engineering. 2008;4. doi:10.2202/1556-3758.1209
30. Salimpour MR. Heat transfer coefficients of shell and coiled tube heat exchangers. Experimental Thermal Fluid Science. 2009; 33(2): 203-207. doi:https://doi.org/10.1016/j.expthermflusci.2008.07.015
31. Gupta PK, Kush PK, Tiwari A. Experimental studies on pressure drop characteristics of cryogenic cross-counter flow coiled finned tube heat exchangers. Cryogenics (Guildf). 2010; 50(4): 257-265. doi: https://doi.org/10.1016/j.cryogenics.2010.01.012
32. Raboh MAA, Mostafa HM, Ali MAM, Hassaan AM. Experimental Study for Condensation Heat Transfer Inside Helical Coil. Evaporation, Condensation and Heat Transfer: Intech Open; 2011. doi: https://doi.org/10.5772/20020
33. Shirgire ND, Panangipalli V. Review on Comparative Study between Helical Coil and Straight Tube Heat Exchanger. Journal of Mechanical and Civil Engineering. 2013; 8:55-59. doi:10.9790/1684-0825559
34. Jaber Habeeb Al-Jabair S, Hussain AA. Experimental Study of Heat Transfer Coefficients of Shell and Helically Coiled Tube Heat Exchangers. Engineering and Technology Journal. 2013; 31:172-196.
35. Suraj R. Gurav. Parametric Comparison of Heat Transfer in Helical and Straight Tube-In-Tube Heat Exchanger. International Journal of Science and Research.2015; 4: 990- 993. https://www.ijsr.net/archive/v4i8/SUB157502.pdf

36. Ankanna C, Reddy S. Performance Analysis of Fabricated Helical Coil Heat Exchanger. International Journal of Engineering Research. 2014; 3: 33-39. ijer.in/publication/v3/188.pdf

37. Naphon P. Thermal performance and pressure drop of the helical-coil heat exchangers with and without helically crimped fins. International Communications Heat Mass Transfer. 2007; 34(3) :321-330. doi: https://doi.org/10.1016/j.icheatmasstransfer.2006.11.009

38. Ghorbani N, Taherian H, Gorji M, Mirgolbabaei H. An experimental study of thermal performance of shell-and-coil heat exchangers. International Communications Heat Mass Transfer. 2010; 37(7): 775-781. doi: https://doi.org/10.1016/j.icheatmasstransfer.2010.02.001

39. Ghorbani N, Taherian H, Gorji M, Mirgolbabaei H. Experimental study of mixed convection heat transfer in vertical helically coiled tube heat exchangers. Experimental Thermal Fluid Science. 2010; 34(7): 900-905. doi: https://doi.org/10.1016/j.expthermflusci.2010.02.004

40. Bandpy MG, Sajjadi H. An Experimental Study of the Effect of Coil Step on Heat Transfer Coefficient in Shell- Side of Shell-and-Coil Heat Exchanger. World Academy of Science, Engineering and Technology International Journal of Mechanical and Mechatronics Engineering 2010;4(11):1209-1214.

41. Nada SA, Alshaer W. Heat transfer and pressure drop characteristics of multi tubes in tube helically coiled heat exchanger. JP Journal Heat Mass Transf. 2014;9:173-202.

42. Nada SA, El Shaer WG, Huzayyin AS. Performance of multi tubes in tube helically coiled as a compact heat exchanger. Heat Mass Transfer. 2015; 51(7): 973-982. doi:10.1007/s00231-014-1469-z

43. Elattar H, Fouda A, Nada SA, Refaey H, Al-Zahrani A. Thermal and hydraulic numerical study for a novel multi tubes in tube helically coiled heat exchangers: Effects of operating/geometric parameters. International Journal of Thermal Science. 2018; 128:70-83. doi:10.1016/j.ijthermalsci.2018.02.020

44. Nada SA, Elattar HF, Fouda A, Refaey HA. Numerical investigation of heat transfer in annulus laminar flow of multi tubes-in-tube helical coil. Heat Mass Transfer. 2018 ;54(3): 715-726. doi:10.1007/s00231-017-2163-8

45. Gore GG, Yarasu RB. Convective Heat Transfer Analysis from Helically Coiled Tube Using CFD and Experimental Methodology. International Journal for Scientific Research & Development. 2015;3 :475-478.
46. Shriyan N. A Review on Heat Transfer of Fluids in Curved and Coiled Geometries. Elixir Mechanical Engineering . 2015; 89: 36998-37007.
47. Karmankar RG. Enhancement of Heat Transfer Coefficient Through Helical. International Research Journal of Engineering and Technology. 2015;2: 2125-2129.
48. Gavade P, Kulkarni P.R. Experimental Evaluation of Helical Coil Tube in Tube Heat Exchanger. International Journal of Emerging Engineering Research and Technology. 2015; 3: 12-17.
49. Sreejith K, Ram T.R. S, Jaivin A, Varghese, Francis M, Mossas V.J, Nidhin M.J, Nithil E.S, Sushmitha S. Experimental Investigation of a Helical Coil Heat Exchanger. International Journal of Engineering and Science. 2015;5 :1-5.
50. Khairul MA, Saidur R, Rahman MM, Alim MA, Hossain A, Abdin Z. Heat transfer and thermodynamic analyses of a helically coiled heat exchanger using different types of nanofluids. International Journal Heat Mass Transfer. 2013; 67: 398-403.
doi: https://doi.org/10.1016/j.ijheatmasstransfer.2013.08.030
51. Izadpanah E, Zarei A, Akhavan S, Rabiee MB. An experimental investigation of natural convection heat transfer from a helically coiled heat exchanger. International Journal Refrigeration. 2018; 93:38-46. doi:https://doi.org/10.1016/j.ijrefrig.2018.06.008.
52. Nada SA, I. Eid E, Abdel Aziz G, A. Hassan H. Heat Transfer enhancement in shell and helical coil with external radial fins. Proceeding of The Twelfth International Conference for Engineering (AEIC), Al Azhar University, Egypt. 2012; 3: 350-369.
53. Nada SA, Eid EI, Abd El Aziz GB, Hassan HA. Performance Enhancement of Shell and Helical Coil Water Coolers Using Different Geometric and Fins Conditions. Heat Transfer - Asian Research.2016; 45(7): 631-647.
doi: https://doi.org/10.1002/htj.21180
54. Gupta A, Kumar R, Gupta A. Condensation of R-134a inside a helically coiled tube-in-shell heat exchanger. Experimental Thermal Fluid Science. 2014; 54: 279-289.
doi: https://doi.org/10.1016/j.expthermflusci.2014.01.003

55. Ali, R., Gulhane, N. P. Experimental Analysis of Condensation in Helical Coil Tube. International Journal of Process Systems Engineering. 2018; 4: 991–1004.
doi: https://doi.org/10.1504/IJPSE.2018.093719
56. Yu J, Chen J, Li F, Cai W, Lu L, Jiang Y. Experimental investigation of forced convective condensation heat transfer of hydrocarbon refrigerant in a helical tube. Applied Thermal Engineering. 2018; 129: 1634-1644.
doi: https://doi.org/10.1016/j.applthermaleng.2017.10.143
57. Saffari H, Naziri V. Theoretical modeling and numerical solution of stratified condensation in inclined tubes. Journal of Mechanical Science and Technology. 2010; 24(12): 2587-2596.
doi: https://doi.org/10.1007/s12206-010-0916-0
58. Waiker. D, Singh. A., Patidar. S., & Parihar. S. Performance Analyses of a Multiple Horizontal Tubes for Steam Condensation, Journal of Mechanical and Civil Engineering.2013; 4:12-18.
59. Mozafari M, Akhavan-Behabadi MA, Qobadi-Arfaee H, Fakoor-Pakdaman M. Condensation and pressure drop characteristics of R600a in a helical tube-in-tube heat exchanger at different inclination angles. Applied Thermal Engineering. 2015;90 :571-578. doi:https://doi.org/10.1016/j.applthermaleng.2015.07.044
60. Ewim DRE, Meyer JP, Abadi SMANR. Condensation heat transfer coefficients in an inclined smooth tube at low mass fluxes. International Journal Heat Mass Transfer. 2018; 123: 455-467.doi: https://doi.org/10.1016/j.ijheatmasstransfer.2018.02.091
61. Abadi SMANR, Mehrabi M, Meyer JP. Numerical study of steam condensation inside a long, inclined, smooth tube at different saturation temperatures. . International Journal Heat Mass Transfer. 2018; 126:15-25. doi: https://doi.org/10.1016/j.ijheatmasstransfer.2018.05.136
62. Abadi SMANR, Meyer JP, Dirker J. Effect of inclination angle on the condensation of R134a inside an inclined smooth tube. Chemical Engineering Research and Design. 2018; 132: 346-357.
doi: https://doi.org/10.1016/j.cherd.2018.01.044
63. Davies WA, Kang Y, Hrnjak P, Jacobi AM. Effect of inclination on heat transfer and flow regimes in large flattened-tube steam condensers. Applied Thermal Engineering . 2019; 148: 999-1006.
doi: https://doi.org/10.1016/j.applthermaleng.2018.11.078

64. Nada SA, Hussein HM. General semi-empirical correlation for condensation of vapor on tubes at different orientations. International Journal Thermal Science. 2016; 100:391-400. doi:10.1016/j.ijthermalsci.2015.10.023
65. Naphon P, Suwagrai J. Effect of curvature ratios on the heat transfer and flow developments in the horizontal spirally coiled tubes. International Journal Heat Mass Transfer. 2007; 50(3): 444-451. doi: https://doi.org/10.1016/j.ijheatmasstransfer.2006.08.002
66. Wu JM, Huang X, Zhang H. Numerical investigation on the heat and mass transfer in a direct evaporative cooler. Applied Thermal Engineering.2009;29:195-201. doi:10.1016/j.applthermaleng.2008.02.018
67. J. Yogesh, Design and optimization of thermal systems. 2nd ed. CRC Press; 2007.
68. YORK, Catalogue, Air Cooled Screw Liquid Chillers, FORM 201.19-EG3 (803), York International Corporation, USA, 2000.
69. J.P. Holmman, W.J. Gajda, Experimental method for engineering, McGrew Hill, New York, 1994
70. Huzayyin AS, Nada SA, Elattar HF. Air-side performance of a wavy-finned-tube direct expansion cooling and dehumidifying air coil. International Journal of Refrigeration. 2007;30:230-244. doi:10.1016/j.ijrefrig.2006.07.023
71. https://www.alibaba.com/product-detail/industrial-air-dehumidifier-withsiemenscontroller_60663659412.html?spm=a2700.details.maylikever.4.ee352a%E2%80%A6
72. https://www.alibaba.com/product-detail/100-tr-Air-Cooled-Water-Chiller_62081786475.html?spm=a2700.7724857.normalList.7.116f1f43BlJLWZ&s=p
73. https://www.alibaba.com/product-detail/High-Efficiency-Recuperator-Heat-Recovery Ventilator_60701360270.html?spm=a2700.7724857.normalList.11.3c6350023onqtx&s=p
74. A. Eslamimanesh, M.S. Hatamipour, Economical study of a small-scale direct contact humidification–dehumidification desalination plant, Desalination, 250, 1, 2010, 203-207, https://doi.org/10.1016/j.desal.2008.11.015.

Appendix (A) Governing Equation for three proposed systems in mathematical model [formatted form equation form EES]

Known Data

$P1 = 101.35$ [kpa]

$Q_r = 352$ [Kw]

$E_{Dw1} = 0.2$

$E_{Dw2} = 0.2$

$E_{HR} = 0.6$

''

Change Data

$\dot{m} = 0.25$

$T_o = 40$ [C]

$w_o = 0.015$ [kg/kg]

''

Constant properties

$T_r = 22$ [C]

$RH_r = 0.3$

$h_r = \mathbf{h}$ ['AirH2O' , $T = T_r$, $P = P1$, $w = w_r$]

$w_r = \omega$ ['AirH2O' , $T = T_r$, $P = P1$, $R = RH_r$]

****

$T_s = 12$ [C]

$RH_s = 0.4$

$h_s = \mathbf{h}$ ['AirH2O' , $T = T_s$, $P = P1$, $w = w_s$]

$w_s = \omega$ ['AirH2O' , $T = T_s$, $P = P1$, $R = RH_s$]

****

$T_3 = T_o$

$w_3 = w_o$ Sensible Heating

$h_3 = h_o$

$RH_3 = RH_o$

$h_o = \mathbf{h}$ ['AirH2O' , $T = T_o$, $P = P1$, $w = w_o$]

$RH_o = \mathbf{RH}$ ['AirH2O' , $T = T_o$, $P = P1$, $w = w_o$]

$T_4 = 120$ [C]

$w_4 = w_3$

$h_4 = \mathbf{h}\left[\text{'AirH2O'}, T = T_4, P = P1, w = w_4 \right]$

$RH_4 = \mathbf{RH}\left[\text{'AirH2O'}, T = T_4, P = P1, w = w_4 \right]$

****

$T_7 = T_{o,wet}$

$RH_7 = 1$ Dehumidification process occurs on the saturation curve

$w_7 = \omega\left[\text{'AirH2O'}, T = T_7, P = P1, R = RH_7 \right]$

$h_7 = \mathbf{h}\left[\text{'AirH2O'}, T = T_7, P = P1, w = w_7 \right]$

$RH_6 = 1$

$T_{o,wet} = \mathbf{WB}\left[\text{'AirH2O'}, T = T_o, P = P1, R = RH_o \right]$

****

$COP = 11.1 - 0.4 \cdot T_o + 7.2 \cdot 10^{-3} \cdot T_o^{\,2} - 5.18 \cdot 10^{-5} \cdot T_o^{\,3}$

****

$$\dot{m}_s = \frac{Q_r}{h_r - h_s}$$

$RR = 0.33$

$$RR = \frac{\dot{m}_{Reg}}{\dot{m}_s}$$

****

$\dot{Q}_{HC} = \dot{m}_{Reg} \cdot 1.005 \cdot \left[T_4 - T_3 \right]$

,,,

Basic system Sys1

,,

Mixing Section

$\dot{m}_o = \dot{m}$

$\dot{m}_r = 1 - \dot{m}$

$$\frac{\dot{m}_o}{\dot{m}_r} = \frac{T_r - T_{1,sys1}}{T_{1,sys1} - T_o}$$

$$\frac{\dot{m}_o}{\dot{m}_r} = \frac{h_r - h_{1,sys1}}{h_{1,sys1} - h_o}$$

$$\frac{\dot{m}_o}{\dot{m}_r} = \frac{w_r - w_{1,sys1}}{w_{1,sys1} - w_o}$$

Where

$$RH_{1,sys1} = \mathbf{RH}\left[\text{'AirH2O'}, T = T_{1,sys1}, P = P1, w = w_{1,sys1}\right]$$

,,,

DW Efficiency

$$E_{Dw1} = \frac{T_{2,sys1} - T_{1,sys1}}{T_4 - T_{1,sys1}}$$

$$E_{Dw2} = \frac{\dot{m}_s \cdot \left[w_{1,sys1} - w_{2,sys1}\right] \cdot 2441.5 \quad [kJ/kg]}{\dot{m}_{Reg} \cdot \left[h_4 - h_3\right]}$$

Where

$$h_{2,sys1} = \mathbf{h}\left[\text{'AirH2O'}, T = T_{2,sys1}, P = P1, w = w_{2,sys1}\right]$$

$$RH_{2,sys1} = \mathbf{RH}\left[\text{'AirH2O'}, T = T_{2,sys1}, P = P1, w = w_{2,sys1}\right]$$

,,,

Cooling coil Capacity

$$\dot{Q}_{CC,sys1} = \dot{m}_s \cdot \left[h_{2,sys1} - h_s\right]$$

,,,

Outlet reactivation temp and humidity from DW

$$T_{5,sys1} = T_4 - \left[\frac{T_{2,sys1} - T_{1,sys1}}{RR}\right]$$

$$w_{5,sys1} = w_4 + \frac{w_{1,sys1} - w_{2,sys1}}{RR}$$

Where

$$h_{5,sys1} = \mathbf{h}\left[\text{'AirH2O'}, T = T_{5,sys1}, P = P1, w = w_{5,sys1}\right]$$

$$RH_{5,sys1} = \mathbf{RH}\left[\text{'AirH2O'}, T = T_{5,sys1}, P = P1, w = w_{5,sys1}\right]$$

$$Twb_{5,sys1} = \mathbf{WB}\left[\text{'AirH2O'}, T = T_{5,sys1}, P = P1, R = RH_{5,sys1}\right]$$

,,,

Outlet humidifer

$w_{6,sys1} = \omega$ ['AirH2O' , T = $Twb_{5,sys1}$, P = P1 , R = RH_6]

$T_{6,sys1}$ = **T** ['AirH2O' , w = $w_{6,sys1}$, P = P1 , R = RH_6]

$h_{6,sys1}$ = **h** ['AirH2O' , T = $T_{6,sys1}$, P = P1 , w = $w_{6,sys1}$]

,,

fresh water production

$$\dot{m}_{w1,sys1} = \dot{m}_s \cdot [w_{2,sys1} - w_s]$$

$$\dot{m}_{w2,sys1} = \dot{m}_{Reg} \cdot [w_{6,sys1} - w_7]$$

$$\dot{m}_{w,sys1} = \dot{m}_{w1,sys1} + \dot{m}_{w2,sys1}$$

,,

Power used

$$COP = \frac{\dot{Q}_{CC,sys1}}{\dot{W}_{c,sys1}}$$

$$\dot{E}_{sys1} = \dot{W}_{c,sys1}$$

,,

Modified system Sys 2

,,

Mixing Section

$\dot{m}_o = \dot{m}$
$m_r = 1 - \dot{m}$

$$\frac{\dot{m}_o}{\dot{m}_r} = \frac{T_r - T_{1,sys2}}{T_{1,sys2} - T_o}$$

$$\frac{\dot{m}_o}{\dot{m}_r} = \frac{h_r - h_{1,sys2}}{h_{1,sys2} - h_o}$$

$$\frac{\dot{m}_o}{\dot{m}_r} = \frac{w_r - w_{1,sys2}}{w_{1,sys2} - w_o}$$

Where

$RH_{1,sys2}$ = **RH** ['AirH2O' , T = $T_{1,sys2}$, P = P1 , w = $w_{1,sys2}$]

,,

DW Efficiency

$$E_{Dw1} = \frac{T_{2,sys2} - T_{1,sys2}}{T_4 - T_{1,sys2}}$$

$$E_{Dw2} = \frac{\dot{m}_s \cdot [w_{1,sys2} - w_{2,sys2}] \cdot 2441.5 \ [kJ/kg]}{\dot{m}_{Reg} \cdot [h_4 - h_3]}$$

Where

$h_{2,sys2} = \mathbf{h}$ ['AirH2O' , $T = T_{2,sys2}$, $P = P1$, $w = w_{2,sys2}$]

$RH_{2,sys2} = \mathbf{RH}$ ['AirH2O' , $T = T_{2,sys2}$, $P = P1$, $w = w_{2,sys2}$]

,,

Heat recovery

$$E_{HR} = \frac{T_{2,HR,sys2} - T_{2,sys2}}{\dot{m} \cdot [T_r - T_{2,sys2}]}$$

$E_{HR}=(h_{2,HR,sys2}-h_{2,sys2})/(\dot{m}*(h_r-h_{2,sys2}))$

Where

$w_{2,HR,sys2} = w_{2,sys2}$

$h_{2,HR,sys2} = \mathbf{h}$ ['AirH2O' , $T = T_{2,HR,sys2}$, $P = P1$, $w = w_{2,HR,sys2}$]

$RH_{2,HR,sys2} = \mathbf{RH}$ ['AirH2O' , $T = T_{2,HR,sys2}$, $P = P1$, $w = w_{2,HR,sys2}$]

$T_{2,HR,sys2}$=TEMPERATURE(AirH2O,h=$h_{2,HR,sys2}$,P=P1,w=$w_{2,HR,sys2}$)

,,

Cooling coil Capacity

$$\dot{Q}_{CC,sys2} = \dot{m}_s \cdot [h_{2,HR,sys2} - h_s]$$

,,

Outlet reactivation temp and humidity from DW

$$T_{5,sys2} = T_4 - \left[\frac{T_{2,sys2} - T_{1,sys2}}{RR}\right]$$

$$w_{5,sys2} = w_4 + \frac{w_{1,sys2} - w_{2,sys2}}{RR}$$

Where

$h_{5,sys2} = \mathbf{h}$ ['AirH2O' , $T = T_{5,sys2}$, $P = P1$, $w = w_{5,sys2}$]

$RH_{5,sys2} = \mathbf{RH}$ ['AirH2O' , $T = T_{5,sys2}$, $P = P1$, $w = w_{5,sys2}$]

$Twb_{5,sys2} = \mathbf{WB}$ ['AirH2O' , $T = T_{5,sys2}$, $P = P1$, $R = RH_{5,sys2}$]

Outlet humidifer

$$w_{6,sys2} = \omega\left['AirH2O', T = Twb_{5,sys2}, P = P1, R = RH_6\right]$$

$$T_{6,sys2} = \mathbf{T}\left['AirH2O', w = w_{6,sys2}, P = P1, R = RH_6\right]$$

$$h_{6,sys2} = \mathbf{h}\left['AirH2O', T = T_{6,sys2}, P = P1, w = w_{6,sys2}\right]$$

,,

fresh water production

$$\dot{m}_{w1,sys2} = \dot{m}_s \cdot \left[w_{2,HR,sys2} - w_s\right]$$

$$\dot{m}_{w2,sys2} = \dot{m}_{Reg} \cdot \left[w_{6,sys2} - w_7\right]$$

$$\dot{m}_{w,sys2} = \dot{m}_{w1,sys2} + \dot{m}_{w2,sys2}$$

,,

Power used and power saving

$$COP = \frac{\dot{Q}_{CC,sys2}}{\dot{W}_{c,sys2}}$$

$$\dot{E}_{sys2} = \dot{W}_{c,sys2}$$

$$Power_{saving,sys2} = \left[\frac{\dot{E}_{sys1} - \dot{E}_{sys2}}{\dot{E}_{sys1}}\right] \cdot 100$$

,,

Modified system Sys 3

,,

Heat recovery

$$E_{HR} = \frac{T_{o,HR,sys3} - T_o}{\dot{m} \cdot \left[T_r - T_o\right]}$$

$E_{HR}=(h_{o,HR,sys3}-h_{o)}/((\dot{m})*(h_r-h_{o)})$

Where

$$w_{o,HR,sys3} = w_o$$

$$h_{o,HR,sys3} = \mathbf{h}\left['AirH2O', T = T_{o,HR,sys3}, P = P1, w = w_o\right]$$

$$RH_{o,HR,sys3} = \mathbf{RH}\left['AirH2O', T = T_{o,HR,sys3}, P = P1, w = w_o\right]$$

$T_{o,HR,sys3}$=TEMPERATURE(AirH2O,h=$h_{o,HR,sys3,P}$=P1,w=$w_{o)}$

Mixing Section

$\dot{m}_o=\dot{m}$
$m_r=1-\dot{\dot{m}}$

$$\frac{\dot{m}_o}{\dot{m}_r} = \frac{T_r - T_{1,sys3}}{T_{1,sys3} - T_{o,HR,sys3}}$$

$$\frac{\dot{m}_o}{\dot{m}_r} = \frac{h_r - h_{1,sys3}}{h_{1,sys3} - h_{o,HR,sys3}}$$

$$\frac{\dot{m}_o}{\dot{m}_r} = \frac{w_r - w_{1,sys3}}{w_{1,sys3} - w_o}$$

Where

$$RH_{1,sys3} = \mathbf{RH}\left[\text{'AirH2O'}, T = T_{1,sys3}, P = P1, w = w_{1,sys3}\right]$$

,,

DW Efficiency

$$E_{Dw1} = \frac{T_{2,sys3} - T_{1,sys3}}{T_4 - T_{1,sys3}}$$

$$E_{Dw2} = \frac{\dot{m}_s \cdot \left[w_{1,sys3} - w_{2,sys3}\right] \cdot 2441.5 \ \text{[kJ/kg]}}{\dot{m}_{Reg} \cdot \left[h_4 - h_3\right]}$$

Where

$$h_{2,sys3} = \mathbf{h}\left[\text{'AirH2O'}, T = T_{2,sys3}, P = P1, w = w_{2,sys3}\right]$$

$$RH_{2,sys3} = \mathbf{RH}\left[\text{'AirH2O'}, T = T_{2,sys3}, P = P1, w = w_{2,sys3}\right]$$

,,

Cooling coil Capacity

$$\dot{Q}_{CC,sys3} = \dot{m}_s \cdot \left[h_{2,sys3} - h_s\right]$$

,,

Outlet reactivation temp and humidity from DW

$$T_{5,sys3} = T_4 - \left[\frac{T_{2,sys3} - T_{1,sys3}}{RR}\right]$$

$$w_{5,sys3} = w_4 + \frac{w_{1,sys3} - w_{2,sys3}}{RR}$$

Where

$$h_{5,sys3} = \mathbf{h}\left[\text{'AirH2O'}, T = T_{5,sys3}, P = P1, w = w_{5,sys3}\right]$$

$$RH_{5,sys3} = \mathbf{RH}\left['AirH2O', T = T_{5,sys3}, P = P1, w = w_{5,sys3}\right]$$

$$Twb_{5,sys3} = \mathbf{WB}\left['AirH2O', T = T_{5,sys3}, P = P1, R = RH_{5,sys3}\right]$$

,,

Outlet humidifer

$$w_{6,sys3} = \omega\left['AirH2O', T = Twb_{5,sys3}, P = P1, R = RH_6\right]$$

$$T_{6,sys3} = \mathbf{T}\left['AirH2O', w = w_{6,sys3}, P = P1, R = RH_6\right]$$

$$h_{6,sys3} = \mathbf{h}\left['AirH2O', T = T_{6,sys3}, P = P1, w = w_{6,sys3}\right]$$

,,

fresh water production

$$\dot{m}_{w1,sys3} = \dot{m}_s \cdot \left[w_{2,sys3} - w_s\right]$$

$$\dot{m}_{w2,sys3} = \dot{m}_{Reg} \cdot \left[w_{6,sys3} - w_7\right]$$

$$\dot{m}_{w,sys3} = \dot{m}_{w1,sys3} + \dot{m}_{w2,sys3}$$

,,

Power used and power saving

$$COP = \frac{\dot{Q}_{CC,sys3}}{\dot{W}_{c,sys3}}$$

$$\dot{E}_{sys3} = \dot{W}_{c,sys3}$$

$$Power_{saving,sys3} = \left[\frac{\dot{E}_{sys1} - \dot{E}_{sys3}}{\dot{E}_{sys1}}\right] \cdot 100$$

,,,

system selection and cost analysis

$$TCS_{sys2} = \dot{m}_{w,sys2} \cdot 3.6 \cdot \dot{W}_{unit} + \left[\dot{E}_{sys1} - \dot{E}_{sys2}\right] \cdot \dot{E}_{rate} \quad \$/h \quad \$/m3 \quad \$/KWh$$

$$TCS_{sys3} = \dot{m}_{w,sys3} \cdot 3.6 \cdot \dot{W}_{unit} + \left[\dot{E}_{sys1} - \dot{E}_{sys3}\right] \cdot \dot{E}_{rate} \quad \$/h \quad \$/m3 \quad \$/KWh$$

$$\dot{W}_{unit} = 2.5$$

$$\dot{E}_{rate} = 0.02$$

Flow chart for mathmetical modeling

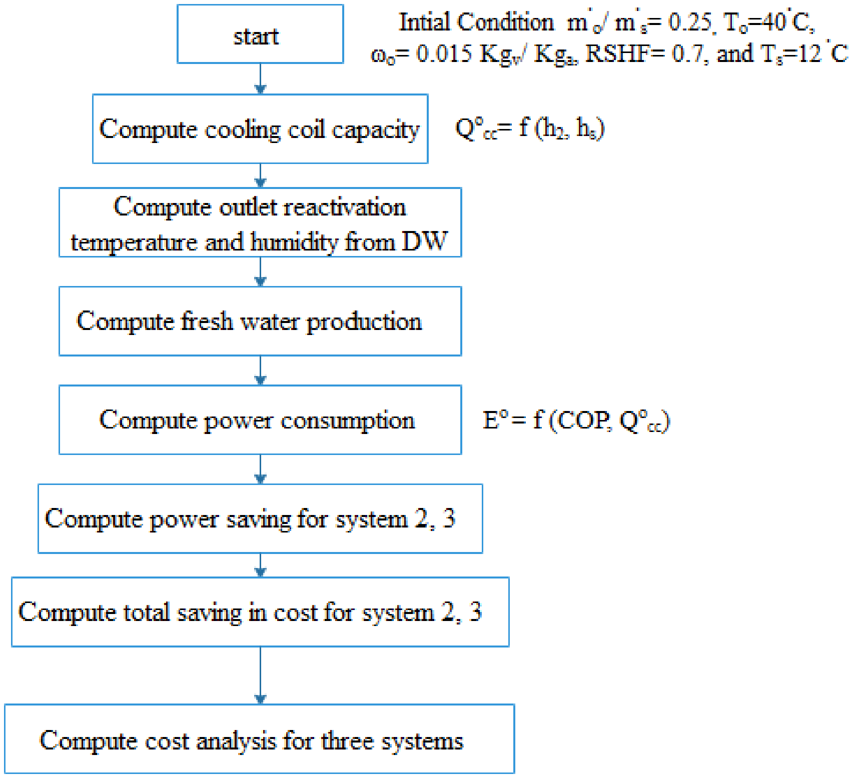

Appendix (B) Pressure drop across honeycomb cooling pad with:

1- Different air flow rate

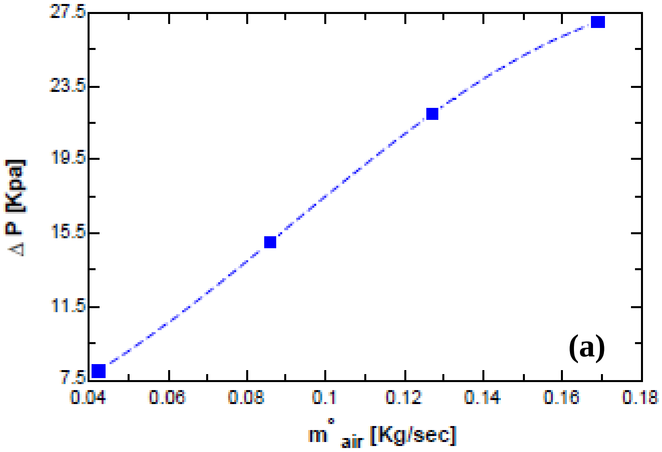

As shown in figure (a) the pressure drops increase by increasing the inlet air flow rate this can be returned to increasing air flow rate will lead to higher maldistribution of flow field at inlet of pads as well as higher air resistance between corrugated sheets.

2- Different water flow rate

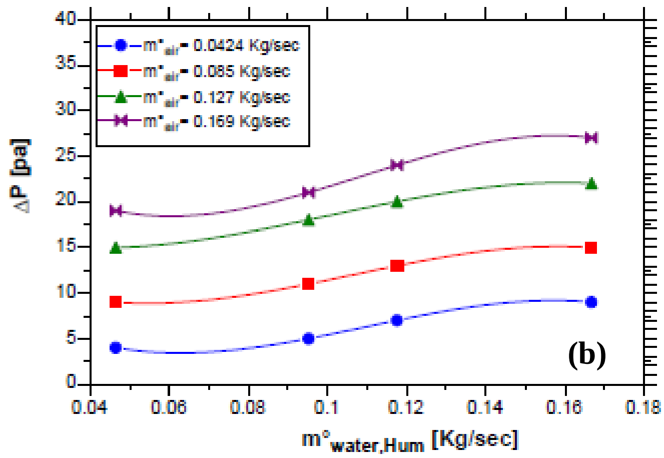

when amount of water inlet to honeycomb pads increased leads to increasing pressure drop across honeycomb pads due to increasing the resistance between air and water molecules which air flow in horizontal stream and water flow in vertical stream. So, pressure drop will be increasing when amount of water increased and air flow rate increased